

Desktop Systems for Manufacturing Carbon Nanotube Films by Chemical
Vapor Deposition

by

David S. Kuhn
Bachelor of Science in Engineering
Stanford University, 1995

Submitted to the Department of Mechanical Engineering in Partial Fulfillment of the
Requirements for the Degrees of

Engineer's Degree in Naval Construction and Engineering
and
Master of Science in Mechanical Engineering

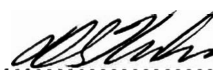
at the

Massachusetts Institute of Technology
June 2007

© 2007 David S. Kuhn
All rights reserved


The author hereby grants to MIT permission to reproduce and to distribute publicly paper
and electronic copies of this thesis document in whole or in part in any medium now
known or hereafter created.

Signature of
Author.....



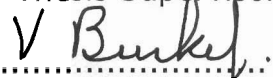
Department of Mechanical Engineering
May 21, 2007

Certified by



Alexander H. Slocum
Professor of Mechanical Engineering, MacVicar Faculty Fellow
Thesis Supervisor

Certified by



David V. Burke
Senior Lecturer, Department of Mechanical Engineering
Thesis Supervisor

Accepted by



Lallit Anand
Chairman, Department Committee on Graduate Students

| REPORT DOCUMENTATION PAGE | | | Form Approved OMB No. 0704-0188 | | |
|---|-------------|-----------------------------------|--|--|--|
| Public reporting burden for this collection of information is estimated to average 1 hour per response, including the time for reviewing instructions, searching existing data sources, gathering and maintaining the data needed, and completing and reviewing this collection of information. Send comments regarding this burden estimate or any other aspect of this collection of information, including suggestions for reducing this burden to Department of Defense, Washington Headquarters Services, Directorate for Information Operations and Reports (0704-0188), 1215 Jefferson Davis Highway, Suite 1204, Arlington, VA 22202-4302. Respondents should be aware that notwithstanding any other provision of law, no person shall be subject to any penalty for failing to comply with a collection of information if it does not display a currently valid OMB control number. PLEASE DO NOT RETURN YOUR FORM TO THE ABOVE ADDRESS. | | | | | |
| 1. REPORT DATE (DD-MM-YYYY) XX-06-2007 | | 2. REPORT TYPE Master's Thesis | | 3. DATES COVERED (From - To) JAN-JUN 2007 | |
| 4. TITLE AND SUBTITLE Desktop Systems for Manufacturing Carbon Nanotube Films by Chemical Vapor Deposition | | | 5a. CONTRACT NUMBER N62271-97-G-0026 | | |
| | | | 5b. GRANT NUMBER | | |
| | | | 5c. PROGRAM ELEMENT NUMBER | | |
| 6. AUTHOR(S) David S. Kuhn | | | 5d. PROJECT NUMBER | | |
| | | | 5e. TASK NUMBER | | |
| | | | 5f. WORK UNIT NUMBER | | |
| 7. PERFORMING ORGANIZATION NAME(S) AND ADDRESS(ES) Massachusetts Institute of Technology | | | 8. PERFORMING ORGANIZATION REPORT NUMBER | | |
| 9. SPONSORING / MONITORING AGENCY NAME(S) AND ADDRESS(ES) Naval Postgraduate School Monterey, Ca 93943 | | | 10. SPONSOR/MONITOR'S ACRONYM(S) NPS | | |
| | | | 11. SPONSOR/MONITOR'S REPORT NUMBER(S) | | |
| 12. DISTRIBUTION / AVAILABILITY STATEMENT 1. DISTRIBUTION STATEMENT A. Approved for public release; distribution is unlimited. | | | | | |
| 13. SUPPLEMENTARY NOTES | | | | | |
| 14. ABSTRACT Carbon nanotubes (CNTs) exhibit exceptional electrical, thermal, and mechanical properties that could potentially transform such diverse fields as composites, electronics, cooling, energy storage, and biological sensing. For the United States Navy, composites potentially provide a significant decrease in lifetime maintenance costs of ships by eliminating hull corrosion. A stronger composite could also improve naval ship survivability or increase combat payloads by reducing the hull weight of ships and submarines. Further, cooling requirements of ship borne electronics have grown exponentially and represent a significant weight penalty for advanced ship designs. Any improvement in thermal transport could significantly improve future naval ship designs. In order to realize these benefits, methods must be discovered to fully characterize CNT growth mechanisms, consistently produce CNTs in manufacturable quantities, and to integrate CNTs into macroscale structures which reflect the properties of individual CNTs. While growth of CNTs in laboratory scale chemical vapor deposition (CVD) tube furnaces has shown great promise, existing low cost tube furnace designs limit the researcher's ability to fully separate critical reaction parameters such as temperature and flow profiles and limit the rate of temperature change during the growth process. Conventional tube furnace designs also provide limited mechanical access to the growth site and prevent optical monitoring of the growth site, removing the ability to observe and interact <i>in situ</i> during growth. This thesis presents the "SabreTube", a low-cost desktop CVD apparatus that decouples temperature and flow variables, provides mechanical and optical access to the reaction site during growth, and provides modular fixturing to enable versatile experimentation with and characterization of CNT growth mechanisms. This thesis also presents the Nanosled, a device designed to translate a substrate through a CVD furnace in order to develop a continuous manufacturing process for CNT films for applications in reinforced structural composites. | | | | | |
| 15. SUBJECT TERMS | | | | | |
| 16. SECURITY CLASSIFICATION OF: | | | 17. LIMITATION OF ABSTRACT | 18. NUMBER OF PAGES | 19a. NAME OF RESPONSIBLE PERSON |
| a. REPORT | b. ABSTRACT | c. THIS PAGE | | | Sean Tibbitts, Educational Technician |
| | | | UU | 147 | 19b. TELEPHONE NUMBER (include area code) (831) 656-2319 civins@nps.edu |

Desktop Systems for Manufacturing Carbon Nanotube Films by Chemical Vapor Deposition

by

David S. Kuhn

Submitted to the Department of Mechanical Engineering on May 21st, 2007
in Partial Fulfillment of the requirements for the Degrees of
Engineer's Degree in Naval Construction and Engineering and
Master of Science in Mechanical Engineering

Abstract

Carbon nanotubes (CNTs) exhibit exceptional electrical, thermal, and mechanical properties that could potentially transform such diverse fields as composites, electronics, cooling, energy storage, and biological sensing. For the United States Navy, composites potentially provide a significant decrease in lifetime maintenance costs of ships by eliminating hull corrosion. A stronger composite could also improve naval ship survivability or increase combat payloads by reducing the hull weight of ships and submarines. Further, cooling requirements of ship borne electronics have grown exponentially and represent a significant weight penalty for advanced ship designs. Any improvement in thermal transport could significantly improve future naval ship designs. In order to realize these benefits, methods must be discovered to fully characterize CNT growth mechanisms, consistently produce CNTs in manufacturable quantities, and to integrate CNTs into macroscale structures which reflect the properties of individual CNTs.

While growth of CNTs in laboratory scale chemical vapor deposition (CVD) tube furnaces has shown great promise, existing low cost tube furnace designs limit the researcher's ability to fully separate critical reaction parameters such as temperature and flow profiles and limit the rate of temperature change during the growth process. Conventional tube furnace designs also provide limited mechanical access to the growth site and prevent optical monitoring of the growth site, removing the ability to observe and interact *in situ* during growth. This thesis presents the "SabreTube", a low-cost desktop CVD apparatus that decouples temperature and flow variables, provides mechanical and optical access to the reaction site during growth, and provides modular fixturing to enable versatile experimentation with and characterization of CNT growth mechanisms. This thesis also presents the Nanosled, a device designed to translate a substrate through a CVD furnace in order to develop a continuous manufacturing process for CNT films for applications in reinforced structural composites.

Table of Contents

| | |
|---|----|
| Abstract..... | 2 |
| Table of Contents..... | 3 |
| Table of Figures..... | 5 |
| Table of Tables..... | 7 |
| Acknowledgements..... | 8 |
| Part One: Introduction and Motivation..... | 9 |
| 1.1 Purpose of the Thesis..... | 9 |
| 1.2 Carbon Nanotube Typology and Characteristics | 10 |
| 1.3 The Potential of Carbon Nanotubes and the Challenges..... | 15 |
| 1.4 Current Production Methods of Carbon Nanotubes..... | 17 |
| 1.4.1 Limitations of Standard, Static Thermal Chemical Vapor Deposition Tube Furnaces..... | 18 |
| Part Two: Carbon Nanotube Furnace and Appliance Designs..... | 21 |
| 2.1 CVD Furnace Material Requirements..... | 21 |
| 2.1.1 The Temperature Challenge..... | 22 |
| 2.1.2 The Chemistry Challenge | 24 |
| 2.1.3 The Flammable Gas Challenge | 26 |
| 2.1.4 The Electrical Challenge..... | 28 |
| 2.2 SabreTube: A Flexible, Low-Cost Desktop Thermal CVD System | 28 |
| 2.2.1 Customer Requirements..... | 29 |
| 2.2.2 Process Variable Decoupling | 30 |
| 2.2.3 Optical Characterization of Carbon Nanotube Growth..... | 32 |
| 2.2.4 Design Philosophy..... | 33 |
| 2.2.5 System Design and Specifications | 34 |
| 2.2.5.1 SabreTube General Description | 34 |
| 2.2.5.2 Substrate Heating..... | 55 |
| 2.2.5.3 Reaction Site Access | 58 |
| 2.2.5.4 Reactor Support and Modular Fixtures..... | 59 |
| 2.2.5.5 Sensing and Control..... | 60 |
| 2.2.5.6 Additional Usability Features | 62 |
| 2.2.5.7 Safety Systems | 65 |
| 2.2.6 SabreTube Components and Price | 69 |
| 2.2.7 Market Competition | 72 |
| 2.3 Enabling the Testing of Continuous Manufacturing of Carbon Nanotubes 72 | |
| 2.3.1 System Requirements and Constraints | 76 |
| 2.3.2 Nanosled design..... | 77 |
| 2.3.2.1 Hertz Contact Stress | 83 |
| 2.3.2.2 Flexure Theory and Design | 84 |
| Part Three: Potential Naval Architecture Applications of Carbon Nanotubes..... | 88 |
| 3.1 Technology Readiness | 88 |
| 3.2 Electronics | 90 |
| 3.2.1 Thermal Management | 91 |

| | | |
|--------------------------------------|--|-----|
| 3.2.2 | Supercapacitors | 94 |
| 3.2.3 | Polymer Composites | 95 |
| Part Four: | Results, Future Work Recommendations and Conclusions | 98 |
| 4.1. | Results..... | 98 |
| 4.1.1. | SabreTube..... | 98 |
| 4.1.2. | Nanosled | 101 |
| 4.2. | Future Work Recommendations | 101 |
| 4.2.1. | SabreTube Future Design Refinements | 101 |
| 4.2.1.1. | Gas Sealing..... | 101 |
| 4.2.1.2. | Substrate Clip Design..... | 103 |
| 4.2.1.3. | Quartz Tube Retraction | 104 |
| 4.2.1.4. | Electrical Safety..... | 105 |
| 4.2.1.5. | Footprint Reduction | 107 |
| 4.2.1.6. | Vertical Tube Holder..... | 108 |
| 4.2.1.7. | Material Changes | 108 |
| 4.2.1.8. | Temperature Feedback Control..... | 108 |
| 4.2.1.9. | Outgas Testing and Conditioning | 109 |
| 4.2.2. | Nanosled Future Work and Refinements..... | 110 |
| 4.2.2.1. | Increase the box CVD size | 110 |
| 4.2.2.2. | Install Graphalloy Bushings..... | 110 |
| 4.2.2.3. | Continuous Harvesting | 111 |
| 4.3. | Conclusions | 111 |
| Appendix A: | SabreTube Technical Drawings..... | 113 |
| Appendix B: | SabreTube Electrical Schematics..... | 127 |
| Appendix C: | SabreTube Parts and Cost Spreadsheet..... | 131 |
| Appendix D: | Nanosled Technical Drawings | 137 |
| Appendix E: | Nanosled Manufacturing | 140 |
| End Fixture Manufacturing | | 140 |
| Shoulder Bushing Manufacturing | | 141 |
| Appendix F: | Department of Defense Technology Readiness Levels | 143 |
| References | | 145 |

Table of Figures

| | |
|--|----|
| Figure 1: Carbon nanotube morphologies..... | 11 |
| Figure 2: Comparison of normalized strength and stiffness of CNTs with common materials..... | 15 |
| Figure 3: Schematic of CNT growth via CVD..... | 19 |
| Figure 4: A typical basic CVD tube furnace | 20 |
| Figure 5: Hydrogen corrosion limits for various steels | 26 |
| Figure 6: Schematic of example CVD system suspended heated platform | 29 |
| Figure 7: Decoupling gas and reaction site temperature profiles | 31 |
| Figure 8: Custom quartz tubes fitted with Kapton windows for X-ray scattering | 32 |
| Figure 9: The SabreTube system including preheater and laser displacement sensor options..... | 35 |
| Figure 10: Schematic of example CVD system suspended heated platform where the platform is coated to permit CNT growth | 35 |
| Figure 11: Schematic of example CVD system suspended heated platform with separate coated substrate | 35 |
| Figure 12: Schematic showing the SabreTube open for loading..... | 36 |
| Figure 13: SabreTube without optional laser sensor..... | 36 |
| Figure 14: Solidworks front view of the SabreTube system with the quartz reactor tube retracted..... | 37 |
| Figure 15: Solidworks plan view of the SabreTube system..... | 37 |
| Figure 16: Solidworks back view of SabreTube system..... | 38 |
| Figure 17: Front end cap..... | 40 |
| Figure 18: Substrate heater mounted between heat sinks and heating a silicon wafer | 41 |
| Figure 19: Modified aluminum heat sinks..... | 42 |
| Figure 20: Aluminum heat sink modification permits thermal expansion along the tube axis. | 43 |
| Figure 21: Quartz tube retracted and at rest on aluminum guide rails, affording easy access to the reaction site and substrate heater for sample loading. | 44 |
| Figure 22: Modular rear right angle bracket with slots for adjusting aluminum rail heights and for passing gas lines..... | 45 |
| Figure 23: Rear end cap with two gas flow lines and one pressure relief check valve and sectioned aluminum guide rails | 46 |
| Figure 24: Aluminum mounting pegboard and adjustable IR temperature sensor | 47 |
| Figure 25: Quartz tube in the resting vertical position on the vertical tube holder | 48 |
| Figure 26: Retractable quartz tube enables easy installation of a stainless steel pipe for routing gas flow | 50 |
| Figure 27: Exploded 3D Cad drawing of the preheater assembly | 51 |
| Figure 28: Optional laser displacement sensor and fixture | 53 |
| Figure 29: Schematic of <i>in situ</i> measurement of CNT film thickness | 54 |
| Figure 30: Laser heating of reaction surface..... | 55 |
| Figure 31: Profile of the Aavid Thermalloy heat sink used in the SabreTube..... | 56 |

| | |
|---|-----|
| Figure 32: CAD Drawing of rear right angle bracket with one Inch slot..... | 60 |
| Figure 33: IR temperature sensor mounting | 61 |
| Figure 34: The SabreTube with a thermocouple used to calibrate the IR temperature sensor..... | 62 |
| Figure 35: Subassembly cost breakdown for the basic SabreTube package..... | 71 |
| Figure 36: Notional Continuous Growth Process | 73 |
| Figure 37: CAD drawing of the Hart and van Laake box CVD furnace system exterior | 74 |
| Figure 38: Box CVD furnace interior details..... | 75 |
| Figure 39: Picture of as built CVD box furnace | 75 |
| Figure 40: Nanosled strategy..... | 77 |
| Figure 41: Nanosled external motor drive with K coupling, wiring, and PTFE tube fitting | 78 |
| Figure 42: Silicon wafer held between round shoulder bushing and cylindrical bottom drive roller | 80 |
| Figure 43: Shoulder bushing detail | 80 |
| Figure 44: Roller assembly model..... | 81 |
| Figure 45: Picture of roller assembly with clamped silicon sled | 81 |
| Figure 46: Picture of roller assembly with shaft collars and Macor washers | 82 |
| Figure 47: Typical crab flexure configuration | 85 |
| Figure 48: Equivalent spring equations | 87 |
| Figure 49: Potential applications of carbon nanotubes in the US Navy..... | 90 |
| Figure 50: Basic electronic cooling model..... | 92 |
| Figure 51: CNT growth in the SabreTube | 99 |
| Figure 52: <i>In Situ</i> measurement of CNT length over time | 100 |
| Figure 53: <i>In Situ</i> measurement of temperature and forest thickness over time | 100 |
| Figure 54: Potential leak path when a moment is applied to a two seal end cap | 102 |
| Figure 55: An end cap with three Viton lip seals adds additional protection against leaks | 103 |
| Figure 56: Possible mechanism for aiding in quartz tube alignment during retraction..... | 105 |
| Figure 57: Ball transfer switch..... | 106 |
| Figure 58: Snap action switches | 106 |

Table of Tables

| | |
|--|----|
| Table 1: Theoretical and reported electrical properties of CNTs vs. common materials. | 13 |
| Table 2: Comparative properties of CNT with selected materials | 14 |
| Table 3: Material suitability | 23 |
| Table 4: Selected material properties | 24 |
| Table 5: Flammability of hydrogen and ethylene..... | 27 |
| Table 6: Required design traits for a basic desktop CVD system | 30 |
| Table 7: SabreTube parts and labor cost..... | 71 |
| Table 8: Comparison of common CVD tube furnaces used to grow CNTs | 72 |
| Table 9: Hertz contact forces on the silicon sled..... | 84 |

Acknowledgements

The design of the SabreTube drew on prior research conducted by John Hart and Luuk Van Laake within Professor Alex Slocum's research group. The author is indebted to all three for their advice and collaboration. John Hart particularly served as the primary customer, sounding board, and collaborator in defining and designing the SabreTube.

John Hart, Luuk Van Laake and Professor Slocum also provided valuable insight and critiques in the design of the Nanosled.

Ken Stone and Hayami Arakawa of the MIT Hobby Shop provided helpful manufacturing tips and a friendly, tolerant, and patient environment for me to relearn the art of machining in producing the two designs.

Part One: Introduction and Motivation

1.1 Purpose of the Thesis

Research into the synthesis of carbon nanotubes (CNTs) is an active field of interest to the scientific and industrial community. Research goals include determining methods to synthesize long aligned CNT strands, to control growth density over a determined area, to control growth conditions to allow for targeted growth sites and configurations (e.g. tangled, aligned), to control defect rates in grown CNTs, to control growth density, and to find low cost, repeatable, and rapid methods to manufacture CNTs. To date, the state of the art has produced CNT forests of less than one cm while individual CNTs of several cm's have been grown.[1]

To achieve these research goals, scientists and technicians require tools to better characterize growth mechanisms and processes. To increase the number of researchers and research groups and to increase the rate of knowledge transfer, the cost of these tools must be kept low. This thesis explores the design of devices that enable the characterization of CVD growth processes for CNT applications and enable development of a process for continuous growth of CNT films. The thesis also highlights potential CNT applications of interest for use in the naval environment.

1.2 Carbon Nanotube Typology and Characteristics

Carbon can take many solid forms, from diamond to graphite to carbon nanotubes. Carbon nanotubes specifically refer to carbon atoms forming a hexagonal ring in a sp^2 bond such that each carbon atom bonds with three adjacent carbon atoms as in graphite. However, rather than existing as planar sheets like graphite, the carbon nanotube is a grapheme sheet 'rolled' into a seamless cylinder. [2]

Individual carbon nanotubes come in a variety of forms referred to as CNT chirality. Depending on how the carbon hexagons arrange relative to the tube axis, the CNT can take on one of three characteristic shapes as shown in Figure 1. Researchers characterize the carbon nanotube type based on two integers known as m and n . If $m=n$, then the pattern known as the 'armchair' results (Figure 1A). Armchair CNTs are notable because these CNTs act as metals. If either m or $n = 0$, then the 'zig-zag' pattern shown in Figure 1B results. All other integer combinations produce a chiral pattern similar to that shown in Figure 1C. Overall, there are hundreds of CNT chiral structures. Zig-zag and Chiral carbon nanotubes both act as semi-conductors though carbon nanotubes where $m-n = 3k$ ($k \neq 0$) have a small bandgap and all other combinations have a bandgap that is inversely proportional to the nanotube diameter. [3]

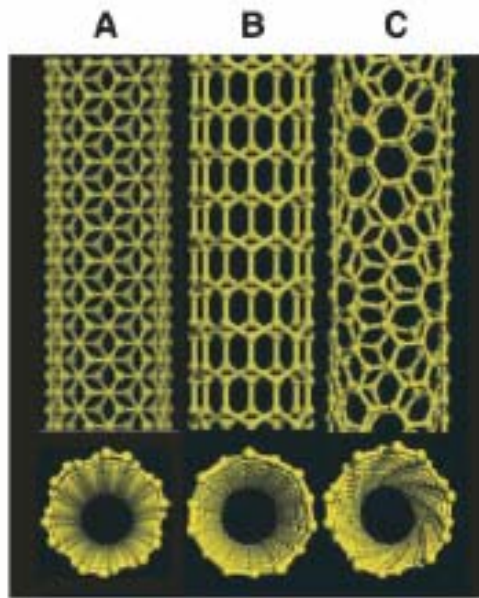


Figure 1: Carbon nanotube morphologies. A shows an 'armchair' layout. B shows a 'zig-zag' layout and C shows a 'chiral' layout. All 'arm chair' nanotubes act as metals. All others are semi-conductors. [3]

CNTs either grow as individual tubes known as single walled nanotubes (SWNTs) or as concentric tubes known as multi walled nanotubes (MWNTs). Both SWNTs and MWNTs have been grown in tangled nets or in aligned forests. While researchers have found ways to control whether SWNTs or MWNTs grow, they have not found ways to control the chirality of the tubes that grow. Examination of SWNT forests show a wide range of lattice structures from the metallic to the semi-conducting and each MWNT has several different lattice structures represented in its concentric tubes. Since MWNTs tend to have a larger diameter and therefore a smaller bandgap (~zero), MWNTs often exhibit metallic characteristics. [2, 4]

The excitement in the academic and industrial communities over CNTs lies in their unique electrical, thermal, and mechanical properties. Both metallic SWNTs and MWNTs exhibit 'ballistic' transport of electrons and phonons over millimeter length scales. Since the electrons and phonons exhibit very little scattering, theory predicts that CNTs may carry currents as high as 10^9 A/cm². Current densities of 10^8 A/cm² have been observed in the lab. In comparison, most common metals achieve current densities of 10^5 A/cm². [3] Research in SWNTs demonstrates that defects in the CNT adversely impact their electrical conductivity and the growth process is an important variable in controlling defect rates.

Serious challenges also exist in establishing electrical contacts between the ends of CNTs in order to preserve the low conductivity properties. Some experiments suggest that methods of establishing electrical contact may be feasible albeit at a lower overall conductivity than for a single CNT. [2, 3] Table 1 tabulates thermal and electrical properties of CNTs versus some common metals.

Theory suggests an achievable thermal conductivity of 6000-6600 W/(m K) in MWNTs though to date experimental values have fallen far short. Baughman reports a measured conductivity of 3000 W/m K while Coleman reports a high of 200 W/m K. [3, 5] This disparity indicates how much CNT properties may vary depending on manufacturing process, impurity level, alignment, grouping, and end connections and demonstrates the need to precisely control manufacturing of CNTs.

Table 1: Theoretical and reported electrical properties of CNTs vs. common materials.

| Material | <u>Electrical Resistivity</u> ($\Omega \cdot m$) | <u>Electrical Conductivity</u> (S/m) | <u>Current Density</u> (A/cm ²) | <u>Thermal Conductivity</u> k (W/m K) at 20°C | Ref |
|-----------------------|---|---|--|---|-----------|
| Reported SWNT | - | - | 10E9 | 200 | [3, 6] |
| Theoretical MWNT | - | - | 10E9 | >6600 | [5, 7, 8] |
| Reported MWNT | - | - | 10E7 | 200-3000 | [3, 5] |
| CNT Spun Yarn | - | 3E4 | - | - | [9] |
| Stainless Steel (304) | 7.2E-7 | - | - | 16.2 / 21.4 ^b | [10] |
| Aluminum | 2.8E-8 | 3.5E7 | - | 250 | [11] |
| Aluminum (5456-H112) | 5.9E-8 | 1.7E7 | - | 116 | [12, 13] |
| Aluminum (6061) | 4.3E-8 | 2.3E7-2.5E7 | - | 154 | [13, 14] |
| Copper | - | 5.8E7 | - | 399 | [11] |

^aThe first set of numbers is measured on graphite parallel to the grain and the second set is measured perpendicular to the grain.

^bMeasured at 100/500°C

^cMeasured at 600°C

Mechanically, CNTs also exhibit exciting characteristics. Theoretically, the stiffness of a single CNT should be on the order of 1 TPa and some experiments have observed a stiffness exceeding 1 TPa. Accompanying this impressive stiffness, some experiments have measured a CNT strength of 63 GPa, making CNTs one of the stiffest and strongest materials known. The low density of CNTs also offers the potential of very strong and stiff materials that are lighter than equivalent structures made from other materials. However, these values represent the upper bound found over several experiments and a wide variation in observed values has been found. It is believed that defects and lattice structure effect the stiffness and strength significantly though much

research is needed to better characterize CNTs. [2, 5] Table 2 provides a summary of some of the ranges of theoretical properties and observed properties for CNTs.

| Material | E (GPa) | σ_t (GPa) | ρ (g/cm ³) | Density Normalized Strength σ_t/ρ | Toughness (J/g) | Ref |
|--|--------------|--------------------------|--------------------------------|--|-----------------------|----------------|
| Observed SWNTs | 1000-1470 | 3-750 | 1.3-1.4 | 2100-58000 ^a | 770 | [2, 5] |
| Arc Discharge MWNTs | 270-950 | 11-63 | - | | ~1240 | [5] |
| CVD-MWNTs | 12-450 | 4 | - | | - | [5] |
| CNT Spun Yarn | - | .460 ^b | .8 | 575 | 14/20/11 ^c | [9] |
| CNT Spun Yarn Sheets | - | .233 / .875 ^b | .5 | 465 / 175 ^d | - | [15] |
| CNT Coagulation Spun Polymer 60% weight | 80 | 1.8 | - | 65 | 570-870 | [5, 9, 15, 16] |
| Stainless Steel (304) | 193 | .621 | 8.03 | 77 ^a | - | [10] |
| High Strength Steel (for High Speed Naval Craft) | - | .49-.62 | 7.83 | 62.58-79.183 | - | [17] |
| HY-80 Steel | 205 | .552 | 7.87 | 70 ^a | - | [18] |
| Aluminum (5456-H112) | 70.3 | .31 | 2.7 | 115 ^a | - | [12] |
| Aluminum (6061) | 68.9 | .241 | 2.7 | 89 ^a | - | [14] |
| PBO | 169 | | 6.2 | | | [19] |
| "S" Class Glass FRP | 18.8 | .357 | 2.491 | 143 ^a | - | [20, 21] |
| Carbon Fiber | 227 | 3.8 | | | | [19] |
| E-Glass | 74 | 3.5 | | | | [19] |
| Silicon Carbide | 280-450 | .35-.65 | 3-3.2 | 109-217 ^a | - | [11] |
| M5 Sample (2001) | 271 | 3.56 | | | | [19] |
| Kevlar ^e | 22.7-112 | .386-3.6 | 1.44 | 268-2500 | 33 | [20, 21] |

Table 2: Comparative properties of CNT with selected materials

^aThese values are derived from the ultimate strength and density.

^bThese values were derived from the Density Normalized Strength and Density

^cToughness values are for singles yarn, two-ply yarn, and PVA infiltrated singles yarn

^dThe first value measures a sheet consisting of aligned fiber layers. The second value is for a composite sheet composed of biaxially aligned layers.

^ePBO stands for poly(p-phenylene-2,6-benzobisoxazole)

^fFor Kevlar, the disparity in Young's Modulus and Tensile Strength come from discrepancies between the ABS rules for High Speed Naval Craft and the DuPont technical guide for Kevlar. The low values in Kevlar ranges come from the ABS standard. The National Research Council's study of high strength composites reports values for Kevlar between the extremes of the ABS rules and the DuPont guide.

1.3 The Potential of Carbon Nanotubes and the Challenges

Considering only theoretical values, CNTs would seem a wonder material with low density, high strength, high stiffness, and excellent thermal and electrical conductivity. However, as shown in Table 1 and pictorially demonstrated in Figure 2, theoretical values have rarely been achieved in experiments and a great deal of difficulty has been experienced in scaling CNT properties for use in macroscale structures. It is presently unknown if all of the scaling challenges can be overcome. While the full properties of the individual CNT may not be achieved in macroscale structures, research activity does demonstrate that progress has been made in addressing some of the challenges and properties of CNT composites may one day surpass present day composites such as CF/epoxy composites.

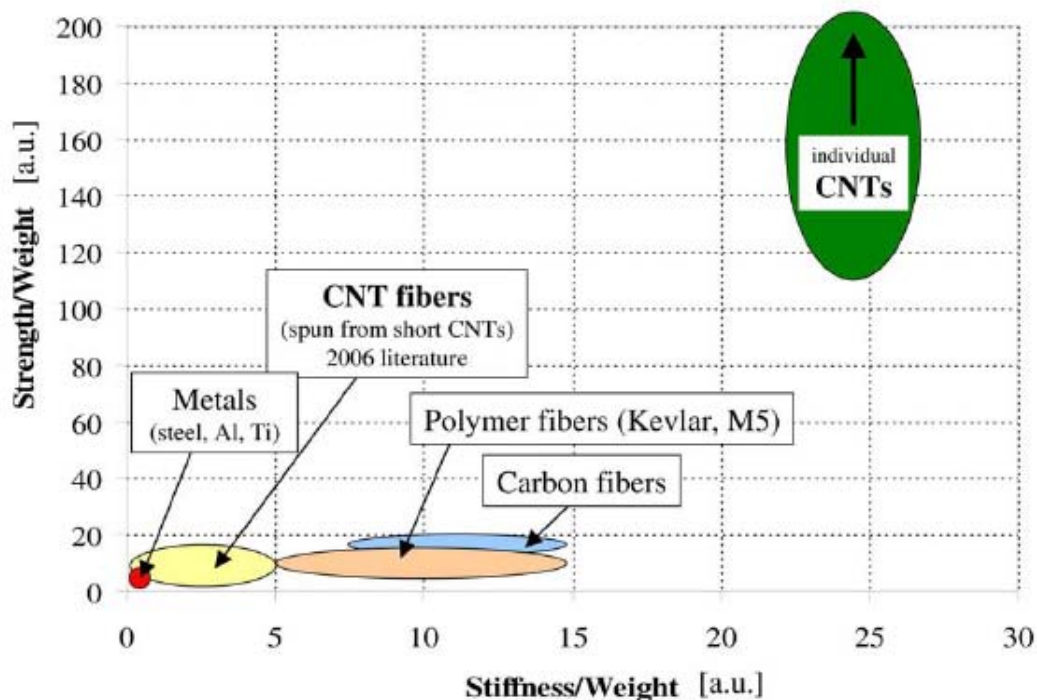


Figure 2: Comparison of normalized strength and stiffness of CNTs with common materials

[2]

Challenges include:

- Growing SWNTs and MWNTs in either forests or in isolation depending on the application.
- Dispersing the harvested CNTs in composite matrices.
- Controlling defect density and chirality of CNTs.
- Maximizing the length of grown CNT fibers.
- Lowering production costs.
- Increasing Production Rates
- Integrating CNTs into devices with good electrical and thermal contact to CNTs

The challenges are great but so is the potential payoff. Dr. John Hart notes that,

“Individual molecular chains boast similarly exceptional properties as CNTs, and the great challenge is in assembling these chains in to macroscopic materials which exhibit nanoscale properties. However, CNTs offer unique promise here because unlike many other molecules, CNTs can grow to macroscopic lengths.” [2]

The recent appearance of CNT augmented flat screen technology, CNT augmented batteries, and CNT plastics for electromagnetic (EMI) shielding demonstrate that commercialization of CNTs is feasible and that research continues to be warranted despite the challenges.

1.4 Current Production Methods of Carbon Nanotubes

Several methods exist to reorganize carbon compounds into CNTs or to 'grow' CNTs from a carbon containing precursor molecule. Some processes involve the use of a metal catalyst to provide an initial growth site and all of the techniques require elevating temperatures to supply the energy of formation. Techniques include arc discharge, laser ablation, thermal chemical vapor deposition (CVD), flame conversion of carbon in an ethylene, oxygen, and argon mix, microwave irradiation of carbon, catalytic gas phase pyrolysis, and many other methods.[2, 3]

CVD is already widely used in industry for other applications and CVD operates at lower temperatures and lower costs than methods such as arc discharge and laser ablation. There have been many demonstrations of CNT growth by CVD. Commercially available MWNT at ~\$100/kg are made by CVD. All of these factors suggest that CVD will be the most promising route to industrial scale production of CNTs. This thesis focuses on enabling the characterization of CNT growth mechanisms via CVD in a particular configuration known as a CNT 'forest'. [2-4, 22]

1.4.1 Limitations of Standard, Static Thermal Chemical Vapor Deposition Tube Furnaces

CVD, a common practice in the chemical engineering discipline and an accepted method of depositing thin films for the semiconductor industry, comprises a class of processes that involve the introduction of a volatile chemical known as a precursor into a furnace region. Energy supplied to the furnace region promotes the adsorption and/or decomposition of the precursor onto a substrate at temperatures inside the furnace up to a limit of 1200 C for the typical CVD furnace. The precursor decomposes and a portion of the dissociated precursor binds to the substrate while the remainder leaves the site as waste product.

A properly prepared substrate can be used to define the adsorption areas via catalyst application and thus control the locations of growth. To produce CNT, an appropriate catalyst and precursor are chosen, and, as precursor material passes the adsorption sites, a carbon nanotube 'grows' from the site as shown in Figure 3.

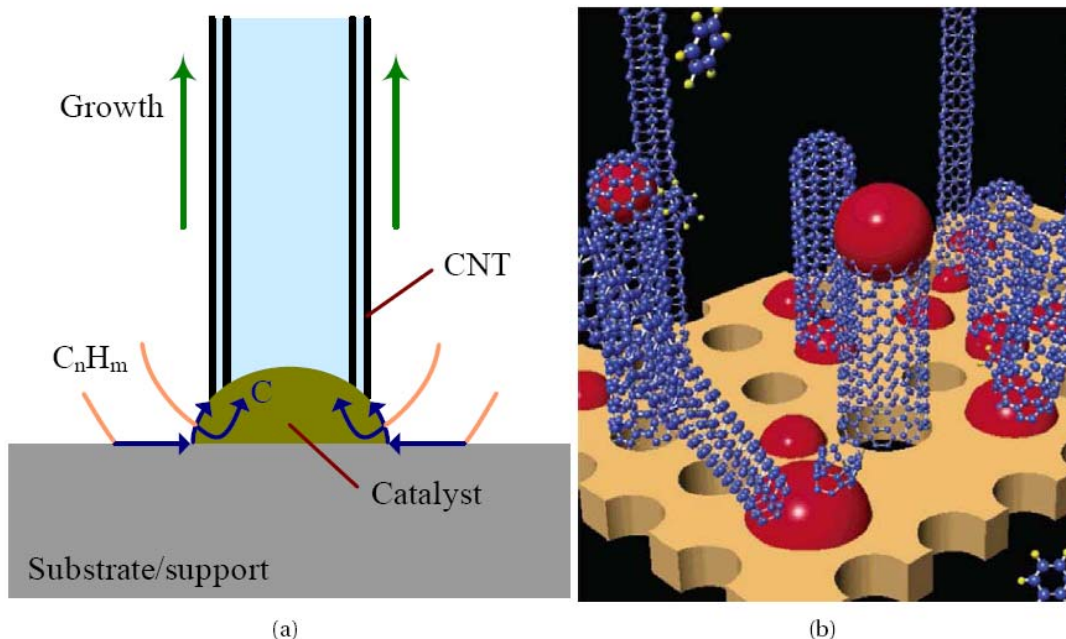


Figure 3: Schematic of CNT growth via CVD

- (a)** A carbon containing precursor molecule adsorbs at the catalyst site on the substrate. The precursor molecule decomposes and the carbon atom binds to the catalyst along with other carbon atoms. The carbon atoms bind into a carbon nanotube and either grow up from the catalyst (shown here) or the nanotube grows between the catalyst and the substrate, lifting the catalyst away from the substrate.
- (b)** A cartoon depicting both nanotube growth mechanisms described above. [2, 23]

A range of reactor vessels can be used to perform CVD. A common laboratory-scale and industrial-scale CVD reactor is a tube furnace, where the reaction is conducted inside a sealed tube. Often heated using an external resistive heater coil, a typical configuration, shown in Figure 4, might place a tube made of a non-reactive material such as quartz inside an insulated enclosure containing coils which encircle the quartz tube. Prior to introducing the precursor, the tube is flushed with gas and the heating coils heat the furnace reactor region to produce a zone of elevated temperature inside the quartz tube. Additional flow control elements and heating zones may be used to pretreat the precursor agent(s) prior to arrival in the reactor tube.

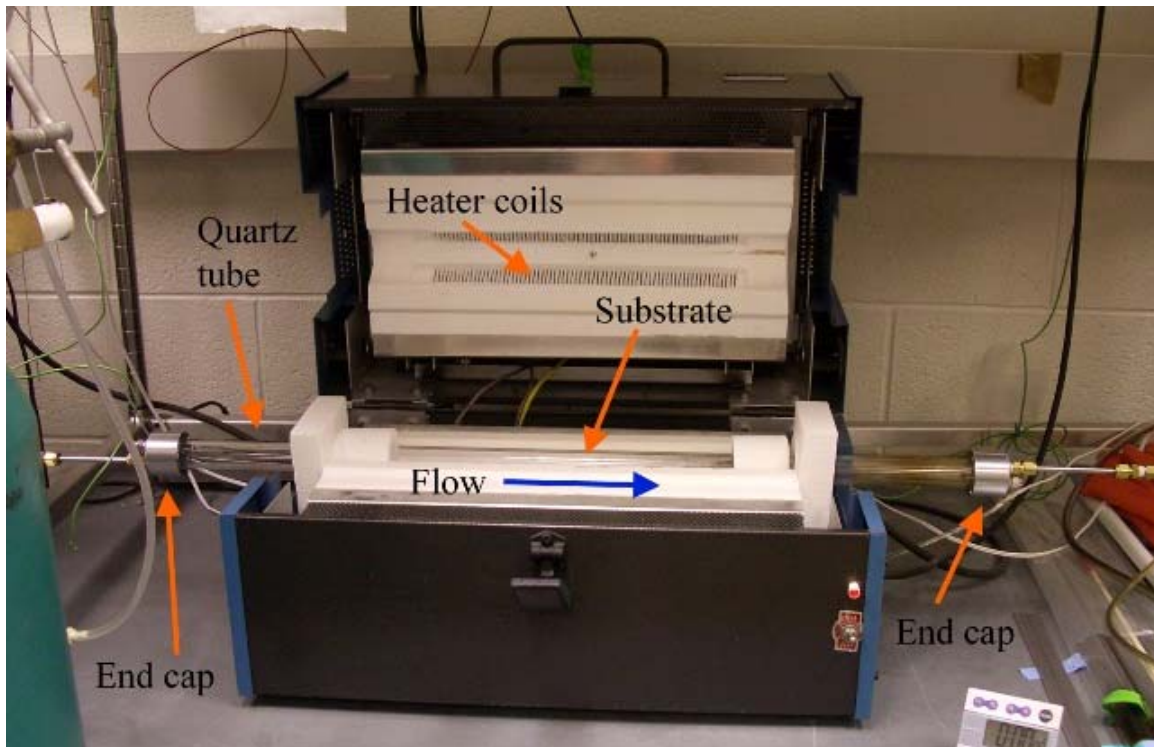


Figure 4: A typical basic CVD tube furnace
The VWR Lindberg system costs approximately \$2300, representing the current entry level cost for a CVD system.

Growth of CNTs within tube furnaces has shown great promise in the production of CNTs. However, existing tube furnace designs limit the researcher's ability to fully separate critical parameters such as temperature and flow profiles. Additionally, the use of heating elements external to the reactor zone necessitates the heating of a large thermal mass, precluding the ability to rapidly vary the reactor zone temperature profile spatially and temporally. In essence, the external heaters provide energy to a region with a diameter on the order of centimeters while CNT growth occurs at the substrate on the order of millimeters for length and on the order of nanometers for the CNT diameter.[2]

The existing tube furnace designs also limit the ability to optically access the reactor region and the growth site, limiting the ability to observe and measure

the reaction *in situ*. These constraints complicate the ability to experiment with and characterize the many variables that govern the synthesis of nanostructures such as CNTs

More advanced tube furnace designs, employing multiple heater arrays to create separately heated zones, automated mass flow controllers, automatic sample loading, and computer reporting of temperature and flow profiles, are available to the researcher at substantially higher prices but do not address the fundamental thermal and optical limitations of the basic design.[24, 25]

Part Two: Carbon Nanotube Furnace and Appliance Designs

2.1 CVD Furnace Material Requirements

While the basics of the chemical process to produce CNTs are known, the nuances and details remain to be investigated. It is known that current techniques require high operating temperatures at the substrate growth site, commonly in the 700-1200°C range for thermal CVD. Most common CVD operations also occur in a reducing environment (e.g. H₂). Finally, it is desirable to maintain a clean environment within the reaction chamber and to eliminate trace quantities of unknown gases from material outgassing at high temperatures. This is essential for reliable control of process variables and for repeatability.

The requirement for a reducing environment necessitates a means to seal the reaction chamber from the external environment and to purge the reactor

internals. Some thermal CVD applications and most CNT growth processes require the use of flammable and explosive gases which furthers the urgency to maintain a barrier to oxidizing agents entering the reaction chamber when these gases are present and to prevent leaks of hazardous agents into the lab.

2.1.1 The Temperature Challenge

The process temperatures of up to 1000 C at the substrate preclude the use of most conventional electrical and sealing materials. Many materials suitable for use at high temperatures may still outgas some chemicals which could interfere with the quality of CNT growth. Other materials simply melt or lose their shape and elasticity. For instance, most standard electrical wiring insulation melts and outgases at temperatures above 120 C though some commonly available insulated wiring may be used at temperatures up to 260 C. Table 3 provides a list of some common materials and their suitability and Table 4 summarizes the strength, thermal, and electrical properties of some suitable materials.

Thermal inertia also affects the CVD growth process. In order to experiment with different heating profiles, a low thermal mass should be employed within the CVD reactor. A low thermal mass also shortens the experiment cycle time by allowing the system to cool faster, enabling the researcher to remove samples and begin a new growth experiment sooner.

Van Laake and Hart propose a prototype suspended resistive heater to lower thermal mass. Initial thermal modeling of the prototype system by Van

Laake and Hart demonstrated that a silicon substrate with stainless steel electrodes would not exceed 500 °C at the electrode to substrate interface. This provides a rough temperature design limit for any materials selected.[26]

| <u>Material</u> | <u>Suitability</u> | <u>Typical Use</u> | <u>Requirement Conflicts</u> |
|--------------------|--------------------|--|---|
| Brass | Unsuitable | Valve Fittings | Ignites Acetylene |
| Solder | Unsuitable | Electrical Connection | Low Melting Point (<350°C) |
| Copper | Unsuitable | Electrical Connection | Ignites Acetylene |
| Low Alloy Steel | Unsuitable | Structural | Hydrogen Corrosion |
| Glass (Pyrex) | Unsuitable | Viewing Window | Lower Temperature Resistance and higher thermal expansion than Quartz |
| Silicon | Suitable | Substrate, Substrate Heater | None |
| Stainless Steel | Suitable | Structural, Electrical Conductor | None |
| Aluminum | Suitable | Structural, Heat Sink, Electrical Conductor | May not be exposed to full process temperature |
| Quartz | Suitable | Viewing Window, Reaction Chamber | None |
| Nickel | Unsuitable | Electrical Conductor | Decomposes Hydrocarbons; Forms toxic gas in CO atmosphere |
| Ceramics (general) | Suitable | Thermal Insulation, Electrical Insulation, Structural | None |
| Alumina | Suitable | Electrical Insulation, Structural Support, Gas Routing and Treatment | |
| Fiberglass | Suitable | Thermal Insulation, Electrical Insulation | May not be exposed to full process temperature |
| Kapton | Suitable | Thermal Insulation, Electrical Insulation | None |
| Viton | Suitable | Sealing Technology | May not be exposed to full process temperature |

Table 3: Material suitability

| <u>Material</u> | <u>Yield Strength</u> (MPa) | <u>Density</u> (g/cm ³) | <u>Service Temperature Limit</u> (°C) | <u>Thermal Conductivity</u> (W/(m·K)) | <u>Electrical Resistivity</u> (Ω·cm) | <u>Ref</u> |
|--------------------------|--------------------------------|--|--|--|---|------------|
| Quartz | 6.8 | | 1500 | 1.2 - 2 | > 10 ² | [27] |
| 99.8% Alumina | | 3.91 | | 8.2 | | [28] |
| Firebrick | | 1.9-2.1 | > 1300 | 1.3 ^a | | [11] |
| Silicon Wafer | | | | | 2-30 | [29] |
| 304 Stainless Steel | 621 | 8.03 | | 16.2 / 21.4 ^b | 7.2E-5 | [10] |
| Aluminum (6061) | | | | 154 | 4.32E-6 | [13, 14] |
| Aluminum | | | | 250 | 2.8E-6 | [13] |
| Fiberglass Wire Sleeving | | | 482 | | | [30] |

Table 4: Selected material properties

^aMeasured at 900°C

^bMeasured at 100/500°C

2.1.2 The Chemistry Challenge

The growth of CNTs and general CVD operations occur in high temperature, reducing environments. Various chemical species such as hydrogen (H₂), ethylene (C₂H₄), acetylene (C₂H₂), methane (CH₄), etc may be used for a specific CNT process or for general thermal CVD. Therefore, all materials selected must show good corrosion/degradation resistance in this environment and must not produce an unsafe condition. Table 3 provides a list of some common materials and their suitability.

The use of acetylene in some typical CVD processes prohibits the use of common materials such as copper and brass within the reaction chamber or

within the gas stream since acetylene can ignite upon contact with copper. This precludes the use of copper for thermal transport or in wiring and precludes the use of standard brass fittings.

Hydrogen (H_2) may also be used in many thermal CVD processes and is used in many CNT growth processes. H_2 , when present at a significant partial pressure and high temperature, can attack carbon steels. The H_2 will remove the carbon to produce methane. This embrittles the steel, potentially causes cracking, and introduces methane to the process environment. Figure 5 shows limit curves for various steels at a given temperature and H_2 partial pressure. A particular steel listed in Figure 5 can be used without risk of hydrogen corrosion if the operating conditions are below and to the left of the respective curves. [31] Since the typical CNT growth process occurs around $800^{\circ}C$ ($\sim 1500^{\circ}F$), materials in the CVD reactor will be at risk of H_2 attack if they are allowed to reach this temperature with even the smallest H_2 partial pressures. At $500^{\circ}C$ ($\sim 932^{\circ}F$), metals are safe below .6 MPa of H_2 partial pressure. Therefore, the designer must carefully match material selection to expected temperature and pressure profiles.

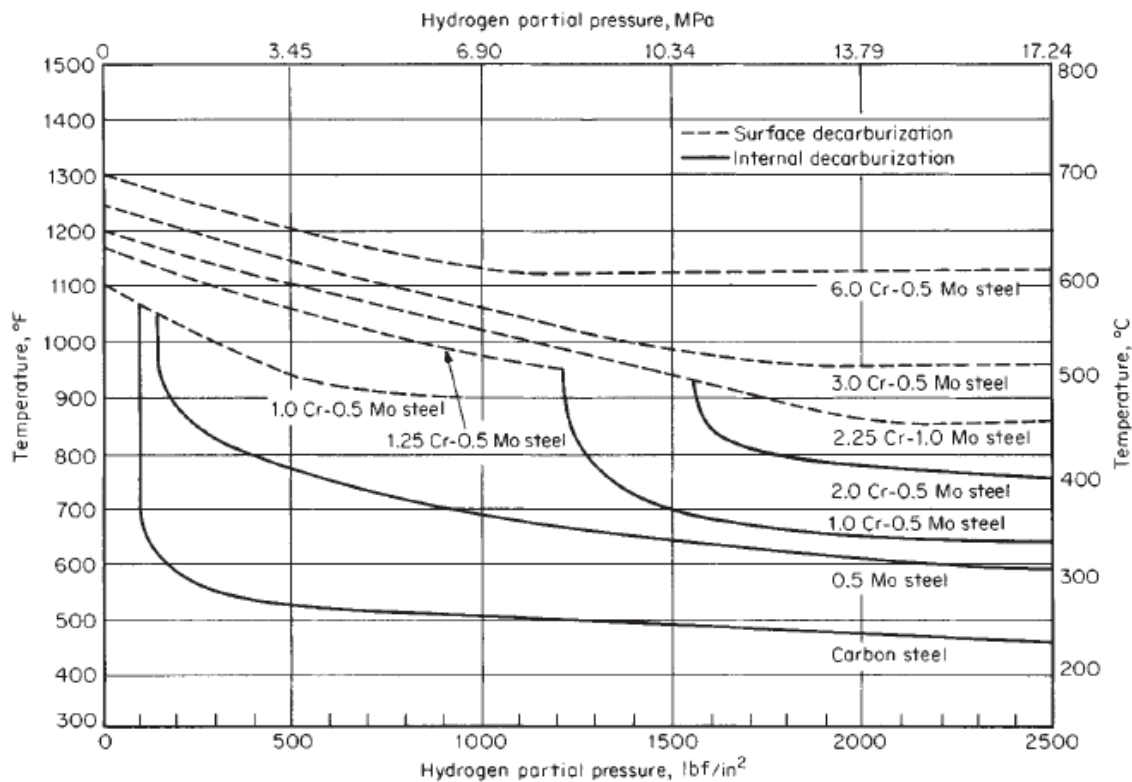


Figure 5: Hydrogen corrosion limits for various steels
[31]

Nickel serves as a catalyst for decomposing many hydrocarbons and is therefore unsuitable for use in the reactor or gas stream. At best, sooting of the reactor would occur and at worst, toxic nickel carbonyl could be formed if a carbon monoxide (CO) atmosphere were ever present.

2.1.3 The Flammable Gas Challenge

Both hydrogen (H_2) and ethylene (C_2H_4) are commonly used in thermal CVD growth of CNTs. Both gases may ignite or explode under the proper circumstances. Hydrogen requires an oxidizer such as air to be present. At high pressures (> 17 MPa) and temperatures above $350^\circ C$, ethylene may ignite without an oxidizer present. [31, 32]

Table 5: Flammability of hydrogen and ethylene

| Chemical Compound | Lower Flammability Limit % v/v | Upper Flammability Limit %v/v | Autoignition Temperature °C |
|---|-----------------------------------|----------------------------------|--------------------------------|
| Ethylene | 2.7 | 36 | 490 |
| Hydrogen | 4 | 75 | 400 |
| Flammability Limit refers to the percent volume of the gas that must be present for ignition to occur | | | |
| Autoignition is the temperature at which the compound is known to ignite in air though compounds have been known to ignite at temperatures lower than the reported Autoignition temperature | | | |

[31]

In order to ensure safe operation, the design must ensure a gas tight seal to prevent explosive gases from leaving the reaction chamber and to prevent oxygen (air) from mixing with the flammable gases. The design also requires a purge capability to remove oxygen from the reaction chamber and gas lines prior to introducing flammable compounds.

The minimum safety requirements would provide a purge capability. The reaction chamber must always be purged and prior to opening. The next level of protection would provide a temperature display to indicate when temperatures sufficient to produce ignition are present within the reaction chamber. Continuing safety improvements would require gas sensing and temperature interlocks. An outer chamber would provide a final level of security. Each level of safety produces additional costs and integration challenges.

2.1.4 The Electrical Challenge

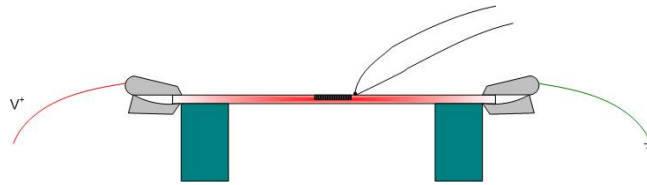
Electrical currents in the milliamp (mA) range passing through the body can kill a person. An individual's bodily resistance may vary considerably based on genetics, current body chemistry, whether the person is sweating, the parts of the body in contact with the electrical source, etc. Generally, a direct voltage of over 30 V should be considered as hazardous and life-threatening in the worst case. The reactor will operate with power sources capable of 100 V_{DC} and potentially up to 10 A of current. Therefore, the reactor could kill the operator if electrical contact is made.

To prevent a hazardous condition, all electrical connections must be suitably insulated or covered. In some cases, electrical interlocks, warning lights, or warning signs may be required.

2.2 SabreTube: A Flexible, Low-Cost Desktop Thermal CVD System

As discussed in section 1.4.1, a need exists to redesign the basic CVD furnace in order to reduce thermal mass and enable optical observation in a convenient, low cost package accessible to as many research groups as possible. Lucas van Laake, Anastasios John Hart and Alex Slocum developed a prototype heated platform CVD furnace. This section details the next step in the evolution of the suspended heater tube furnace prototype proposed by van Laake et al.¹[33] The basic configuration of the suspended heater platform is shown in Figure 6.

¹ The SabreTube was designed and developed with Dr. A. John Hart



**Figure 6: Schematic of example CVD system
suspended heated platform**

2.2.1 Customer Requirements

Numerous discussions with John Hart, Luuk Van Laake, Alex Slocum and Onnik Yaglioglu as well as my observations of CNT growth procedures in the laboratory led to the list of traits required for a low cost, basic research level desktop CVD system shown in Table 6. While the focus of my research group was on expanding the selection of means to measure and characterize nanotube growth and to enable the researcher to decouple the gas and temperature variables in order to better understand the CNT growth process, the intent of these design traits is to produce a CVD system that enables research in many reactions and annealing processes as well as CNT growth.

Table 6: Required design traits for a basic desktop CVD system

| Traits | Importance | Purpose |
|---|-------------------|---|
| Low Thermal Mass | High | Enable rapid temperature changes during operation |
| Resistively Heated Substrate | High | Decouple Ggas temperature from reaction site temperature; build upon prior research with resistive heating |
| Electrical Access to the Substrate | High | Enables resistive heating |
| Substrate Heater Power of 0-10 A, 0-100 V _{DC} | Medium | Past experiments used ≈ 50 V _{DC} at 3 A. Range permits flexibility in experimentation. (assumes silicon used for the substrate resistive heater) |
| Optical Access (top, side, bottom) | High | Allow optical and non-contact measurement and characterization of in situ growth (i.e. IR sensing, hi speed photography, and Laser displacement sensing); Allow non-contact manipulation of the growth site (i.e. laser); |
| Non-Contact Temperature Measurement | High | Reduce work required in attaching thermocouples at growth site; Reduce potential sources of sample contamination |
| Process Gas Preheater | High | Process gas conditioning to enable nanotube growth |
| Flexibility in means to provide gas to the Reaction chamber | Medium | Allows for testing different gas profiles and delivery paths. |
| Flexible Sensor Mounting | High | Provide means to accommodate different sensing methods to maximize research utility |
| Reaction Chamber Temperatures ≤ 1000 C | High | Research to date suggests a temperature of ≈ 800 C to promote good CNT growth. 1000 C limit provides room for experimentation. |
| System Operating Pressure | Medium | Slight Vacuum to Atmospheric Pressure |
| Easy Substrate Loading | Medium | Save time and labor for the researcher. |
| Adequate Heat Dissipation at Electrode Contact Points on the Substrate Heater | High | Prevent thermal failure of electrical contacts |
| Low Cost | High | Lower the barrier to entry into nanotube research |
| Electrical Safety | Critical | Prevent electrocution |
| Gas Safety | Critical | Prevent flammable gas ignition |

2.2.2 Process Variable Decoupling

Many variables including the temperature at the reaction site, the temperature pretreatment of the precursor gases, catalyst choice, precursor gas

choice, etc are thought to affect the growth mechanism and defect rates of CNTs. The number of variables creates a large design space to explore and decoupling the variables is essential to a successful exploration of the design space. Figure 7 depicts the design requirement to decouple temperature process variables.

In the typical tube furnace, the precursor gases are heated as they flow across the entire heating zone. It is desired to be able to independently heat the precursor gas to control the gas decomposition and then to separately heat the reaction site to control the catalyst temperature.[34]

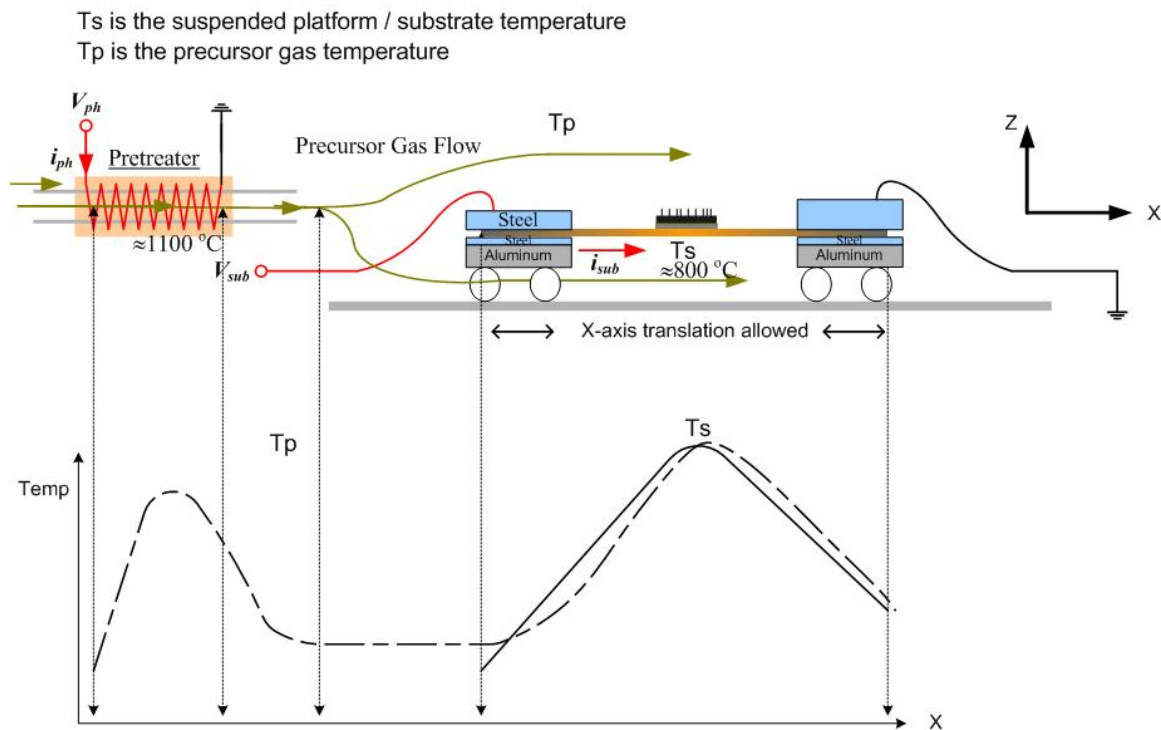


Figure 7: Decoupling gas and reaction site temperature profiles
The figure shows how removing the external heating coils used in the basic CVD furnace enables different temperature profiles for the Precursor Gases and the Reaction site. Since the gas is no longer dependent on residence time in the tube furnace for preheating, gas flow rates may also be varied.

2.2.3 Optical Characterization of Carbon Nanotube Growth

In order to enable IR sensing, photography, laser sensing, and other sensing methods, materials capable of passing wavelengths in the infrared and visual spectrum must be used. Quartz is a typical reactor tube material and is highly IR transparent.[27]

X-Ray scattering requires a different material as Quartz interferes with the X-ray beam. Custom quartz tubes fitted with Kapton windows may be used when employing X-ray scattering.[35]

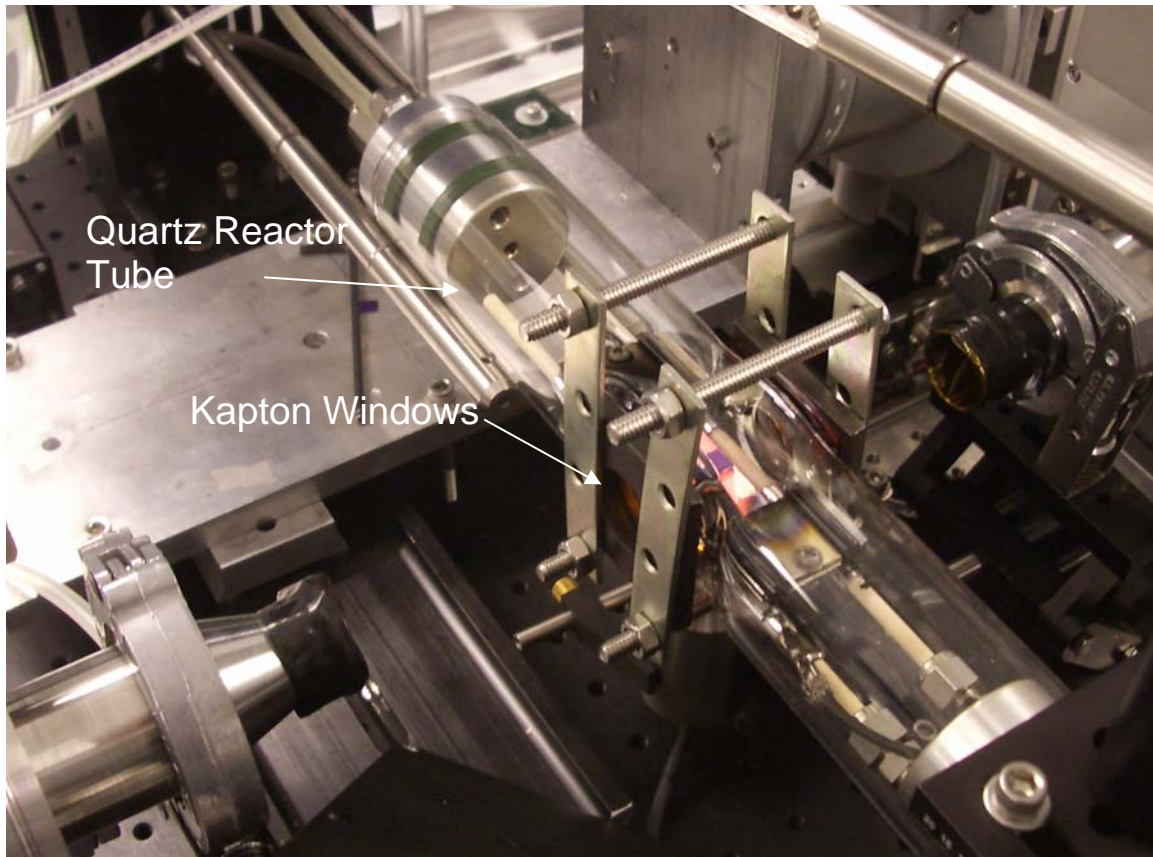


Figure 8: Custom quartz tubes fitted with Kapton windows for X-ray scattering

2.2.4 Design Philosophy

The SabreTube is intended to enable research by many groups in order to enable the rapid characterization of the process variables that control the growth of CNTs, to improve the level of knowledge of CNT growth dynamics, and to enable rapid process discovery. To meet this goal, the SabreTube would have to be available at a relatively low cost but provide more functionality than the basic tube furnace.

In order to control costs, the decision was made to utilize off the shelf components whenever possible and to minimize the number of custom components required. Where possible, common materials vice exotic materials were used and, if the option existed, less expensive components were selected.

Ease of use and ease of reconfigurability also empower the researcher. Modular and standard connectors (1/4-20 and #8-32 size screw holes) were used throughout the design and fixtures were designed to allow degrees of freedom in positioning instrumentation. Space was reserved around the quartz tube of the furnace to maximize optical sight lines and to maximize the space available for mounting experimental equipment and sensors not sold as part of the SabreTube basic package.

Finally, it was desired to keep the footprint of the system small to enable space constrained research groups to use the SabreTube and to allow the SabreTube to be transported to be used with immovable equipment. For instance, after construction, the SabreTube was taken to Cornell and mounted in

an X-ray beamline in order to characterize *in situ* growth of CNTs by small angle X-ray emission (SAXS).

2.2.5 System Design and Specifications

Complete technical drawings and electrical schematics for the SabreTube are in Appendices A and B. The following sections describe the SabreTube system with illustrative graphics and pictures.

2.2.5.1 SabreTube General Description

The SabreTube (Figure 9) is a system for conducting chemical vapor deposition (CVD) and catalytic chemical vapor deposition (CCVD) within a reactor vessel designed to allow for separate heating of precursor fluids and of the reaction growth site. (Figure 7) The precursor fluids (gases or liquids) are routed separately or jointly through pretreatment zones and any associated heaters to enter the reactor chamber through any of the sealable pressure ports and into the reactor tube. Within the tube, a suspended platform is used to provide a low thermal mass to enable rapid change in the temperature of the reaction surface. The reaction surface can be integral to the suspended platform or resting on or attached to the suspended platform. For instance, if a silicon wafer is used as the platform, a portion of the silicon wafer may be coated with catalyst to provide a growth site for nanostructures such as CNTs or a separately treated silicon wafer could be placed on top of the silicon heating platform. (Figure 6, **Figure 10**, Figure 11)

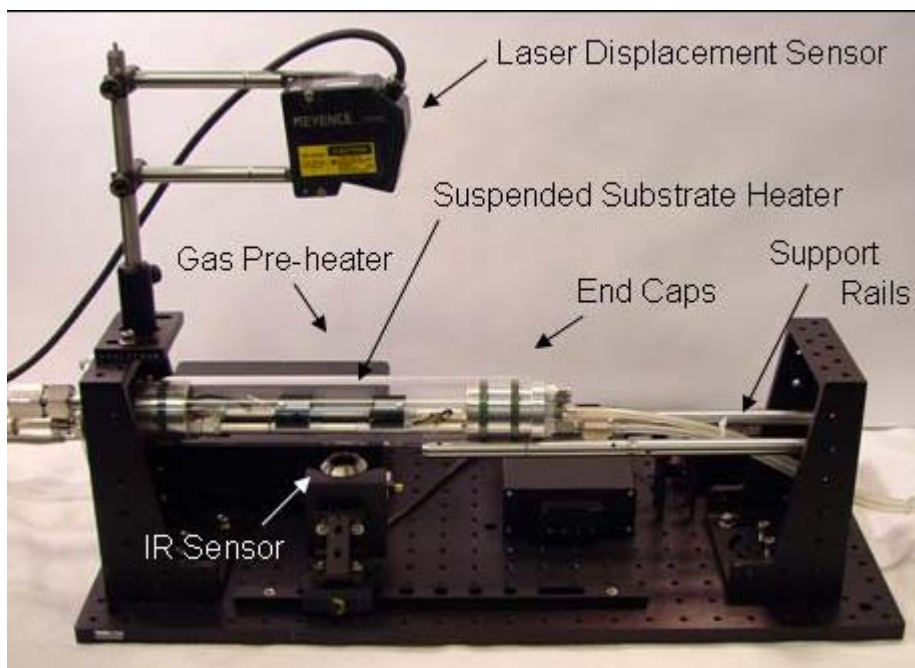


Figure 9: The SabreTube system including preheater and laser displacement sensor options



Figure 10: Schematic of example CVD system suspended heated platform where the platform is coated to permit CNT growth



Figure 11: Schematic of example CVD system suspended heated platform with separate coated substrate

The reactor chamber consists of a quartz tube for the main body and machined aluminum end caps to provide pressure sealing and to route power and fluid services to the inside of the reactor. Each aluminum end cap uses two Viton lip seals to provide a sealing surface between the quartz tube and the end cap. The end caps fit inside the quartz tube, allowing the user to observe the lip seal compression as the end cap is inserted and during operation. The design

also permits the quartz tube to be easily slid off of the front end cap to enable easy access to the reaction site for loading and unloading of samples. (Figure 12, Figure 13, Figure 17)

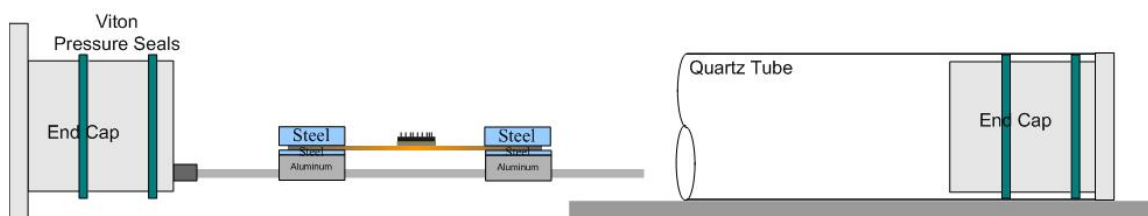


Figure 12: Schematic showing the SabreTube open for loading
Note the dual rings of pressure seals on the end caps and the tube retraction to permit access to the substrate sample.

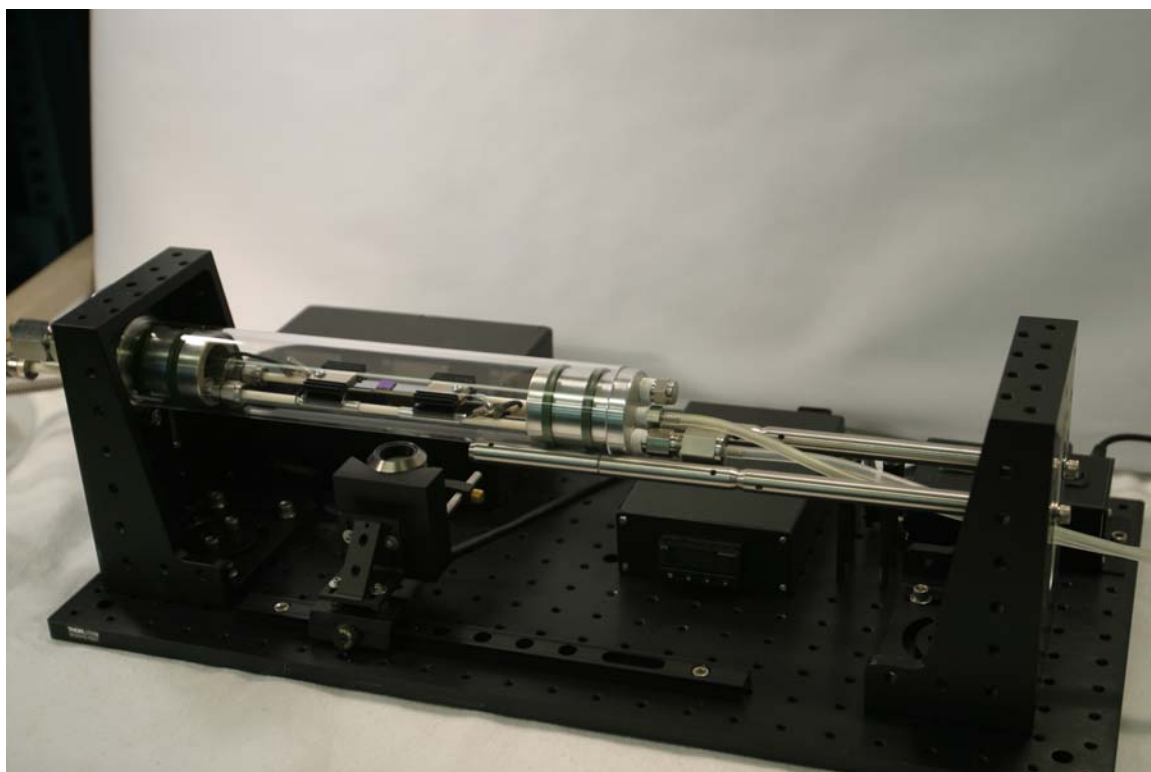


Figure 13: SabreTube without optional laser sensor

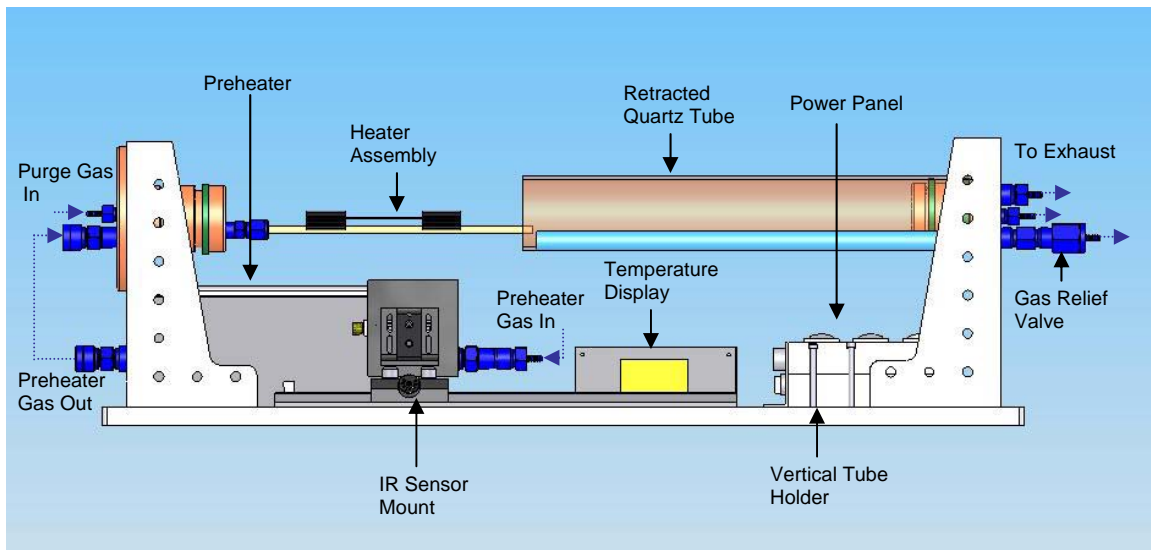


Figure 14: Solidworks front view of the SabreTube system with the quartz reactor tube retracted

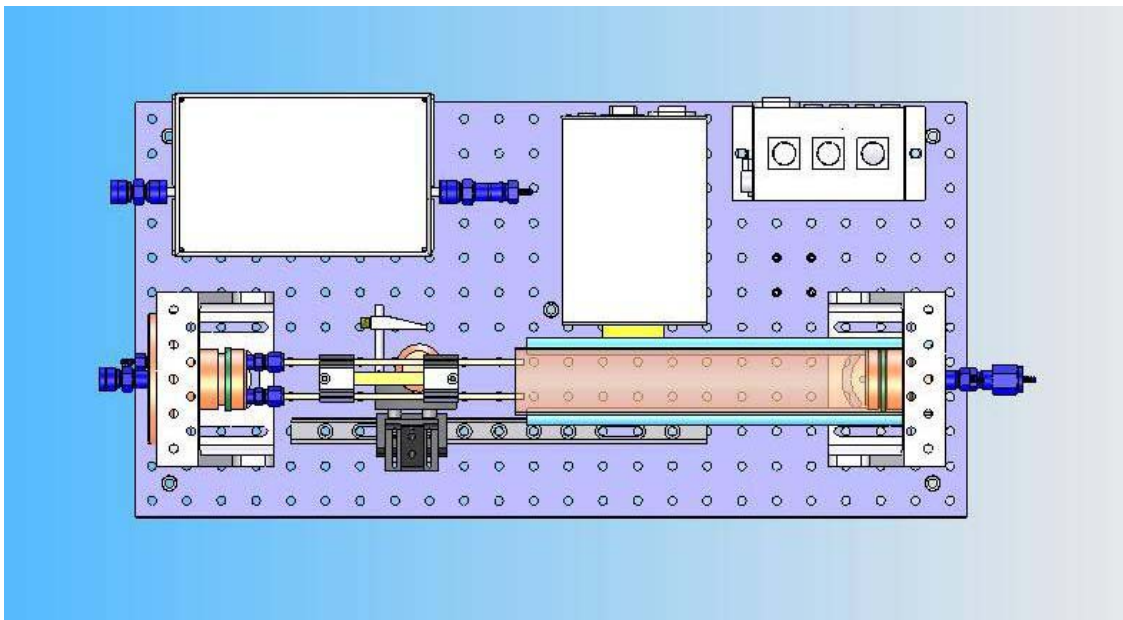


Figure 15: Solidworks plan view of the SabreTube system

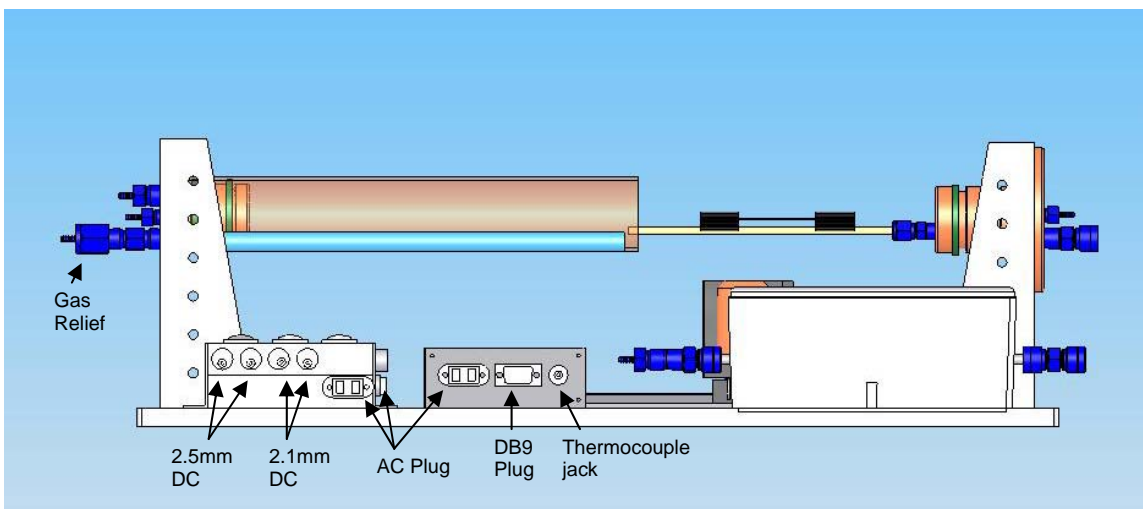


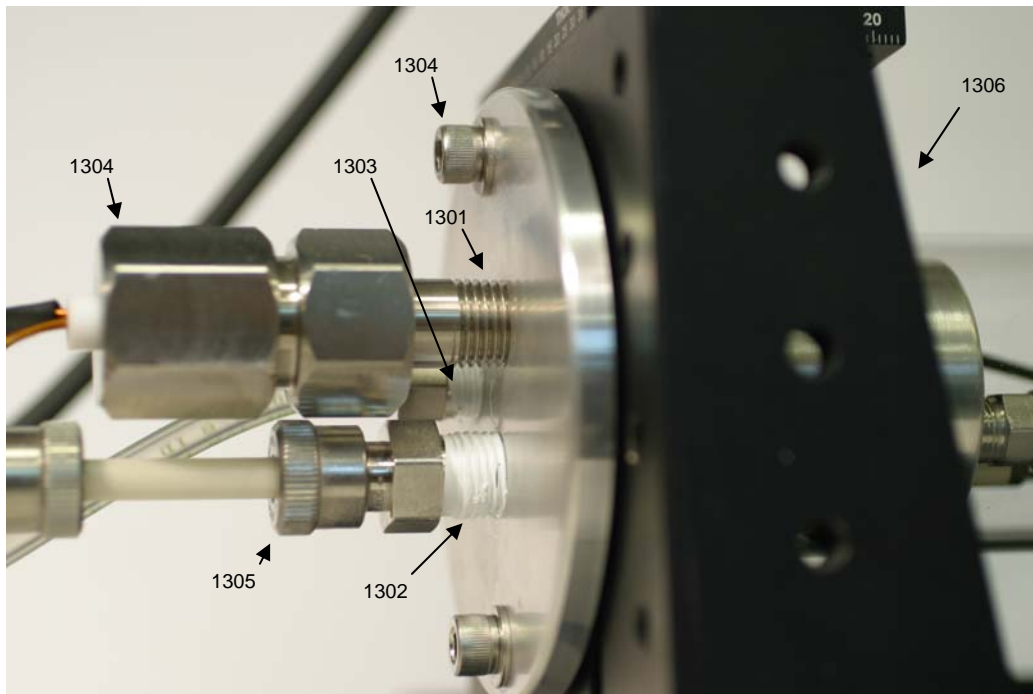
Figure 16: Solidworks back view of SabreTube system

The 'front' end cap, (Figure 17) contains three pass through ports consisting of two ¼" NPT interfaces (1301, 1302) and one 1/8" NPT interface (1303) on the external face of the end cap. To route two heater power lines and two K type thermocouple lines, a Conax-Buffalo pressure tight power sealing gland² (1304) attaches to one of the ¼" NPT female threads on the external face of the front end cap. A ¼" tube adapter to ¼" NPT Swagelok pressure fitting (1305) attaches to the second ¼" NPT female port on the external face of the front end cap to permit routing of precursor fluids to the reactor. The 1/8" NPT female port (1303) on the external face of the front end cap may be used to route additional precursor or purge fluids or is blanked when not used. On the reactor side face of the front end cap, two 3/16" tube adapter to 1/8" NPT Swagelok fittings are used to hold 3/16" alumina rails (Vesuvius McDanel Ceramics). These fittings are used to provide an easy means of changing out alumina rails in the event of breakage and for changing the extension length of the rails into the reactor quartz tube. The two alumina rails, spaced .98 inches apart (center to

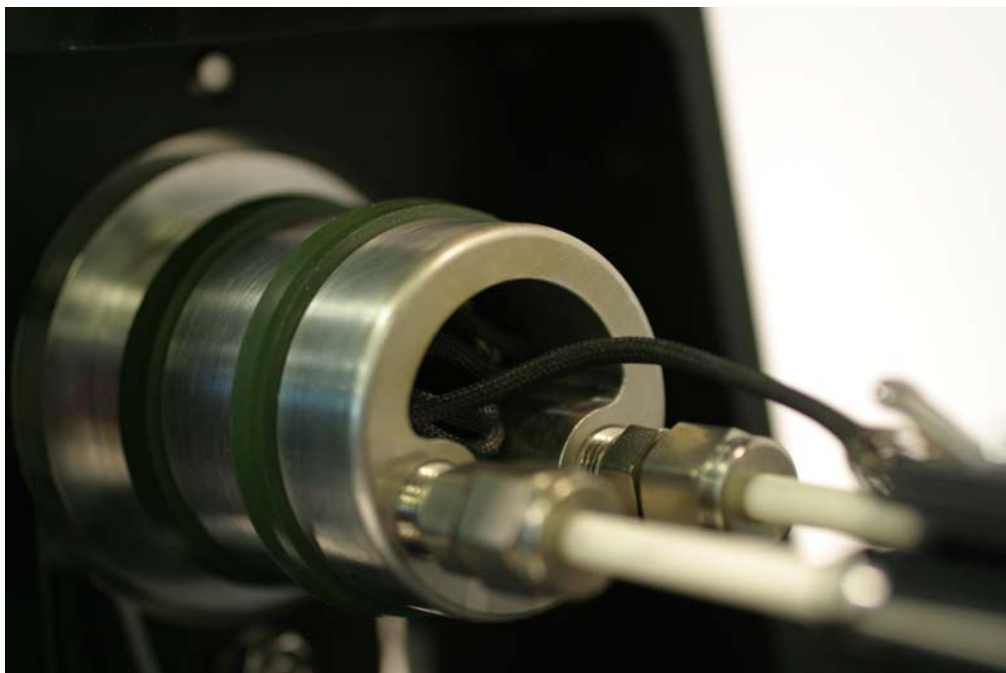
² Exact part number is provided in Appendix C.

center) on a horizontal plane, extend along the axis of the reactor tube to provide an electrically insulating cantilever support for the heating mechanism and substrate. (Figure 17)

Four two inch aluminum tubing sections of .222" inner diameter and .25" outer diameter are slid over the alumina rails to form the four corners of a planar rectangle to provide mechanical support and electrical contact for the heating mechanism atop the alumina rods. One electrical power line consisting of 18 AWG alumel wiring with a fiberglass insulating sleeve is routed to one of the two aluminum tubing sections that define the edge of the rectangle closest to the front end cap. This wire attaches to the tubing via a flat-toothed stainless steel alligator clip. The second electrical power line routes to one of the aluminum tubing sections that define the edge of the planar rectangle furthest from the front end cap. Together with the substrate and its mount, the aluminum tubing sections serve to form a complete electrical circuit. Two of the four aluminum tubing sections are not electrical contacts but ensure level mounting of the substrate on the alumina rails. The aluminum tubes can be easily slid along the alumina rails to accommodate different substrate lengths. Steel 'E' clips hold the insulated electrical wiring against the alumina rails. (Figure 18)



(a)



(b)

Figure 17: Front end cap

(a) Front end cap Viton lip seals and alumina rail mounting

(b) Front end cap showing one power feed through connection, two gas feed through connections, and two rail mounting holes.

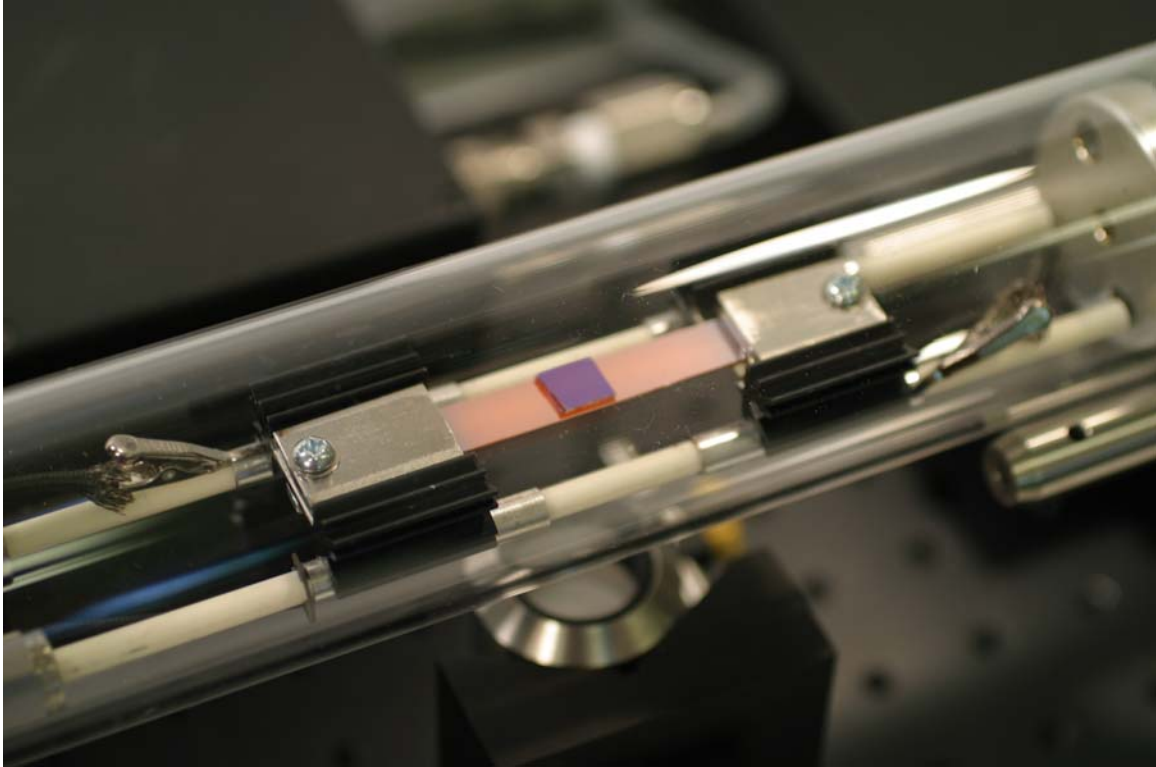


Figure 18: Substrate heater mounted between heat sinks and heating a silicon wafer

Black anodized aluminum heat sinks (Aavid Thermalloy 63620) mount atop the aluminum tubing sections. The aluminum heat sinks are modified to have $\frac{1}{4}$ " radius cuts along the undersides to fit smoothly on the aluminum sleeves. This limits lateral motion while permitting the heat sinks to slide longitudinally on the aluminum tubes to provide thermal stress relief due to substrate thermal expansion during heating. (Figure 19) A .03" polished 304 stainless steel plate rests on top of the heat sink flat. The narrow edge of the substrate, typically a .3 mm thick by 10 mm wide by 50 mm long piece of silicon wafer in our implementation, is held between this flat steel plate and a $\frac{1}{8}$ " thick 304 stainless steel bar. A screw, spring washer, and nut compress the two stainless steel bars, the substrate heater, and the heat sink together to improve electrical contact and hold the substrate heater in place. (Figure 20) Removal of

the anodization along the radial cuts and along the top surface of the heat sink produces a low resistance electrical path from the aluminum tube sleeves to the .03" steel plate. The insulating alumina rail ensures that the only electrical path between the heat sinks is through the suspended platform.



- (a) (b) (c)
- Figure 19: Modified aluminum heat sinks**
- (a) Underside of the modified aluminum heat sink. A 1/4" ball end mill is used to make two cuts spaced 1.0115" apart along the length of the heat sink.
 - (b) Top of the modified aluminum heat sink. The anodization has been removed from the top flat to improve electrical contact.
 - (c) Profile of the modified heat sink showing the spacing of the radial cuts.

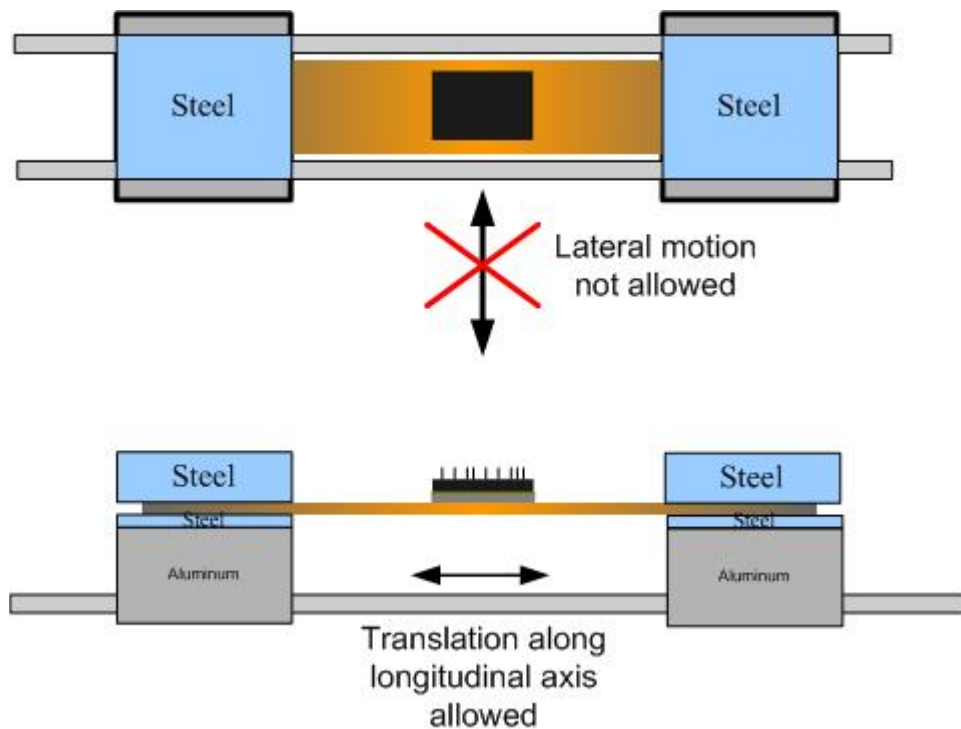


Figure 20: Aluminum heat sink modification permits thermal expansion along the tube axis.

When closed, the reactor assembly, consisting of the quartz tube, the two end caps, the alumina rails, and the heat sink and heating assembly with the substrate, is held in place by the front end cap. Mounted by two screws to a ninety degree bracket (Thorlabs) modified with a pass through hole, the front end cap can provide full support to the reactor assembly. (Figure 12, Figure 13, Figure 17) However, to minimize bending stresses on the quartz tube which can cause unequal pressure on the lip seals, two ½" aluminum rails extend from a second (Thorlabs) ninety degree bracket to provide two lines of contact to the quartz tube near the rear end cap. These aluminum rails also serve as a linear guide and support for use when opening and closing the quartz tube to access the interior. When sliding the quartz tube back from the front end cap, the

aluminum guide rails aid the user in smooth operation of the tube to avoid hitting the heater assembly. The guide rails extend far enough to allow the quartz tube to rest securely atop them while the user accesses the substrate. (Figure 21) The aluminum rails may be built up of sections to allow for tailoring the rail length to various applications.³ (Figure 23) The ninety degree angle bracket for the rear end cap contains slots to allow for adjusting the height of the aluminum rails via a hex bolt or for removing the aluminum rails. The rear bracket also contains a slot to allow for the passage of service lines to the rear end cap. (Figure 22)

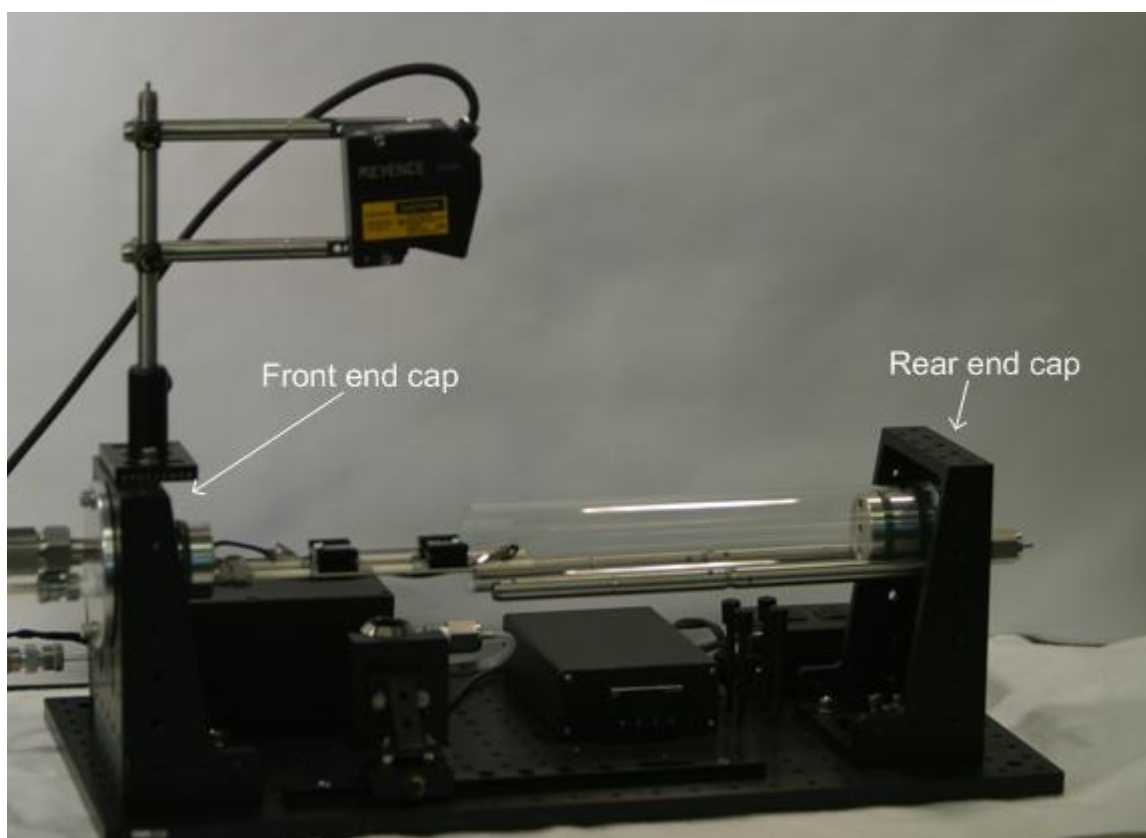


Figure 21: Quartz tube retracted and at rest on aluminum guide rails, affording easy access to the reaction site and substrate heater for sample loading.

³ For instance, in order to perform x-ray scattering experiments, a special quartz tube with flat kapton windows was installed. The location of the windows required the ability to shorten the aluminum rails while the reactor was open and then lengthen the rails when the reactor was closed.

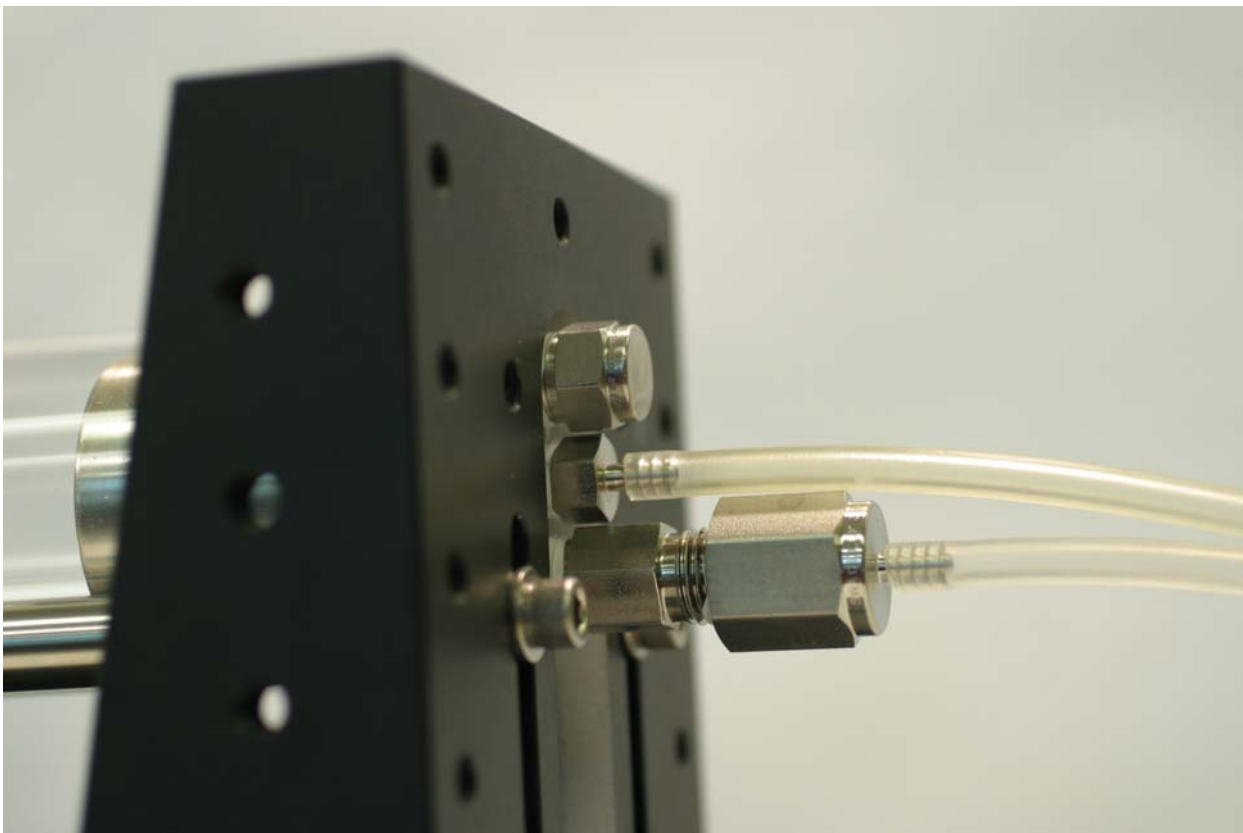


Figure 22: Modular rear right angle bracket with slots for adjusting aluminum rail heights and for passing gas lines

The rear end cap fits inside the quartz tube and seals via two lip seals. Two holes pass through the end cap to route the precursor and purge gases to one or more exhaust lines which lead to an exhaust hood. The two gas routing holes contain 1/8" NPT female threads to allow the connection of modular fittings. If only one gas routing hole is used, the second may be fitted with a plug. In this implementation, one of the gas routing holes is fitted with a 1/8" NPT male hose barb. A third fluid access path with a 1/8" NPT female thread is fitted with a Swagelok 1/8" NPT check valve rated to .3 psi to guard against reactor tube overpressure. (Figure 23) In the event of an overpressure, the check valve relieves to a tygon tube that is routed to an exhaust hood. The reactor process

employed typically occurs about .1 psi above atmospheric and is governed mechanically by a bubbler fluid level on the gas output line. With a 48 mm tube inner diameter, an internal pressure of .3 psi corresponds to 4.4 N or 1 lbf against the end cap, ensuring the check valve will relieve before the end caps eject except under a sudden pressure pulse condition.



Figure 23: Rear end cap with two gas flow lines and one pressure relief check valve and sectioned aluminum guide rails

Both ninety degree angle brackets are mounted to a 12"x24"x1/2" aluminum pegboard (Thorlabs) via 1/4-20 hex head screws such that the reactor tube axis is parallel to the long axis of the pegboard. The aluminum pegboard, built for standard optical mountings, contains 1/4-20 holes spaced one inch apart along the length and breadth of the pegboard to permit modular fixturing. Under

the reactor tube, a 12" dove tail rail holds a slide with a v-clamp (Thorlabs). The v-clamp holds an infrared (IR) temperature sensor (Exergen). The slide allows for positioning the IR sensor along the tube axis and a slotted angle bracket that holds the v-clamp to the slide permits positioning the IR sensor along the axis perpendicular to the tube axis. The v-clamp itself allows for adjusting the focal distance from the IR sensor head to the substrate. (Figure 24)

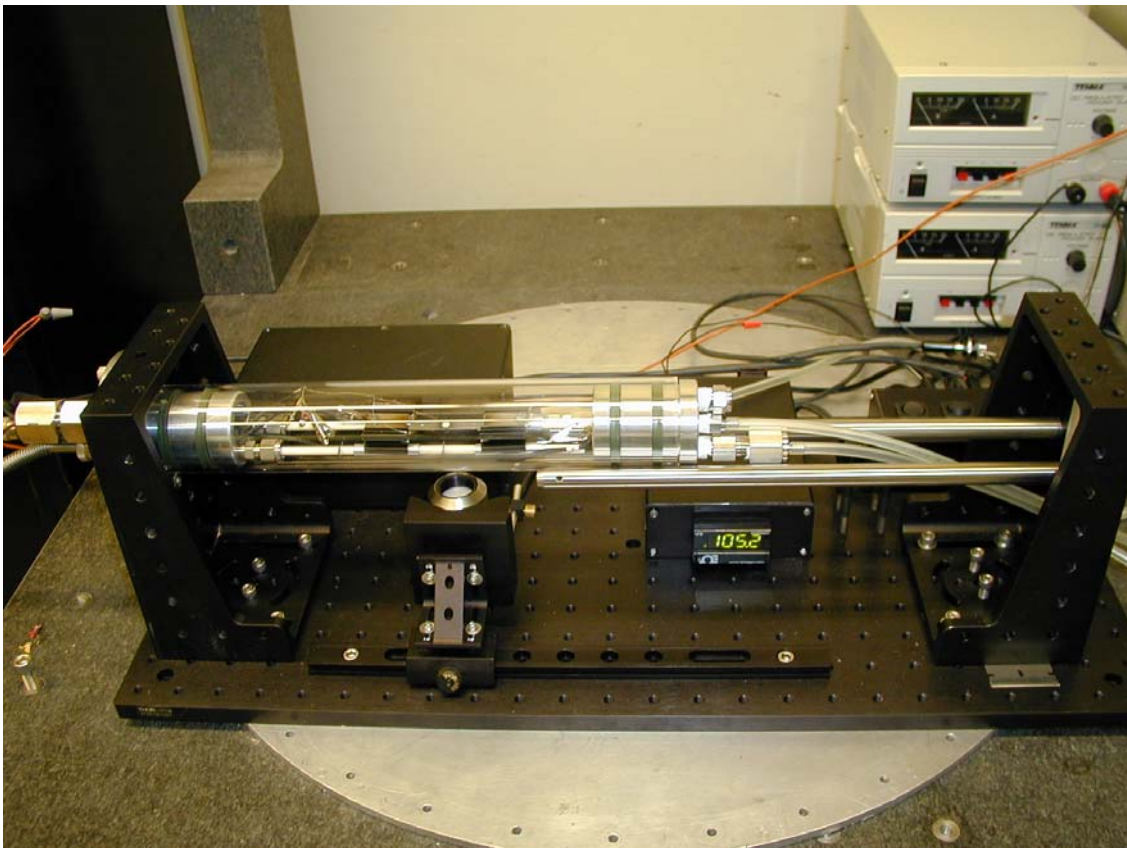


Figure 24: Aluminum mounting pegboard and adjustable IR temperature sensor

Behind the reactor tube brackets, when looking from right to left from the front of the reactor system, a power panel, a vertical tube holder, and a temperature display are mounted to the pegboard. (Figure 14, Figure 25)



Figure 25: Quartz tube in the resting vertical position on the vertical tube holder

The power patch distribution panel provides a single place for the user to ascertain the power status of the reactor system. A variable DC power supply plugs into the rear of the power panel and the power panel routes power to the wires for the power sealing gland on the front end cap via a single position single throw (SPST) switch. DC plugs for the substrate heater use 2.5 mm ID and 5.5 mm OD lockable jacks. 120 V AC wall power plugs into the power panel and routes power to the temperature display and controller via a 20 mm, 100 mA fuse and a SPST switch. The power panel is constructed from a standard die cast anodized aluminum flanged enclosure but ABS (plastic) may also be used for the housing. All interfaces are panel mounted. (Figure 16) Electrical schematics can be found in Appendix B.)

The vertical tube holder exists to provide a secure resting place for the tube at times when the user wishes to adjust the horizontal rails or perform other actions where the user is concerned about impacting the horizontally mounted tube. The tube holder consists of four rubber tipped ¼-20 hex head bolts that form a snug fit with the inside of the quartz tube. (Figure 25)

The temperature display / controller enclosure, made of extruded aluminum, may also be constructed from ABS. The enclosure houses an Omega i32 temperature display and controller with the display mounted so that it is perpendicular to the aluminum pegboard plane and is viewable from the front of the reactor system during operation. The rear of the enclosure holds a panel mounted AC jack, a 2.1 mm ID / 5.5 mm OD DC style jack with type K thermocouple wiring for interfacing to the IR sensor or the thermocouples, and a 9 pin D-sub miniature female jack to permit R232 interface between the i32 temperature display and a computer. (Figure 16)

In general, fluids are routed to the CVD system via separately procured flow controllers. High-purity tygon tubing from the flow controllers connects to a male hose barb fitted to ¼" tube adapter Swagelok Ultra-Torr fitting. A flexible ¼" stainless steel hose mates to the Swagelok fitting. The other end of the stainless steel hose connects to a Swagelok Ultra-Torr ¼" tube adapter to ¼" male NPT that fits to the front end cap to route gases to the reactor tube. Two inlet connections on the front cap allow for routing two separate gas lines to the reactor tube if desired. The user may also opt to use one of the pass through holes on the front end cap to hold a rigid or flexible pipe to route gases to a

specific point within the reactor as shown in (Figure 26). If this option is used, the user would route the purge gases to a separate port to ensure the hollowed region of the front end cap is fully purged prior to opening the reactor tube.

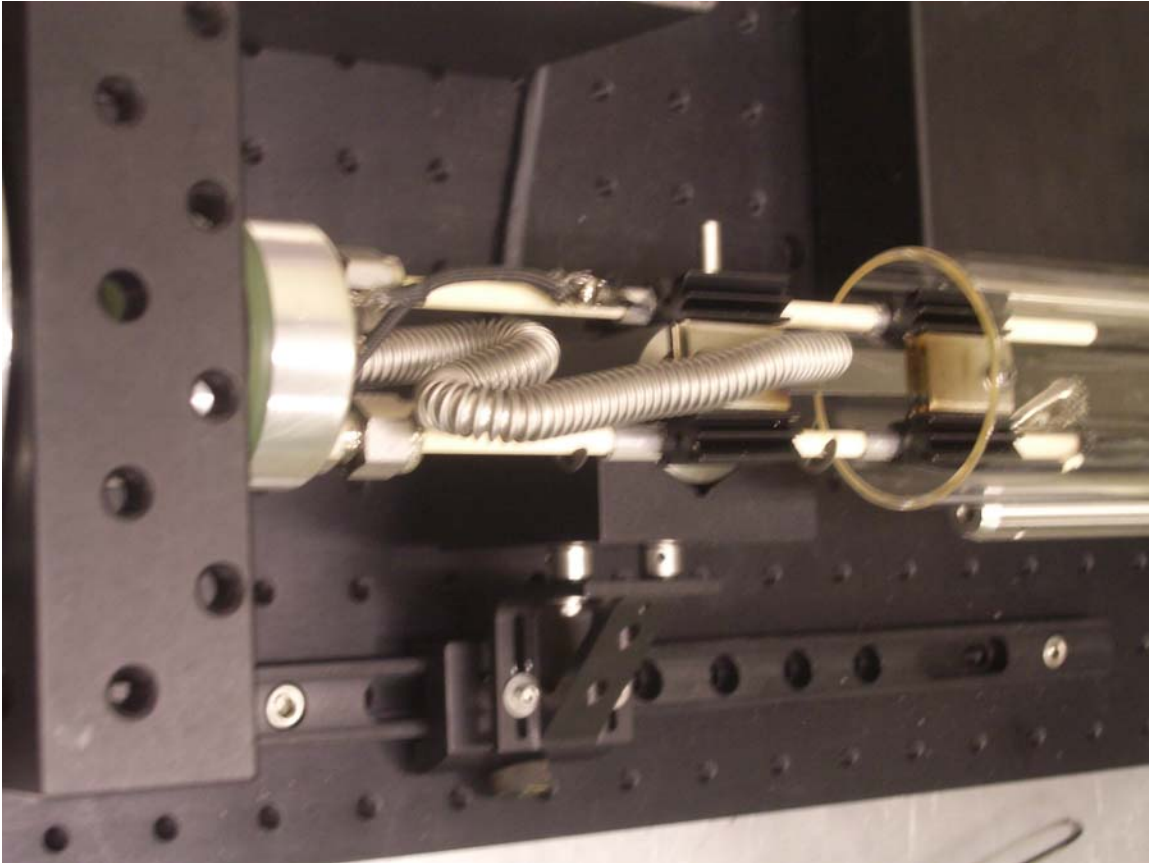


Figure 26: Retractable quartz tube enables easy installation of a stainless steel pipe for routing gas flow

An optional gas preheater assembly may also be mounted on the aluminum pegboard to the left of the temperature display and behind the ninety degree angle bracket that holds the front end cap. The preheater assembly consists of a die cast aluminum enclosure, a rectangular fire brick cut in half with a 1 inch hole drilled parallel to the long axis of the brick. A coil of 30 AWG alumel heater wire is wrapped around a $\frac{1}{4}$ " quartz or alumina heating tube. A variable DC power supply under voltage control provides power to the preheater via a 2.1

mm ID / 5.5 mm OD DC jack and SPST switch on the power patch panel. (Figure 27) A Swagelok Ultra-Torr ¼" tube adapter to ¼" male NPT connected with a ¼" NPT to male hose barb fitting on the inlet side of the heater tube provides a pressure sealed connection for routing inert purge gases and precursor gases to the preheater via tygon tubing. The outlet side of the preheater tube utilizes a Swagelok Ultra-Torr ¼" tube adapter to ¼" tube adapter to connect to a stainless steel flexible hose with ¼" tube ends on either end. The stainless steel hose connects to a Swagelok Ultra-Torr ¼" tube adapter to ¼" male NPT that fits to the front end cap to route gases to the reactor tube.

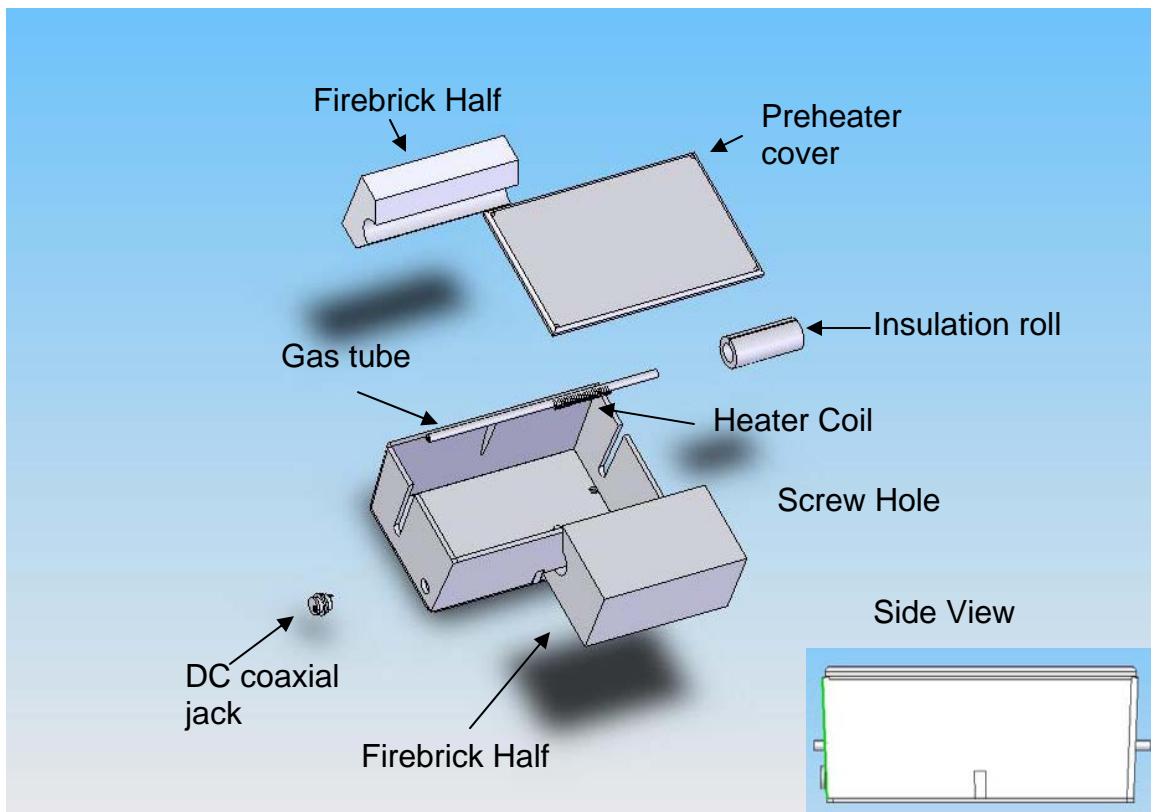


Figure 27: Exploded 3D Cad drawing of the preheater assembly

The modular fixture holes on the angle brackets enable the mounting of an optional laser displacement sensor. A base plate with an adjustable post (Thorlabs) mounts atop the front end cap right angle bracket. The adjustable post allows adjustable positioning along the front to back axis (perpendicular to the tube) of the aluminum pegboard and connects to a ½" post holder. An eight inch round aluminum post (Thorlabs) extends vertically up from the post holder to provide the required height for the laser displacement sensor. Two ½ inch diameter aluminum posts (Thorlabs) extend horizontally from the vertical post and over the reactor tube. Two right angle mounting adapters (Thorlabs) slide over the 8 inch vertical post and the horizontal posts and enable degrees of freedom about the longitudinal axis of the vertical post and along the longitudinal axis of the horizontal mounting posts. Machined flats with a series of 8-32 screw holes on the ends of the horizontal posts permit the mounting of a Keyence LKG 152 laser displacement sensor at an angle of 8.5° to the vertical. (Figure 28, Figure 29)

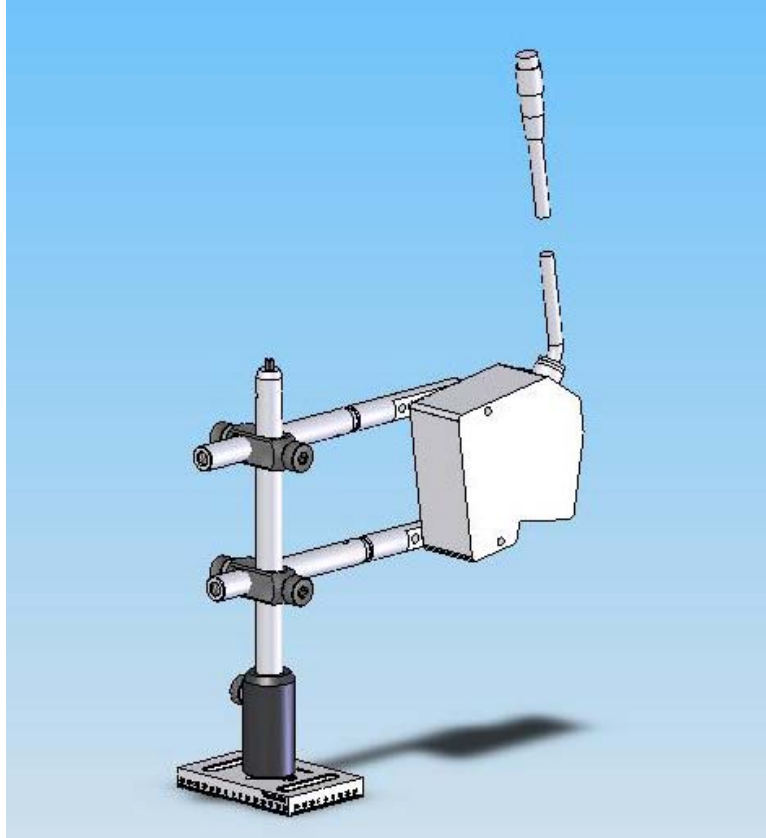


Figure 28: Optional laser displacement sensor and fixture

Additional means of heating the suspended platform such as laser heating may be used due to the presence of modular fixturing outside the quartz tube. (Figure 30) Depending on the method used, windows may need to be fitted to the quartz tube or the user may need to use a different material tube.

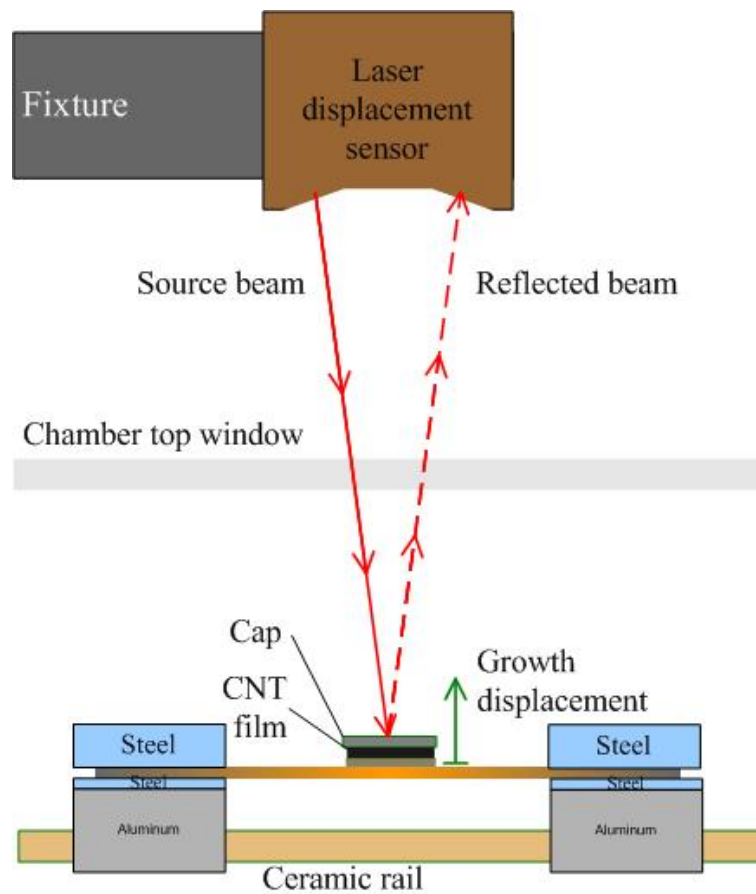


Figure 29: Schematic of *in situ* measurement of CNT film thickness

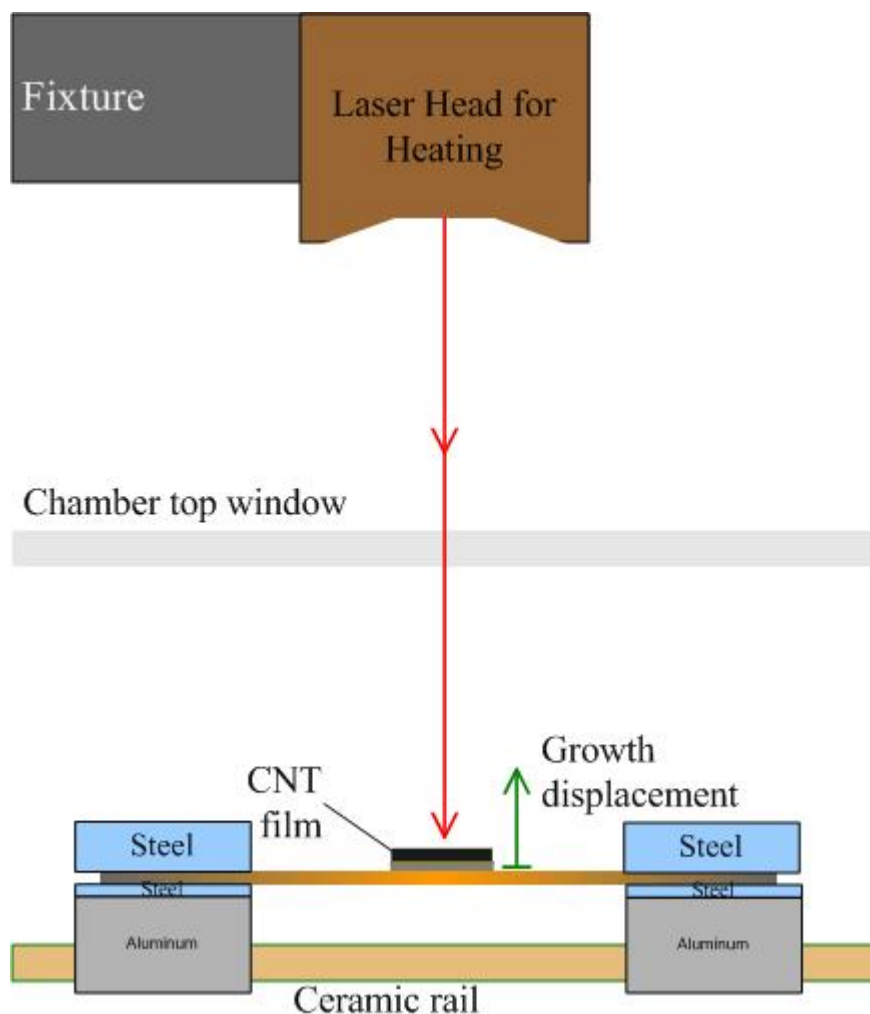


Figure 30: Laser heating of reaction surface

2.2.5.2 Substrate Heating

The basic heating method proposed by van Laake et al. [33] was adapted for use in the SabreTube. Van Laake, using a silicon wafer clamped between steel blocks, found via modeling and experimentation that the steel electrodes remained below 500°C over a wide range of currents and process temperatures up to 1000°C.[33]

For the SabreTube, the steel blocks were thinned to minimize thermal mass by replacing the top steel piece with .125" thick AISI 304 stainless steel

and the bottom steel piece with .03" thick AISI 304 mirror polished stainless steel. The full surface area of the mirrored side of the .03" thick stainless steel plate rests on an extruded aluminum heat sink. The aluminum heat sink (Figure 31) uses extruded radial fins to maximize surface area and black anodization to improve emissivity to maximize heat transfer through the heat sink.

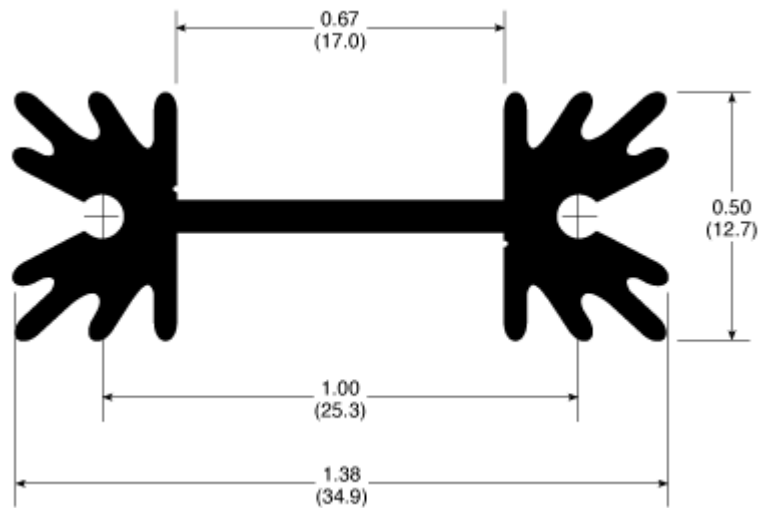


Figure 31: Profile of the Aavid Thermalloy heat sink used in the SabreTube
This heat sink, cut to one inch long, has a thermal resistivity of 17.17°C/W in the as bought condition.[36]

The heat sink, whose construction is explained above on page 42, enables the heater assembly to passively relieve thermal stresses produced by thermal expansion.

Current flows through a wire to an aluminum tube to the heat sink to the steel plate and along the flat silicon wafer. The current then exits the wafer via the steel plates and aluminum heat sink at the far end of the wafer. Silicon has an electrical resistivity that is greater than four orders of magnitude higher than aluminum and stainless steel, and the silicon acts as a resistive heater (Table 4).

A new thermal model, similar to the one in [33] was not built. Aluminum has an order of magnitude higher thermal conductivity than stainless steel, the heat sink gives a much higher surface area, and the stainless steel block has been thinned. All of these factors would indicate increased ability to dissipate heat and self-cool by the heat sink assembly.

Consider the formulas for resistance to heat loss by conduction (R_{cd}), convection (R_c), and radiation (R_r)[33].

$$R_{cd} = \left(\frac{L}{k * A} \right)$$

$$R_c = \left(\frac{1}{h * S} \right)$$

$$R_r = \frac{T}{\sigma \varepsilon T_{\infty}^3 \left((T + 1)^4 - 1 \right)}$$

Where:

$L \equiv$ Thickness of the plate (m)

$k \equiv$ Thermal Conductivity (W/m·K)

$A \equiv$ Cross-sectional Area (m²)

$h \equiv$ Convection Heat transfer coefficient (W/m²K)

$S \equiv$ Surface Area (m²)

$T \equiv$ Temperature at the element (K)

$T_{\infty} \equiv$ Ambient Temperature (K)

$\sigma \equiv$ Stefan-Boltzmann constant [5.67E-5 W/(m² K⁴)]

$\varepsilon \equiv$ Emissivity

In the case of the smaller steel blocks,

$$R_{cd_SS} = \left(\frac{L \downarrow}{k * A} \right) \Rightarrow R_{d_SS} \downarrow$$

The aluminum heat blocks have a higher emissivity and surfaces area and a lower thickness than the steel blocks they replaced. Similar qualitative analysis of the thermal resistance equations indicates that R_d , R_c , and R_r would all be lower for the heat sink.

Since the steel block design maintained electrode temperatures under 500°C in all temperature cases, then the steel / aluminum design should have an even greater margin and is guaranteed to stay below 500°C. Further testing is required to validate this theory.

2.2.5.3 Reaction Site Access

In order to place wafers treated with catalyst within the reactor, users of the conventional CVD tube furnace shown in Figure 4 must remove the aluminum end cap and use an implement such as a metal spatula to push the sample into the tube and into the heating zone. Even more difficult, a spatula or very long tweezers must be used to gently remove the wafer with the grown product from the tube. Wafers must also be placed in proper sequential order in the tube.

Higher end machines employ motor driven sample sleds to place the wafers inside the CVD. To save costs, the SabreTube removes the tube to provide access to the reaction site. The quartz tube retracts by hand and rests on the aluminum rails, allowing the user to mount samples directly on the

substrate or to replace the silicon substrate heater with a catalytically heated silicon wafer if the user desires to grow directly on the heating element. If separate wafers are placed on the substrate heater, then the wafers can be placed in any order and easily relocated.

The mechanical access provided by the retracting tube also permits the user to easily adjust or repair reactor internals if required. It also enables the user to put in custom fixtures such as the gas flow router shown in Figure 26.

2.2.5.4 Reactor Support and Modular Fixtures

The aluminum pegboard base plate and the aluminum right angle brackets that hold the end caps all contain numerous ¼-20 screw holes spaced 1" apart. The pegboard and angle brackets employ a square grid pattern though the angle brackets use a diamond pattern across the top. The right angle brackets also contain slots which permit continually varying the height of mounted items. These two slots are used to mount the aluminum support rails. A dovetail slide is also attached to the peg board. All of these components enable a great deal of flexibility in mounting sensors and components. Though the prototype utilized Thor Labs Components (www.thorlabs.com) for mounting, the standard interfaces allow any system that can accept ¼-20 screws to be used or custom parts to be made.

The large right angle brackets that hold the end caps were modified using an OMAX waterjet. A 2.25" diameter hole cut in the front end bracket permits mounting the front end cap directly to the bracket (Figure 17). The end cap could

not mount without the pass through hole due to the need to route gases and the power sealing gland to the flange face.

A one inch wide slot cut by waterjet in the rear angle bracket enables the gas fittings on the rear end cap to extend through the bracket plane when the quartz tube is retracted.

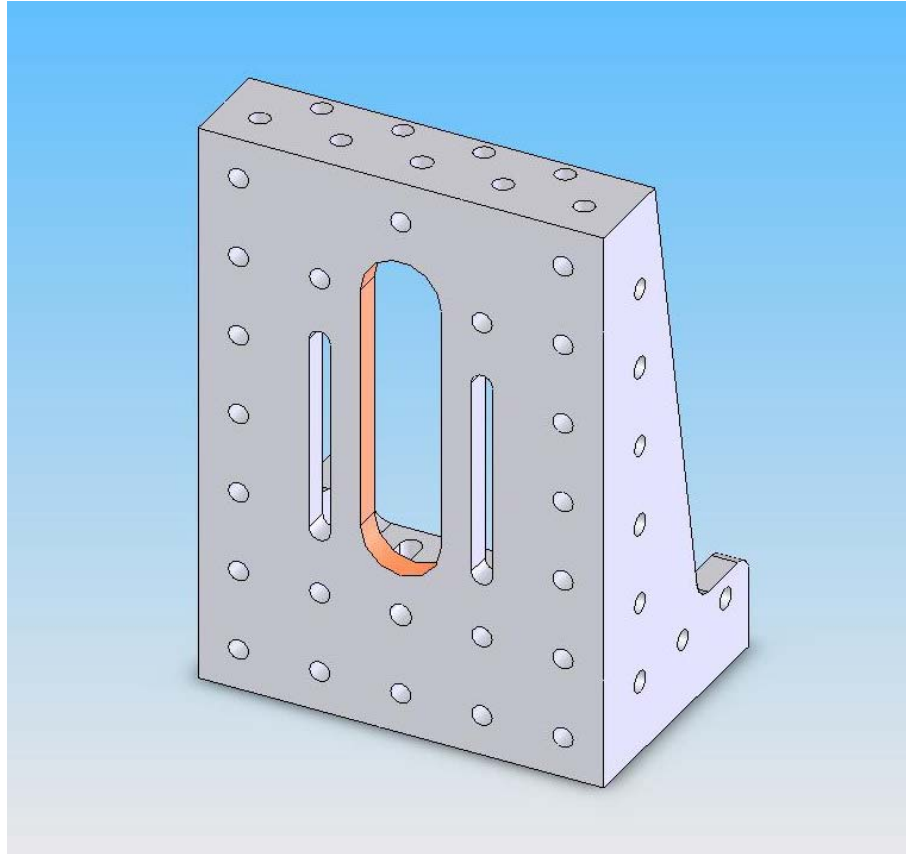


Figure 32: CAD Drawing of rear right angle bracket with one Inch slot

2.2.5.5 Sensing and Control

An Exergen IRT/c.2ACF-K-LoE infrared temperature sensor is placed 20 mm below the substrate heater. The sensor is held in place by a vee block with a mounting arm which allows the sensor to be translated up and down by the user. The vee block mounts to a right angle block. The right angle block mounts

via slots to a carriage that rides on the dovetail rail. The slots on the right angle block allow adjusting how far the IR sensor extends underneath the reactor tube and the carriage allows adjusting the longitudinal position of the IR sensor, enabling the user to adjust the location monitored by the temperature sensor.

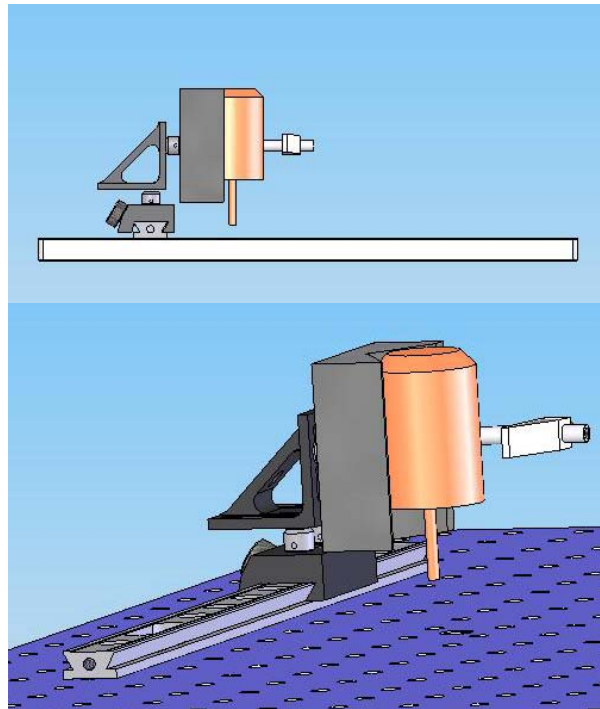


Figure 33: IR temperature sensor mounting

Type K alumel thermocouples are routed through the power sealing gland and terminate inside the front end cap. If desired, the user may connect thermocouples to these alumel wire ends to monitor internal reactor temperatures (Figure 34). The thermocouple leads also enable calibrating or validating the calibration of the IR temperature sensor display as described in [2].

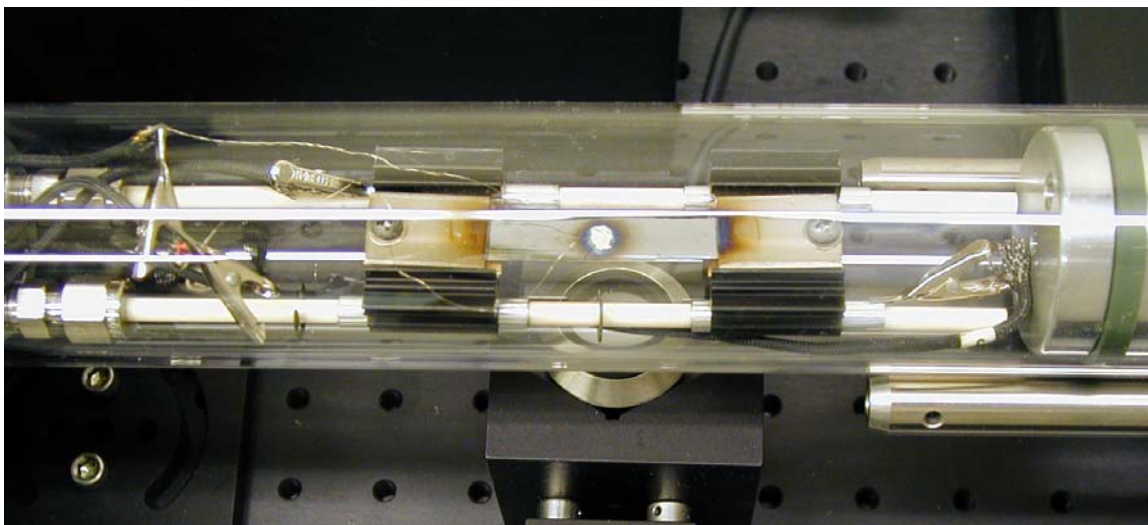


Figure 34: The SabreTube with a thermocouple used to calibrate the IR temperature sensor

An Omega i32 temperature controller and display is mounted to the aluminum pegboard. The rear of the temperature display enclosure contains a 2.5 mm ID / 5.5 mm OD DC jack with K type thermocouple wiring from the jack to the controller. A 9 pin D sub miniature jack in the rear of the enclosure allows the user to interface with the display and controller via the R232 standard. (Figure 16)

2.2.5.6 Additional Usability Features

2.2.5.6.1 Alumina Rail Replacement

Alumina rods provide a chemically inert, electrically insulated cantilever support for the substrate heater assembly. The dual rail cantilever permits longitudinal thermal expansion of the heater assembly while minimizing the thermal mass inside the reactor.

Though not intended as a consumable, the user may have to replace the alumina rails if the user accidentally breaks the rails by dropping an instrument on the rail or other accidents. Rather than requiring the user to replace the entire front cap assembly, the rails are mounted using 1/8" NPT to 3/16" tube adapters. With a crescent wrench, the user can simply and easily remove an alumina rail and replace it.

2.2.5.6.2 Aluminum Support Rails

The aluminum support rails provide end support when the quartz tube is closed but they also support the tube in the open configuration and aid in maintaining tube alignment when opening and closing the reactor.

The aluminum support rails are held at their height by compression using hex cap 1/4-20 bolts and a 1/4" washer against the aluminum right angle bracket. The vertical slots are used to permit changing the height of the aluminum support rails in case a larger diameter quartz tube is ever used with the SabreTube. (This would also require replacing the front end cap)

The aluminum support rails can be a single foot long 1/2" aluminum rod or can be built of shorter aluminum rod segments connected end to end. The built up rail may be desired in cases where modifications to the quartz tube have been made or to shorten the rails to fit some sensor. (Figure 23)

2.2.5.6.3 Power Panel

Two DC power lines and one AC power line are routed through a single enclosure. Each power line requires a SPST switch to be closed in order for

power to be applied to a portion of the reactor system. This provides the user with a single place from which to activate the CVD reactor system and from which to discern the electrical status of the system at one glance.

The AC power line routes to the temperature display / controller. A 100 mA, 20 mm fuse is in the circuit to protect the temperature unit. This fuse is also located on the power panel to consolidate all electrical operations in one location.

2.2.5.6.4 Size and Weight

The layout of the SabreTube and the predominantly aluminum construction give the SabreTube a compact form and low weight. Small labs or labs with little open space will have an easier time finding a place for the SabreTube than many larger systems. Most users can lift the system on their own by grasping both right angle brackets. (It is recommended that the user remove the substrate heating assembly and quartz tube but I have successfully relocated the SabreTube without doing so.)

The relatively small form factor and open space around the quartz tube also enable the user to take the SabreTube to permanently mounted sensors such as X-ray scattering machines, enabling research synergies.

2.2.5.7 Safety Systems

2.2.5.7.1 Gas

2.2.5.7.1.1 Flammable Gases

Protection from flammable gas ignition is provided by procedural compliance, pressure tight boundaries, external exhaust hoods⁴, and appropriate material choices. Prior to introducing a flammable gas to the reactor, the tube must be closed against the pressure tight Viton seals and all gas ports on the end caps must be blanked or connected to appropriate gas lines. The gas exhaust lines and the relief valve fittings should all be routed to an exhaust hood to prevent flammable gas accumulation.

The user must first flush the gas preheater (if used) and the quartz tube with an inert gas to remove any oxidizing agents such as air prior to introducing any flammable gases. Electrical power for the substrate preheater and the gas preheater should not be applied until the inert gas purge is complete. Purges should flush at least ten times the volume of the unit to be flushed.

Following reactor use, the preheater and quartz tube should again be flushed with an inert gas to ensure all flammable gases are removed prior to opening the reactor which introduces air, an oxidizing agent. Power to the heaters should also be secured and the reactor allowed to cool prior to opening the reactor. This removes heat sources and potential spark sources that could provide ignition energy to a flammable mixture.

⁴ Exhaust hoods would not be provided with the SabreTube but should be separately procured and present for safe operation.

If the user employs a means to route gas directly to the substrate, the user should use the second gas inlet line to route purge gases. This ensures adequate purging of the entire reactor, including the cavity in the front end cap.

It is strongly recommended that the lab where the SabreTube is used also contain a hazardous gas detector as a means to alert the user of hazardous gas leaks into the lab.

Some CVD processes incorporate acetylene so neither copper nor brass are used in the construction of the SabreTube since both can lead to ignition when in contact with acetylene.

2.2.5.7.1.2 Reactor Pressure Integrity

The SabreTube is only meant for CVD processes that occur at atmospheric pressure.⁵ The reactor process employed typically occurs around .1 psi above atmospheric. To guard against overpressure, a third gas pass through hole with a 1/8" NPT female thread on the rear end cap is fitted with a 1/8" NPT check valve rated to .3 psi to guard against reactor tube overpressure. (Figure 23) In the event of an overpressure, the check valve relieves to a tygon tube that is routed to an exhaust hood.

Quartz serves as the main body of the Reactor vessel. Quartz exhibits an adequate tensile strength of 6.8 MPa⁶. Hoop stress is twice as much as

⁵ If the tygon tubing is replaced with stainless steel tubing, the system could be used with vacuum processes.

⁶ Quartz tensile property has been reported as high as 47 MPa. However, the quartz supplier recommends using the lower value to account for quartz's sensitivity to surface flaws and scratches in the tensile region.

longitudinal stress in cylinders and Hoop stress for a circular cylinder is defined as:

$$\sigma_{hoop} = \frac{P * r}{t}$$

where:

$P \equiv$ Pressure (Pa)

$r \equiv$ Thin walled tube radius (m)

$t \equiv$ Wall thickness (m)

For the SabreTube, at check valve relief, $\sigma_{hoop} = .026$ MPa, far less than the quartz tensile strength. An internal overpressure of .5 MPa or 5.3 atm would be required to cause the quartz to fail. Any overpressure should cause the .3 psi check valve to fail first followed by ejection of the tygon to male barb pipe fitting and then ejection of the end caps since a 5.3 atm overpressure would generate 1000 N or 230 lbf against each end cap.

2.2.5.7.2 Electrical

Section 2.1.4 demonstrates an electrical hazard exists if the user comes into contact with the current supplied to the CVD system. To guard against electrical shock, proper size wires and sufficient electrical insulation is used to protect the user.

The Quartz's resistivity of $\geq 10^6 \Omega \cdot \text{cm}$ protects the user against shock from the tube. [27, 37] At 100 V_{DC} and with a 2 mm tube thickness, the current generated by a loose wire touching the quartz tube would not exceed .02 mA. The Aluminum 6061 end caps do not provide electrical protection. To guard

against an electrical short, the power wiring is shielded by a fiberglass sleeve rated to 482°C, far in excess of the temperature it will see. The fiberglass sleeve is provided with the Conax-Buffalo Power Gland and is certified by Conax-Buffalo to provide adequate insulation against electrical shocks.

18 AWG wiring is used throughout the entire reactor system. For standard copper wiring, the load limit for 18 AWG is 16 A. Internal to the reactor and for the gas preheater, the wiring is changed to 18 AWG Alumel and 30 AWG Ni80/Cr20 Alumel respectively. The higher AWG for the preheater enables a lower amperage of around 3 A to produce a temperature of 1000°C.[38]

The greatest electrical hazard to the user is operating the substrate heater while the reactor tube is open. The aluminum heat sinks, steel blocks, and silicon substrate are all energized to the heater voltage and current. Procedurally, the tube furnace should never be operated with the substrate heater exposed.

2.2.5.7.3 Thermal Safety

Experience with the SabreTube shows that the quartz tube in the vicinity of the substrate heater becomes uncomfortably hot to the touch but the temperature does not appear to present a burn hazard. We have used a small air blower to cool the exterior of the tube so that at the conclusion of a growth cycle, the tube can be handled immediately. This enables even faster cycle times.

2.2.6 SabreTube Components and Price

One of the goals of the SabreTube is to minimize cost in order to enable the maximum number of research groups to use the system, thereby increasing the pace of discovery. The modular design of the system also means that not all functionalities will be needed by all groups. Therefore, to lower cost and tailor the system to user needs, it is envisioned that the SabreTube would be offered as a basic package with the PreHeater and the Laser Displacement Sensor as optional add-ons.

The basic SabreTube would include:

1. Front End and Rear End Caps
2. Quartz Reactor Tube
3. Substrate Heating Assembly with replacement silicon substrates
4. IR and Thermocouple Temperature Sensing, Display, and Control with software interface
5. Modular Fixtures (Pegboard, Brackets, 12" Aluminum Support Rails, etc.)
6. Vertical Tube Holder
7. Gas Routing Fixtures

The PreHeater option would include:

1. PreHeater Enclosure
2. Firebrick
3. Three Quartz and Four Alumina Tubes
4. Heater Wire

The Laser Displacement Sensor option would include:

1. Laser Displacement Sensor
2. Laser Mounting Fixture
3. Software interface

Though research was not done into the cost of manufacturing the SabreTube commercially, the cost of creating the prototype may be used as a rough guide for the order of magnitude of the cost of each option. Material costs will reflect the cost of ordering small quantities at retail prices. Manufacturing costs, where known, do not reflect production scale costs because custom components were machined. The end caps, for instance, may be far cheaper to cast if the initial cost of a mold can be paid off due to anticipated demand. For the cost exercise, the retail cost of machining the end caps is known since the MIT Central Machine Shop was commissioned to machine the parts. All other parts were machined by me on an end mill or using an OMAX waterjet. I am not a proficient machine shop operator so I did not include the time I spent machining as a part of the estimate. Overall, the costs provided in Table 7 are rough orders of magnitude for the SabreTube. Figure 35 shows the costs for the basic SabreTube package by subassembly. A full itemized cost is provided in Appendix C.

Table 7: SabreTube parts and labor cost
The majority of the cost for the laser option is from the \$8,000 cost of the laser itself.

| Parts and Labor Costs | |
|----------------------------|------------|
| SabreTube Basic Package | \$3,321.37 |
| PreHeater Option | \$55.51 |
| Laser Displacement Sensing | \$8,076.01 |

SabreTube Basic Package Subassembly Cost Breakdown

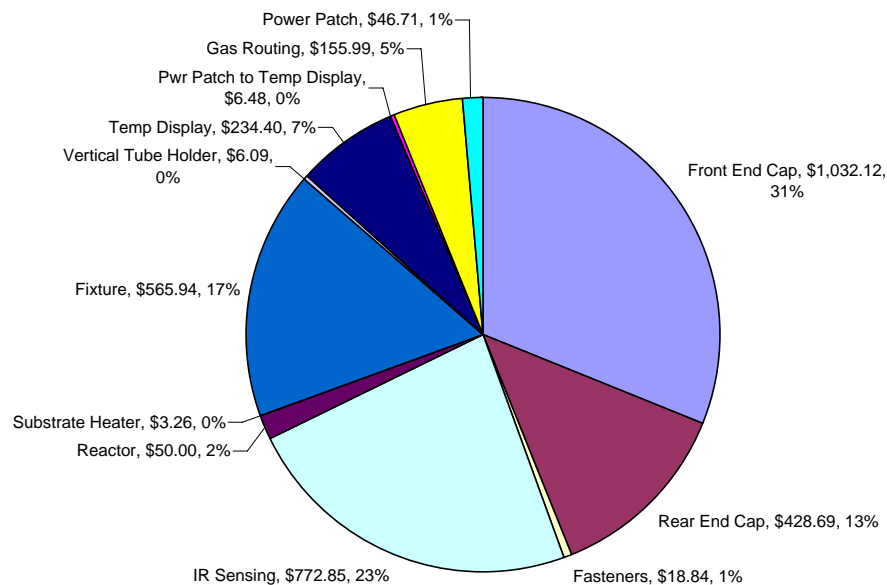


Figure 35: Subassembly cost breakdown for the basic SabreTube package

As can be seen from Figure 35, the greatest costs are in the front end cap and the IR sensing. Though little can be done about the cost of the IR sensor, hopefully a casting or some other manufacturing method can lower the end cap costs significantly.




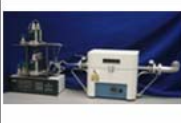

To cut the end caps on the waterjet requires about half an hour when set-up and fixturing is included. The actual cuts are less than 10 minutes. The end

plates for the temperature display require about 20 minutes of fixturing and cutting on the waterjet. The greatest time is spent on drilling the holes for the power patch panel enclosures and would require about an hour.

2.2.7 Market Competition

Table 8 compares common basic CVD tube furnaces used for growing CNTs. The table shows a large price range and a large range of functionalities. Though a price is not shown, the SabreTube would probably be available for less than \$9,000. The SabreTube provides significant functionality improvements at a relatively low cost in the existing market.

Table 8: Comparison of common CVD tube furnaces used to grow CNTs

| | SabreTube | Microphase Desktop CVD | VWR Lindberg Blue M Single Zone Tube Furnace | Atomate | Firstnano EasyTube 2000 |
|----------------------------------|---|---|---|---|---|
| |  |  |  |  |  |
| Size (WxDxH) in | Large Desktop 32"x15"x8" | Desktop 12"x8"x≈10" + 8"x8"xUnk for Pwr Supply | Desktop 21"x13"x12" (Length changes to ~36" when tube is added) | Large Desktop | Cabinet 64"x64"x29" |
| Cost | | \$12,271 (\$10,600 academic) | \$2,293 | \$36,000 (starting price on basic package) | Unknown |
| Heating Rate | 100°C/s | 1.33°C/s | 1°C/s | Unknown | Unknown |
| Optical Access | Yes | Yes | | | |
| Modular Fixtures | Yes | | | | |
| Fully Automated Control | | | | Yes | Yes |
| Automatic Gas Flow Controller | | | | Yes | Yes |
| Notes: | | Ethanol Based Processes Only | | | |
| URL: | www.sabretube.com | www.microphase.jp/ desktop-cvd.htm | www.vwr.com | www.atomate.com | www.firstnano.com |

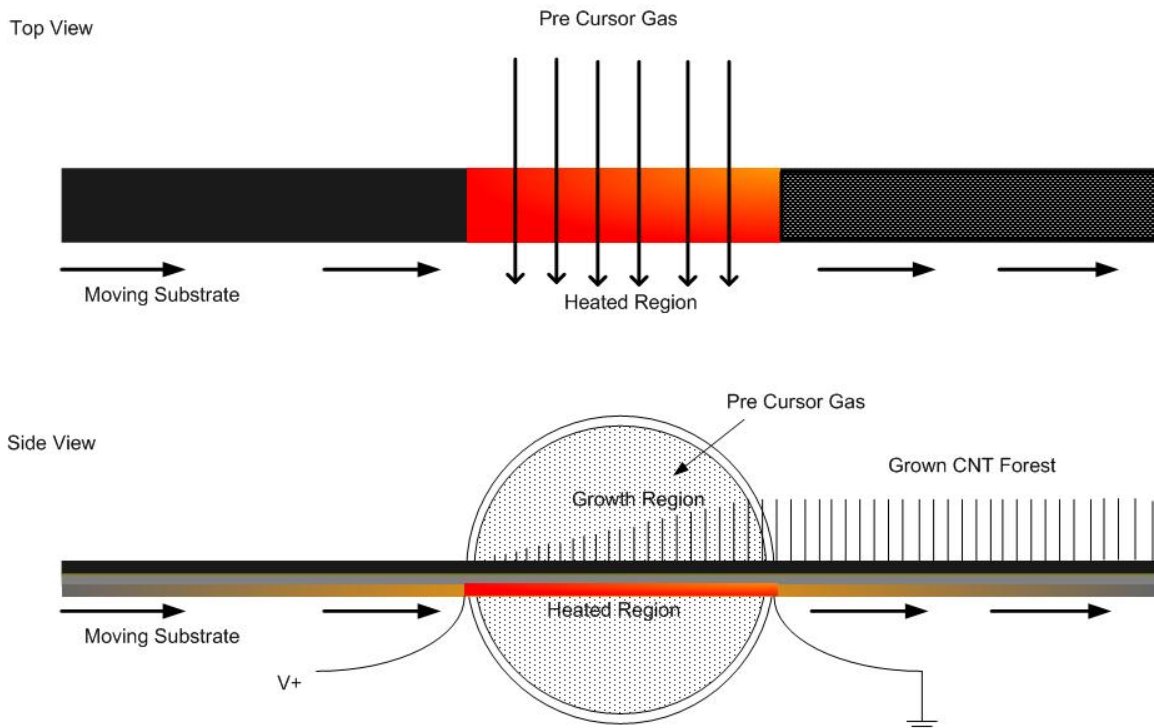


Figure 36: Notional Continuous Growth Process

Whether a continuous growth process would be cheaper and faster at producing CNTs depends on such things as the rate of growth and the required system complexity. Research and experimentation is required to understand the variables affecting continuous growth in order to optimize the process and make a cost-benefit analysis.

In addition to lower production costs of CNT forests, a continuous growth process might enable integration with an entire composites production line. Research by a PhD student at MIT, Enrique Garcia, involves using a roller impregnated with resin pre-preg to lift CNT forests directly off of silicon substrates. If a continuous growth process can be devised and combined with Garcia's roller method, then a new means of manufacturing CNT composites can be created.

Ideally, any continuous growth process would recycle the growth substrate for further use in growing CNTs after the CNTs have been harvested. At this stage, it was decided to first experiment with continuous growth processes with one time use silicon wafers. Devices to enable this experimentation were required.

Hart and van Laake previously created a box CVD furnace to enable increased *in situ* mechanical access to the substrate during growth by increasing the internal reactor volume around the substrate. Constructed of aluminum, the box shape facilitates mounting mechanisms inside the reactor.[2] Figure 37, Figure 38, and Figure 39 show details of the CVD box furnace design. (Figures courtesy of Dr. John Hart.)

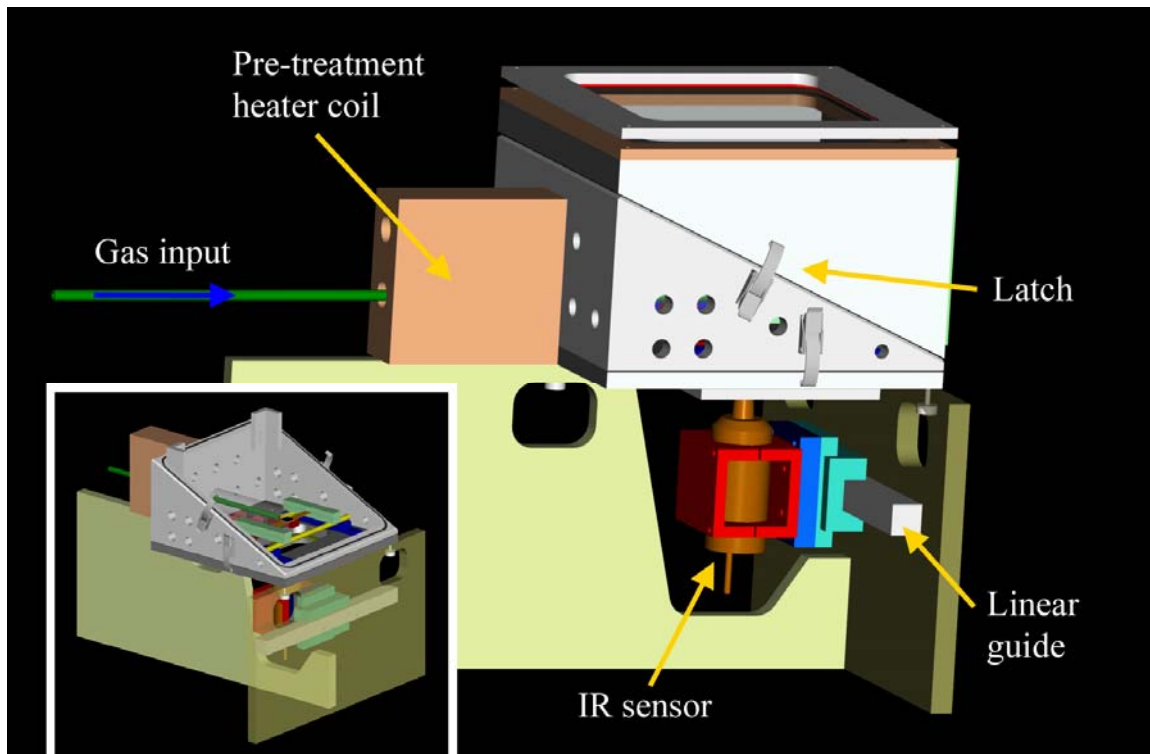


Figure 37: CAD drawing of the Hart and van Laake box CVD furnace system exterior

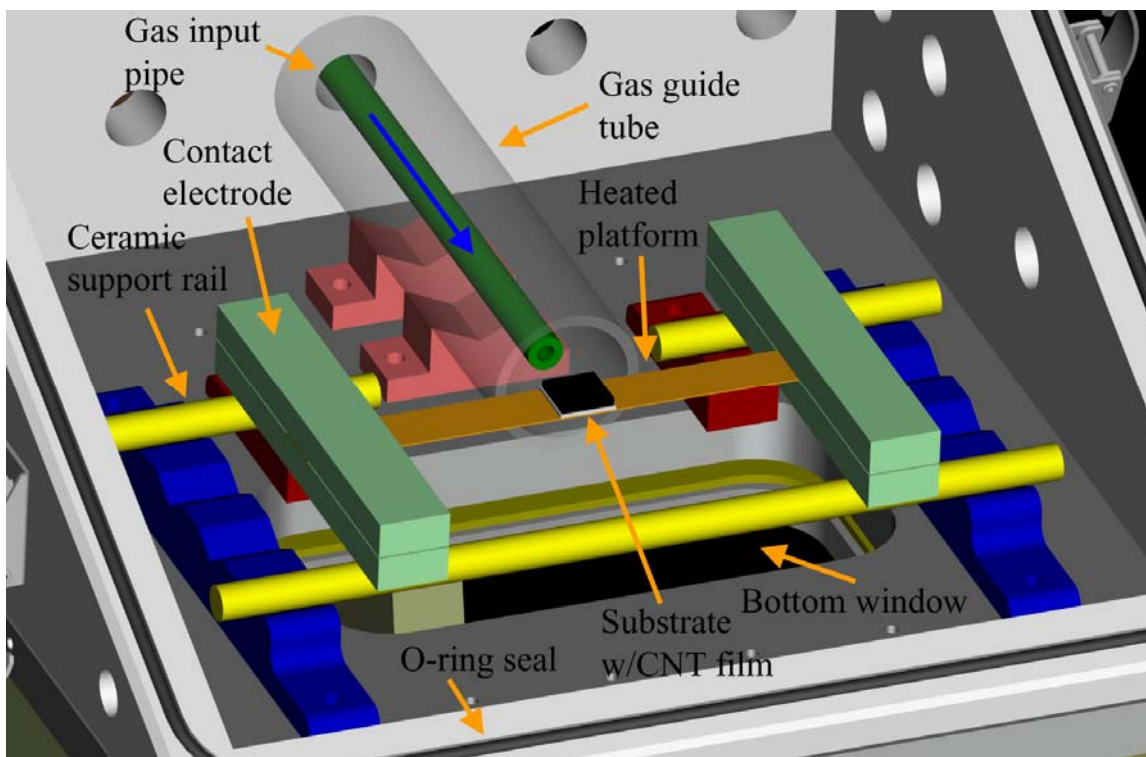


Figure 38: Box CVD furnace interior details

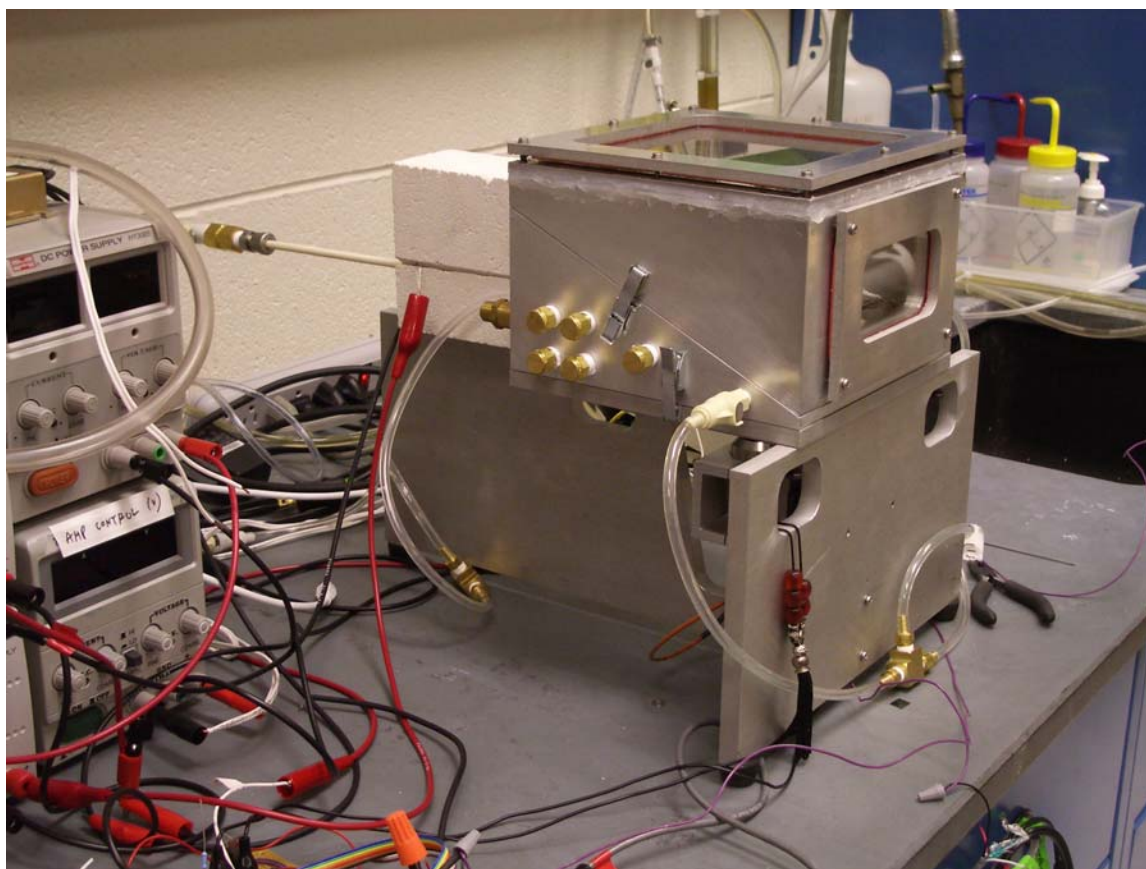


Figure 39: Picture of as built CVD box furnace

This section of the thesis focuses on the design of a mechanism, known as the Nanosled, which enables experimenting with continuous growth processes for CNTs within the CVD box designed by Hart and van Laake.

2.3.1 System Requirements and Constraints

- Resistive heating of the substrate for rapid temperature response when the reaction site is in the growth zone
- Resistive heating of the substrate growth zone only
- Precursor gas application to the growth zone
- Continuously moving growth zone or continuously moving reaction site that passes through the growth zone. Linear motion should be variable and on the order of one inch / minute
- Variable growth zone length
- Able to fit within the box CVD furnace interior of 7" long x 6.87" deep x 4.75" high
- Able to maintain substrate rolling alignment
- Able to remove and load rolling silicon substrate
- Able to accommodate variable substrate width (15-26mm) and thickness(.3-1mm)
- Growth Zone remains within optical window footprints and within focal lengths for box furnace IR sensor and laser displacement sensor

- Electrical isolation of the substrate from the Aluminum walls of the CVD box furnace
- CVD compatible materials employed

2.3.2 Nanosled design

A roller design was selected to translate a catalyst treated silicon wafer resting on a silicon sled across the box furnace. Stainless steel rollers provide a means to both drive the sled and create an electrical circuit to heat only the growth region. The basic strategy is depicted in Figure 40.

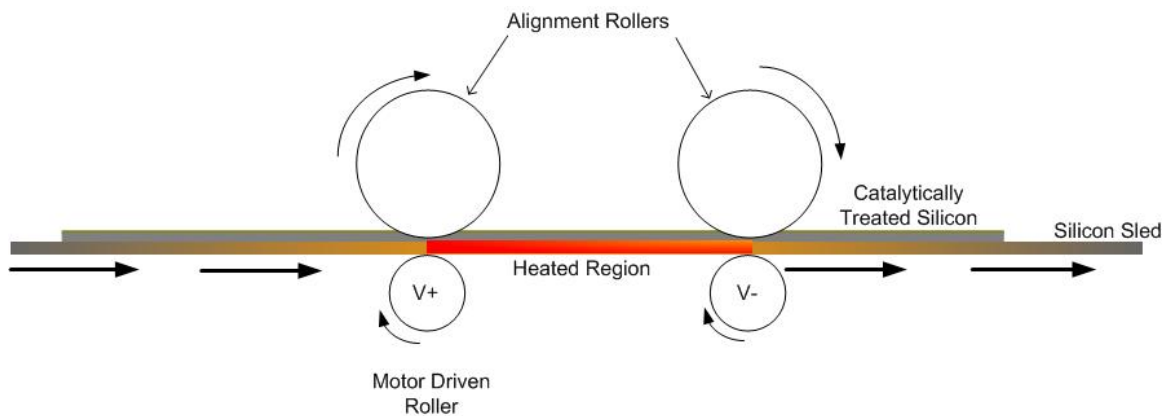


Figure 40: Nanosled strategy

Quarter inch 304 stainless steel shafts were selected for the bottom drive rollers to enable one shaft to fit through one of the CVD box modular ports. This longer shaft passes through a PTFE $\frac{1}{4}$ " NPT to $\frac{1}{4}$ " tube fitting (4401) to electrically isolate the shaft from the CVD furnace. The shaft terminates at a K style coupling (4402) which also electrically isolates the shaft from an electric drive motor (4403) but permits shaft rotation. A wire is attached to the shaft (4404) outside of the reactor to minimize the potential for sparking within the reactor itself. The low speeds and the

limited length of travel due to space constraints within the reactor allow for a wire to wrap around the shaft as it turns. The portion of the bottom roller shaft that is outside of the reactor requires a Plexiglas box or other electrically insulating material around it because it carries current during operation. (Figure 41)

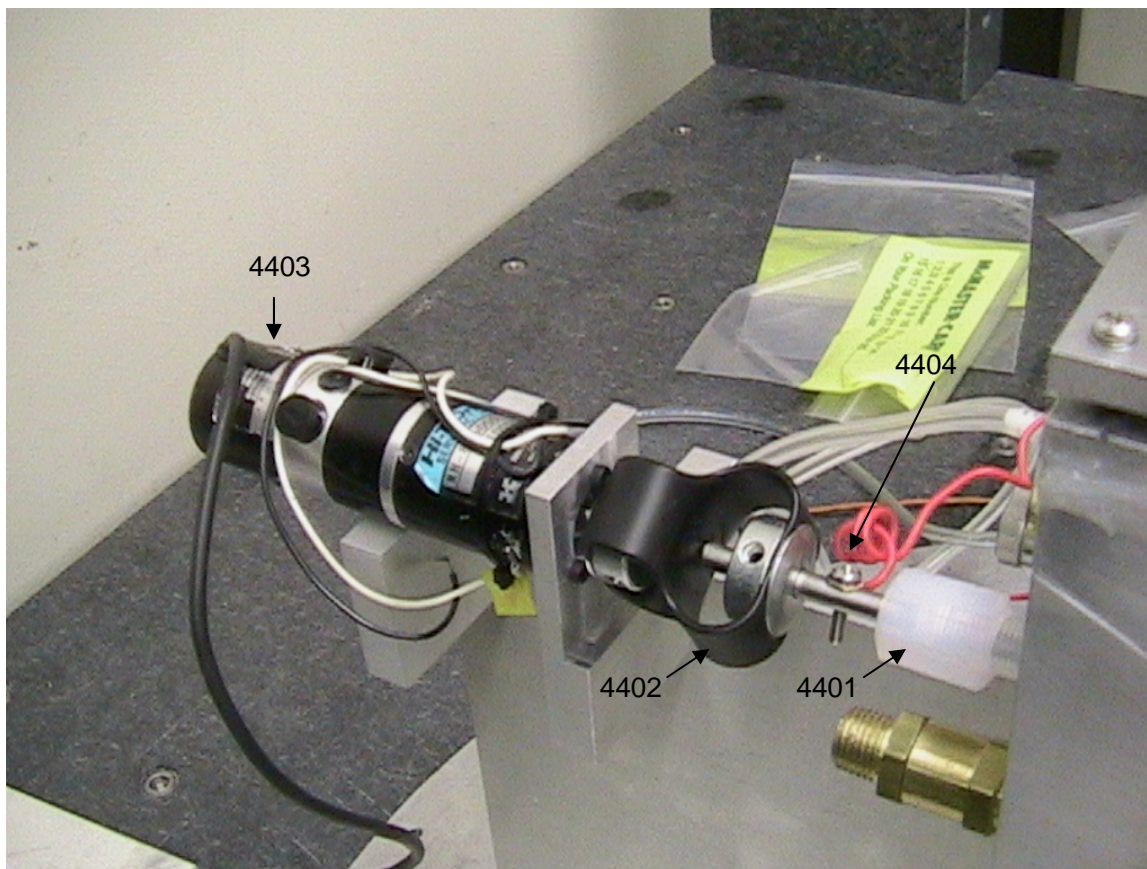


Figure 41: Nanosled external motor drive with K coupling, wiring, and PTFE tube fitting

The other quarter inch bottom roller shaft is contained fully within the box. An attached ground wire exits the CVD box furnace via a sealed port to allow the user to complete the electric circuit. The bottom roller drive shafts are maintained at a constant diameter across the width of the sled to promote more uniform electrical flow through the silicon wafer. (Figure 42)

To insure good traction of the silicon sled against the bottom roller and a good electrical connection, a downward normal force is required on the silicon sled. As discussed below in Section 2.3.2.1, a larger radius wheel is desirable give low contact stresses on the brittle silicon sled. Also, the top rollers cannot make contact across the full width of the sled in order to provide clearance for grown CNTs to pass under the roller and out of the electrically heated zone. This also prevents the top roller from inadvertently damaging the catalyst surface. The top roller must also be able to accommodate different width sled heaters and different width growth wafers. Finally, the top roller should be used to aid in maintaining the silicon sled alignment.

All of these requirements led to a two piece shoulder bushing design. The shoulder bushings slide over a 3/16" stainless steel shaft and maintain their position via a M3 set screw. The set screw allows the user to vary the gap between the bushings. The shoulder of the bushing contains a .2 mm right angle lip that is designed to fit over the edges of the silicon sled. The .2 mm depth prevents contact between the bushing and the bottom roller while guiding the silicon sled

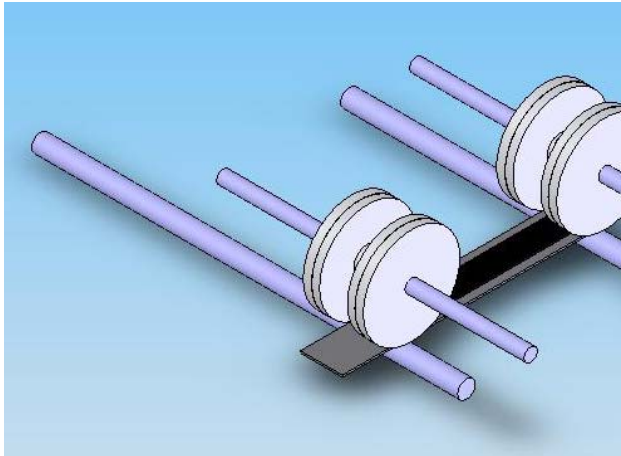


Figure 42: Silicon wafer held between round shoulder bushing and cylindrical bottom drive roller

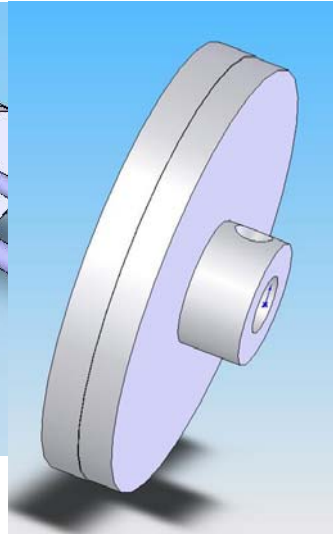


Figure 43: Shoulder bushing detail

Two roller assembly fixtures constructed of Aluminum (6061) provide support to the four shafts. The two roller assembly fixtures are aligned via two Macor electrically insulating ceramic rods (4801). The rods, clamped in place by M6 screws (4802), allow the user to vary the gap between the two fixtures which allows the user to change the length of the growth zone. The Macor guide rods also aid in maintaining drive alignment and preventing a short from developing between the fixtures. Each fixture rests on Macor disc pads to electrically isolate the fixture from the reactor aluminum floor. Each roller assembly employs a manually driven screw (4803) to lower the shoulder bushing via a crab flexure. The crab flexure provides a compliant fit and feel while ensuring motion only along the vertical axis (see Section 2.3.2.2). (Figure 44, Figure 45) Note the bowing in the crab flexures in Figure 45 as the screw holds the shoulder bushing against the silicon sled.

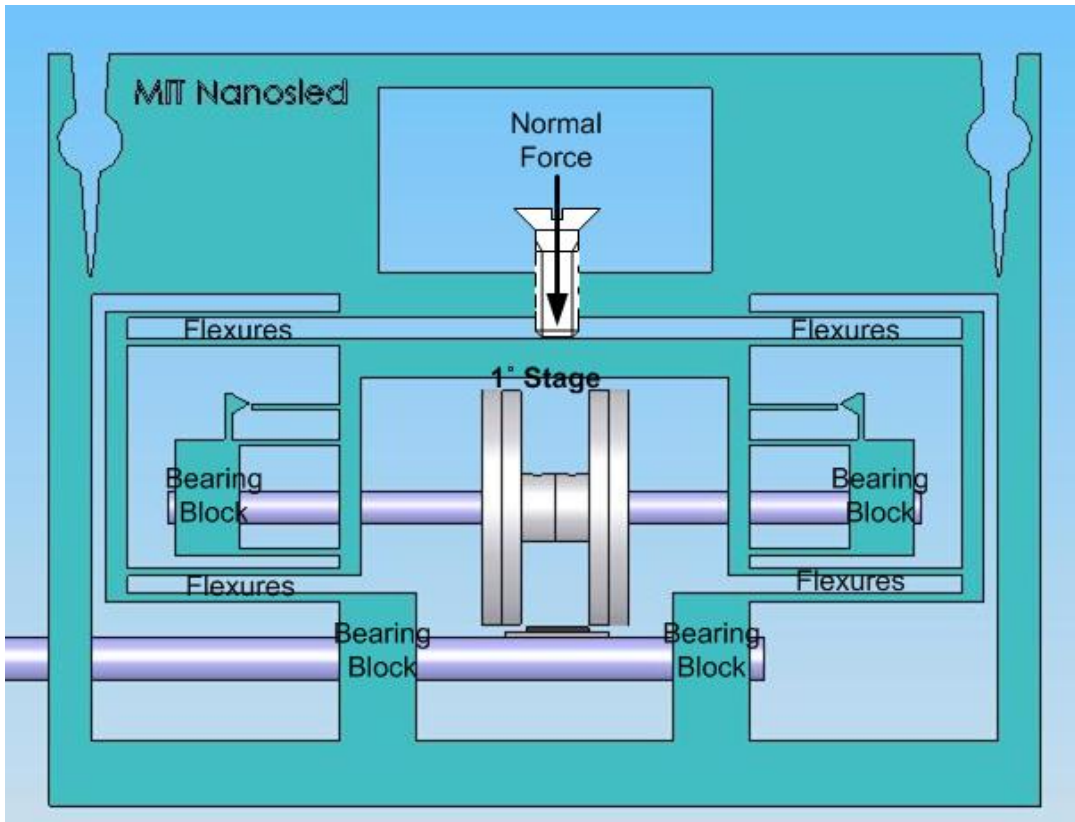


Figure 44: Roller assembly model

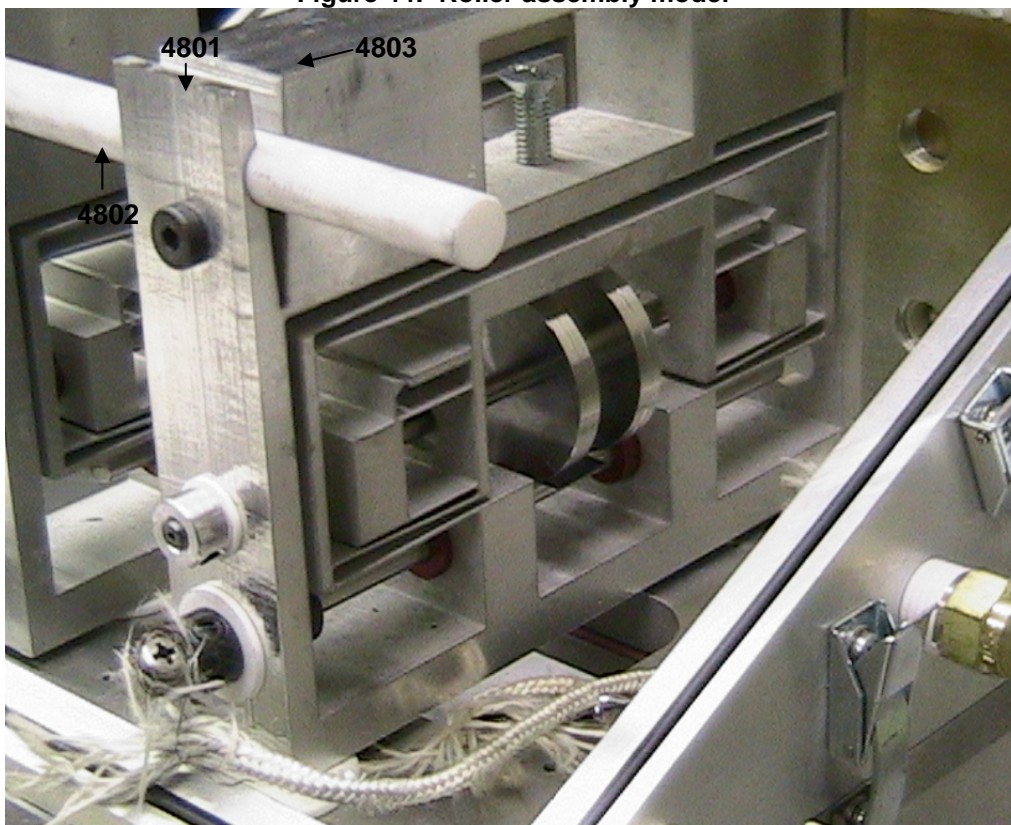


Figure 45: Picture of roller assembly with clamped silicon sled

The top and bottom shafts are supported by aluminum bearings with Frelon linings to meet temperature and chemical requirements for the CVD process. (Figure 44) The Frelon also provides an electrically insulating barrier between the energized shafts and the fixtures. The bearings are held in the roller assembly fixtures by 'C' style bearing retaining clips. Two aluminum shaft collars or two steel shaft collars (4901) (depending on what was available from the vendor) are placed on each shaft to restrict lateral motion of all shafts and a Macor washer (4902) fits between the shaft collar and the fixture to prevent electrical contact.

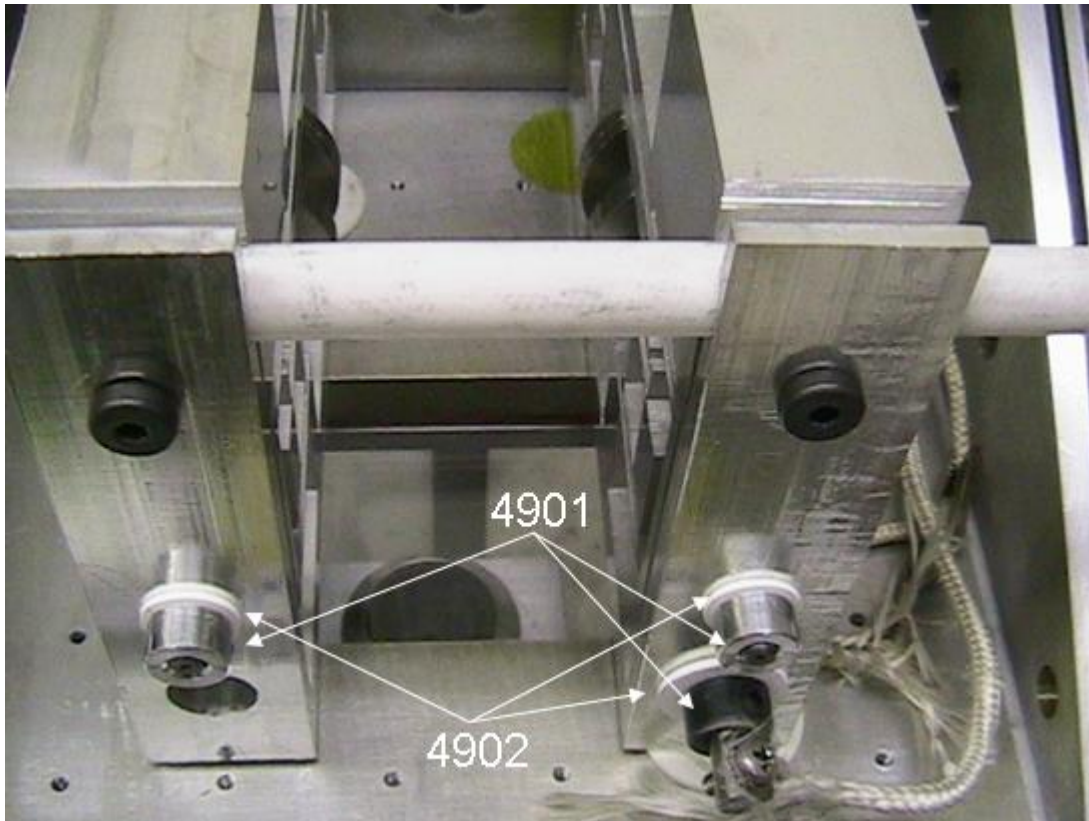


Figure 46: Picture of roller assembly with shaft collars and Macor washers

2.3.2.1 Hertz Contact Stress

Hertz Stress theory enables us to predict whether a material will fail when subject to contact by round surfaces. The smaller the radius, the smaller the area of contact available to transmit a given force, which results in a higher contact stress. In the case of the Nanosled, the silicon wafer is held between the steel shoulder bushings and the bottom roller (Figure 42). The bottom roller with a radius of 6.35 mm (1/8") has a smaller radius than the shoulder bushing. Therefore, the bottom roller provides the limiting stress case.

A spreadsheet created by Professor Alex Slocum at MIT for calculating Hertz point contact stresses was used to calculate the allowed force on the silicon wafer. Since the silicon wafer is flat, the radius of the wafer is set at one hundred times the radius of the bottom roller in the spreadsheet. Silicon is a brittle material so the flexural strength vice the ultimate tensile strength sets the failure criteria. Microsoft Excel Solver was used to determine the maximum force that could be used without exceeding a shear stress / (flexural strength/2) ratio of one, resulting in an allowed force of .5 N (.112 lbf) as shown in Table 9. If the safety factor of two is removed, then the allowable force jumps to 2.9 N (.65 lbf). Though the allowable force seems small, experience with mounting silicon in stationary resistive heating fixtures and in the Nanosled has shown that the silicon sled can be clamped relatively easily.

Table 9: Hertz contact forces on the silicon sled

| Hertz_Point_Contact.xls | |
|--|-----------------|
| To determine Hertz contact stress between bodies | |
| By Alex Slocum, Last modified 1/17/2004 by Alex Slocum | |
| Enters numbers in BOLD , Results in RED | |
| Be consistent with units! | |
| Ronemaj (mm) (steel roller) | 3.175 |
| Ronemin (mm) | 3.175 |
| Rtwomaj (mm) (Silicon wafer) | 317.500 |
| Rtwomin (mm) | 317.500 |
| Applied load F (N) | 0.534 |
| Silicon Flexural Strength (MPa) | 270 |
| Phi (degrees) | 90 |
| Elastic modulus Eone (steel roller) (Mpa) | 1.93E+05 |
| Elastic modulus Etwo (silicon wafer) (Mpa) | 1.63E+05 |
| Poisson's ratio vone (steel roller) | 0.27 |
| Poisson's ratio vtwo (silicon wafer) | 0.22 |
| Equivalent modulus Ea | 9.40E+04 |
| Equivalent radius Re | 1.5718 |
| ellipse c (mm) | 2.38E-02 |
| ellipse d (mm) | 2.38E-02 |
| Contact pressure, q | 4.50E+02 |
| Stress ratio (must be less than 1) | |
| Maximum shear stress/(flexural strength/2) | 1.00 |
| Deflection at the one contact interface | |
| Deflection (µunits) | 179.2 |
| Stiffness (load/µunits) | 0.0 |
| for circular contact a = c, a | 2.38E-02 |
| Depth at maximum shear stress/a | 0.627 |
| Max shear stress/flexural strength | 0.566 |

2.3.2.2 Flexure Theory and Design

The fixture must hold the shoulder bushing in such a way that it accomplishes the following:

- Maintains silicon wafer alignment
- Provides a gradual engagement of the silicon by the shoulder bushing as the bushing lowers vertically
- Minimizes shoulder bushing motion in other axis
- Able to vertically retract the shoulder bushing from the silicon sled to enable change out of the silicon sled

These requirements lead to the use of a crab flexure (a.k.a double parallelogram flexure). A basic crab flexure is shown in Figure 47.

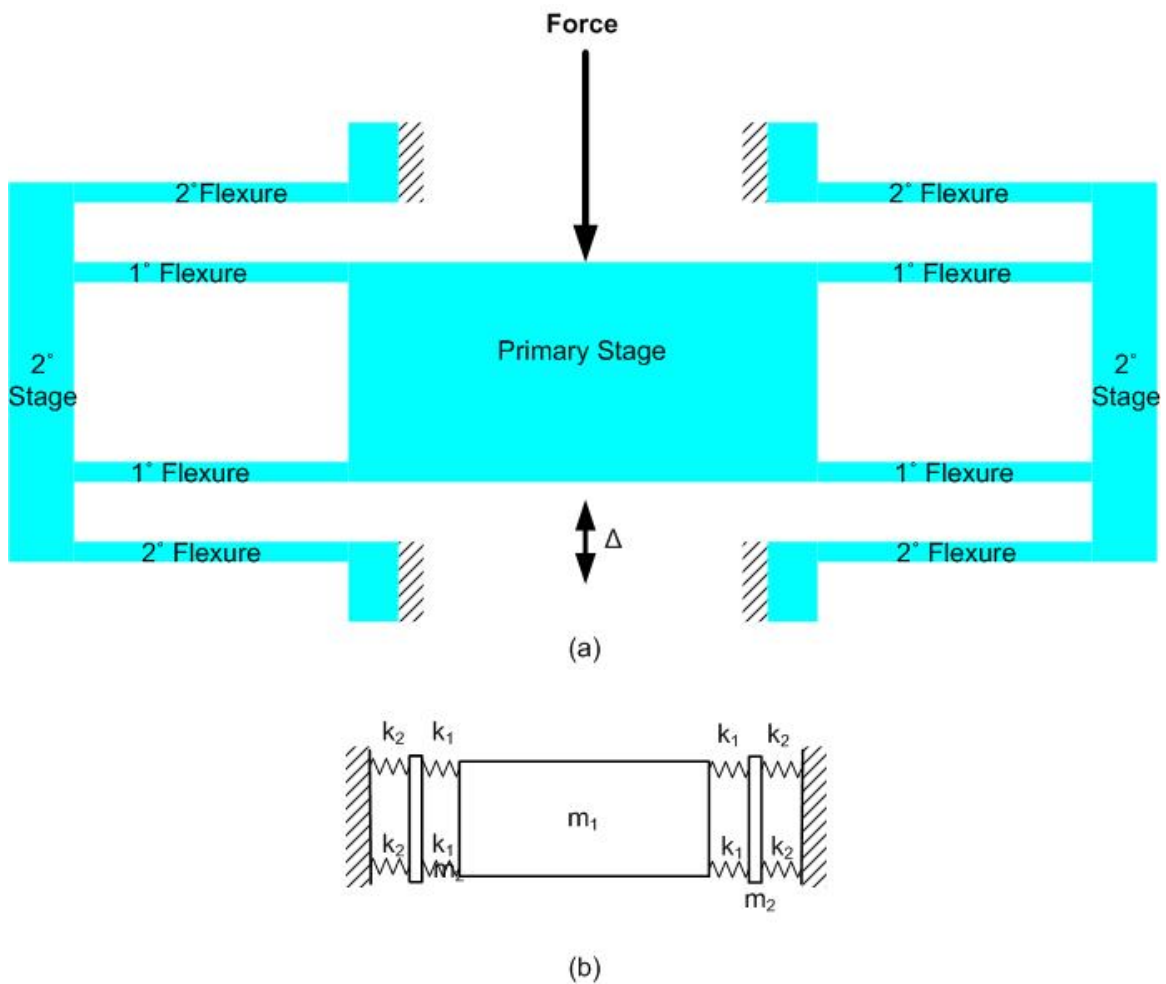


Figure 47: Typical crab flexure configuration
(a) Schematic of a typical crab flexure. Flexure thicknesses are 1mm for the nanosled. 1° and 2° refer to the primary and secondary flexures.
(b) Crab flexure modeled as a spring network.

The flexure arms on the crab flexure are cantilever beams that act as flat springs. The spring constant for one flexure in the vertical direction is:

$$k = \frac{E * b * t^3}{4 * L^3} = 1.3 \times 10^4 \frac{\text{kg}}{\text{s}^2}$$

where

E = Young's Modulus = 69 GPa for Al6061

b = Beam Width (m) = 25.4 mm

t = Beam Thickness (m) = 1 mm

L = Beam Length (m) = 32 mm

The flexure thickness is driven by the minimum width able to be cut with reliability on the MIT Hobby Shop waterjet. One inch aluminum stock is used to ensure the fixtures are stable and to provide good lateral stiffness to the flexures. The beam length is limited by the space available within the CVD box furnace. (A larger furnace would enable longer lengths and thicker sections for the flexure)

The spring constant for lateral motion of the primary stage (motion out of the page plane in Figure 47) is much higher at $8.6 \times 10^6 \text{ kg/s}^2$ due to the one inch (25.4mm) thickness in this direction.

And the force on a spring is linearly related to displacement by the spring constant so that:

$$F = k * \Delta$$

where

F = Force (N)

Δ = Deflection (m)

If we think of the crab flexure as a spring network we arrive at Figure 47b.

If we treat the spring constants as resistances, then we can add the spring constants according to the following rules:

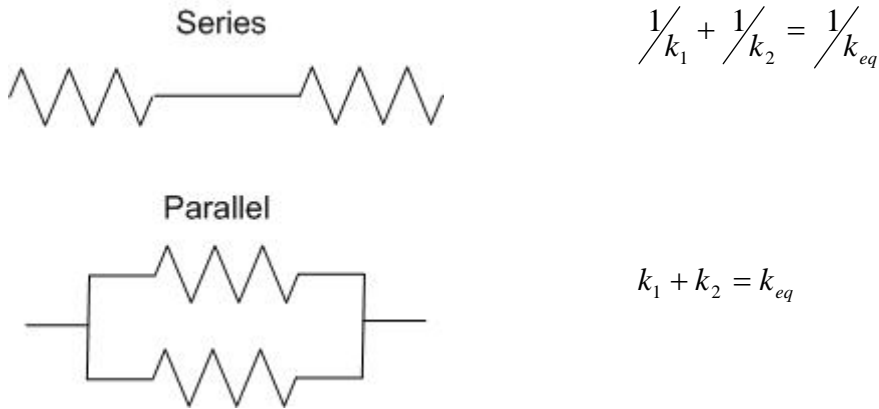


Figure 48: Equivalent spring equations

For the Nanosled, all of the flexure arms possess the same breadth, length, and thickness so all have the same spring constant. Treating m_2 as insignificant, the equivalent spring constant is:

$$k_{eq_vertical} = \left(\frac{1}{4 * k_1} + \frac{1}{4 * k_2} \right)^{-1} = 2k = 2.6 \times 10^4 \frac{N}{m}$$

$$k_{eq_lateral} = 1.7 \times 10^7 \frac{N}{m}$$

This means that the fixture is 645 times stiffer in the lateral direction than in the vertical direction, inhibiting out of vertical deviations. Vertically, 26.7 N or 6 lbf is required to move the shoulder bushing across the 1 mm design gap to contact the silicon sled. Experience shows that the user can feel the contact as it is made and avoid breaking the silicon with this arrangement.

The stress in a cantilever beam is defined as

$$\sigma_{bend} = \frac{3 * E * t * \Delta}{2 * L^2}$$

At the design deflection of 1mm, the maximum bending stress is 101 MPa.

This is less than half of Aluminum 6061's fatigue strength of 214 MPa (at 10^5 cycles). A deflection of 2.117 mm corresponds to the fatigue limit and a deflection of 2.75 mm equates to the yield limit of 275 MPa.

Part Three: Potential Naval Architecture Applications of Carbon Nanotubes

3.1 Technology Readiness

When considering a technology, the Department of Defense assigns a 'Technology Readiness Level' (TRL) to the candidate technology or research. TRL 1 refers to the veritable 'inventor's light bulb', the point where basic research starts to be applied to an application, even if only via theoretical equations. At the highest readiness level, TRL 9, the application has been fully implemented and used during missions. Appendix F provides a detailed description of each level.

In the case of CNTs, a large number of research fields may be impacted. Some applications exist as marketed products while most exist as paper studies or basic research in a laboratory, representing a TRL range from one to six. Most of the applications discussed below are between a TRL of two, "Technology Concept or Application Formulated," and a TRL of four, "Component or Breadboard Evaluation in a Laboratory." [39] At these TRL levels, one can only

speculate on actual properties and characteristics of the application and must approach any claims with skepticism. However, in order to determine whether a technology merits further development, the research sponsor must cautiously estimate the potential costs and payoffs of a technology. Overall, the potential of CNTs are such that resources are warranted to see if the strength, thermal and electrical properties can be harvested for applications in ten or twenty years.[19]

Below, I outline several possible applications of CNTs in the naval environment. Where able, I try to quantify the possible impacts of the technology if the theoretical claims are achieved. In other cases, I engage in a qualitative discussion of the naval architectural impact. Areas explored include supercapacitors, electronics cooling, and composites. Figure 49 summarizes some of the potential applications of CNTs in the US Navy.

Potential Applications of Carbon Nanotubes in the Navy

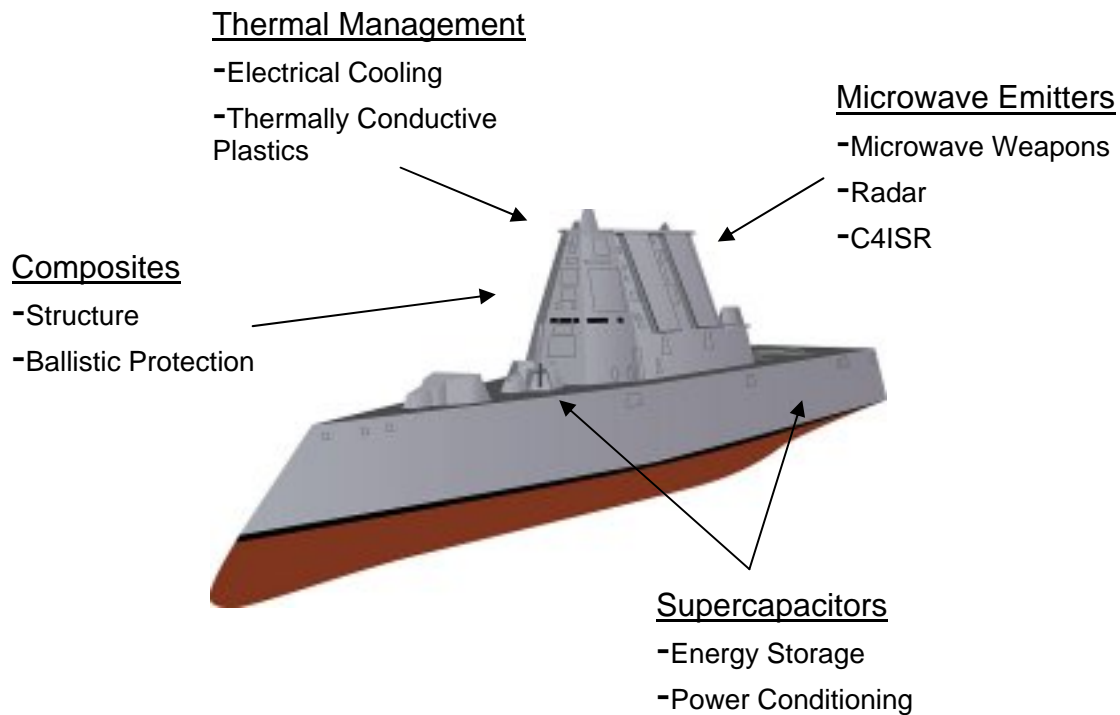


Figure 49: Potential applications of carbon nanotubes in the US Navy
The graphic is the DDG1000 hull form and is used as a representation of the future Navy only. Its use is not meant to imply that CNT technology is present in the DDG1000.

3.2 Electronics

As we move into the 21st Century, the US Navy requires greater and greater electrical loads for radars, communications, and weapons. Theater Ballistic Missile radars may require up to 20 MW of power and over the horizon, cruise missile detecting radars may require greater than 6 MW to operate. Proposals for Electromagnetic (EM) Rail guns could also impose loads on the order of 20 MW. To date, US Navy warships have only carried ship service electrical generating capacity on the order of 10 MW or less. Ships have motors

capable of much more but those motors have been slaved solely to propulsion.[40]

If the Navy is to realize these radars and weapons, then technologies to address power conditioning, energy storage, high power discharge rates, and thermal management of resistive waste heat are required. Table 1 from section 1.2 provides information on electrical and thermal characteristics of CNTs and common materials. The thermal and electrical conductivity of CNTs may provide some solutions if even a fraction of these properties can be preserved in macroscale structures.

3.2.1 Thermal Management

As the Navy moves towards the all electric ship, high energy weapons, and more powerful radars, some studies suggest that electrical thermal loads on the order of 20 MW will require dissipation.[19, 40]

Theory has predicted a maximum thermal conductivity of 6600 W/(m*K) for MWNTs though nothing approaching that value has been achieved. We consider a range of potential thermal conductivities that might be achieved for CNTs in a very basic heat transfer treatment to highlight the potential improvement offered by a high thermal conductivity compound on a notional future warship that must dissipate $Q_{waste} = 20$ MW of waste heat.

Assume a basic electronic model as shown in Figure 50 where we assume that all thermal loads are transferred via conduction to a heat sink and

then via convection to a fresh water heat exchanger. We ignore other modes of heat transfer.

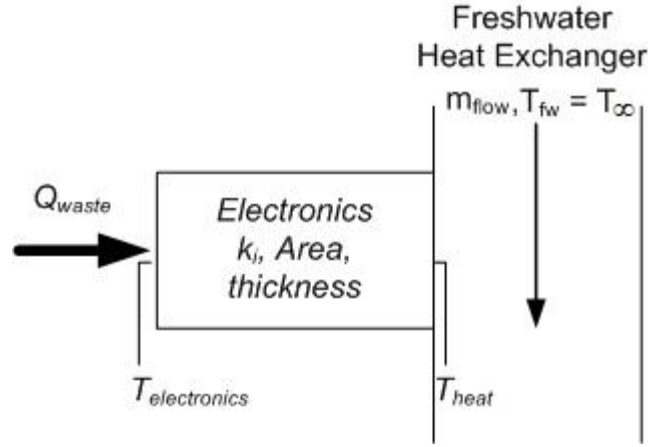


Figure 50: Basic electronic cooling model

This model suggests the following formulas:

$$Q_{waste} = \left(\frac{Area}{thickness} \right) * k_i * (T_{electronics} - T_{heat}) \text{ where } i = Al, CNT \quad \text{Eq (1)}$$

$$\left(\frac{Area}{thickness} \right) * k_i * (T_{electronics} - T_{heat}) = \dot{m}_{flow} * C_{p_fw} * (T_{heat} - T_{fw}) \quad \text{Eq (2)}$$

We compare the thermal conductivity of Aluminum ($k_{Al} = 250 \frac{W}{m * K}$) to a range of thermal conductivity values for a notional CNT heat sink.

$$(k_{CNT} = (250, 500, 1000, 2000, 3000, 6000) \frac{W}{m * K})$$

We consider the following variables to be constant parameters: Q_{waste} and T_{fw} .

Considering Eq (1), if $k_i \uparrow$,

$$Q_{waste}^{\leftrightarrow} = \frac{Area}{thickness} * k_i \uparrow * (T_{electronics} - T_{heat}) \text{ so the temperature delta must drop}$$

or the heat sink size must drop to maintain the equation in balance. Smaller heat

sinks would reduce electronic rack sizes and allow a higher density of electronic cabinet, reducing the volume occupied by electronics and reducing fresh water piping runs. Less piping results in lower head loss, allowing a smaller freshwater pump.

A lower temperature delta could mean a lower electronics interior temperature if we assume the fresh water system holds the heat sink temperature at a given value. This would permit a higher power circuit for a given amount of cooling if temperature is the limiting factor for the circuit.

A lower temperature drop could also result from a reduction in the size of the freshwater system. If the mass flow rate is allowed to drop, then the temperature delta between the fresh water and the heat sink will increase, resulting in a higher heat sink temperature.

Lower fresh water flow rates would mean smaller piping runs and smaller fresh water pumps, which frees up additional space and weight on any ship. Consider an ideal scenario where a heat load of 20 MW is cooled directly by a fresh water flow with ideal efficiency. Assuming a fresh water temperature delta of 7°C (20°F), the required ideal flow rate would be 683 kg/s or 10,820 gallons per minute in the most optimistic scenario. Any significant reduction in flow rates would have profound impacts.

3.2.2 Supercapacitors

The all electric ship concept will require a large amount of energy storage to enable the rapid fire of rail guns and to allow the ship to remain combat ready during casualties. Supercapacitors offer one potential energy storage solution. Additionally, the magnitude of the power loads passed via solid state power conditioners will create 'ripple' currents which can be damped using capacitors. However, current electrolytic capacitors and current polymer capacitors are either very large or very heavy for this application. For instance, an electrolytic capacitor bank sized to 1000 V has a volume density of about 6 F/cm³ with a current density of 50 mA/cm³ and an energy density of .8 J/cm³. [41]

CNTs provide a large surface area with a capacitor separation on the order of a nanometer as opposed to millimeter separations for conventional electrolytic capacitors. This suggests that CNTs might enable very capable capacitors. As would be expected, SWNTs and MWNTs in general produce different capacitances and the treatment of the CNTs also affects the overall results. Experiments have produced capacitors with capacitances from 2.2-283F/g. [3, 22] A power density of 20 kW/kg and an energy density of about 7 W*hour/kg were produced in one experiment.[3] Additionally, discharge rates on the order of 10 mS have been observed. The maximum voltage in any of these experiments was 10 V so no direct comparisons are possible but these results do suggest that further research into creating CNT supercapacitors is warranted.[16, 22]

3.2.3 Polymer Composites

The US military pioneered the research and development of composite technologies for use in high performance areas such as space craft, missiles, and jet aircraft. Today, the Navy is building radar cross section reducing mast enclosures and the new DDG1000 design calls for a deckhouse constructed of composites[19]. Kevlar is credited with saving hundreds of lives by containing the debris caused by the impact of an airliner into the Pentagon on September 11, 2001. Composite body armor saves lives everyday within the military.

Composites probably offer the most likely area where CNT technology will make the great contribution. Manufacturers currently offer plastics with CNTs dispersed in the matrix to provide electrostatic charge dissipation.

At root, individual CNTs have the highest combination of specific strength and stiffness of any known substance and CNTs can be grown to the millimeter scale so they are natural composite fibers if means to mass produce them in a cost effective way can be found and if effective means to incorporate them in resin matrixes can be discovered. Many of the research efforts focus on ways to effectively disperse the CNTs within the resin matrix.

Composites can be produced by several manufacturing methods including coagulation, melt spinning, dry spinning, and direct injection to name a just a few. Experiments with CNT composites span the field of manufacturing methods. The purpose of this thesis is not to explain the many ways to create composites so I will only summarize some of the intriguing results and potential applications.

Zhang et al. report on a process by which they treat CNTs as yarn and spin a CNT fiber. Knitting wool consists of taking cm long fibers and twisting them to make a continuous fiber. Zhang and his group instead take CNTs with lengths on the order of hundreds of micrometers and spin them to form a strong composite yarn. In 2004, Zhang reported creating CNT yarns that exhibited strains at failure of up to 13% and strengths on par with many steels. When impregnated with a PVA resin, strength could be increased to 850 MPa though strain-to-failure dropped to a still respectable 3%. Though nowhere near the theoretical value for electrical conductivity of CNTs, the plain CNT yarn achieved an electrical conductivity of 3000 S/cm². The conductivity dropped to about 2000 S/cm² when the yarn was impregnated with PVA. Toughness close to Kevlar and a tolerance to knotting were also demonstrated.[9] A year later, Zhang et al reported on the ability to create transparent sheets from the spun CNT fibers. Table 2 summarizes the results for the yarn strands and the sheets.

Zhang's process draws the CNTs directly from MWNT forests grown by CVD. The yarns were spun from MWNT forests of not greater than 300 μm in height. However, Zhang points out that the ratio of yarn strength to fiber strength is governed by the helical angle, the fiber length, and the fiber diameter as well as a few other parameters.[9, 42]

$$\sigma_{yarn} / \sigma_{fiber} \approx \cos^2 \alpha * [1 - (k * \csc \alpha)]$$

where

$$k = \frac{\left(\frac{d * Q_m}{\mu} \right)^{1/2}}{3 * L_{fiber}}$$

and

$$\alpha = \arctan(Tw * \pi * D_{yarn})$$

| | |
|-------------------------|--|
| $\alpha \equiv$ | Helical angle of the fiber yarns about the yarn axis |
| $d \equiv$ | Fiber diameter |
| $\mu \equiv$ | Inter-fiber coefficient of friction |
| $L_{fiber} \equiv$ | Fiber length |
| $Q_m \equiv$ | Fiber migration length |
| $D_{yarn} \equiv$ | Yarn diameter |
| $\sigma_{yarn} \equiv$ | Tensile strength of the yarn |
| $\sigma_{fiber} \equiv$ | Tensile strength of the fiber (CNT) |
| $Tw \equiv$ | Yarn twist in turns/meter |

Note that as $k \downarrow$, the fiber strength ratio improves and $k \downarrow$ when $L_{fiber} \uparrow$

and when $d \downarrow$. Enabling researchers to discover processes to control for CNT diameter and to increase fiber length are both objects of the SabreTube and the Nanosled.

CNT composite research has also discovered composites with high toughness and high strain, indicating the potential to use CNT composites for ballistic protection.

The potential strength, stiffness, and toughness of CNT composites are sufficient reasons to invest in basic research into CNTs. Combining these

composites with CNT electrical properties could truly revolutionize naval applications. One paper suggests that the DDG1000 deckhouse will weigh approximately 500 tons and the deckhouse will incorporate planar arrays for radar and communications antennas.[19] It turns out that CNTs can act as field emitters. Current densities of up to 5 A/cm^2 have been observed, well above the $.5 \text{ A/cm}^2$ required for commercial microwave transmitters. If composites that act as microwave emitters can be developed, then planar arrays and deckhouses may be further integrated.[3]

The National Research Council, in a report prepared for the Department of Defense, noted that a key challenge for high performance composites is lowering the manufacturing cost. This once again points to the need to develop tools that enable us to understand the process of CNT growth and tailor CNT growth to meet specific composite requirements.

Part Four: Results, Future Work Recommendations and Conclusions

4.1. Results

4.1.1. SabreTube

The SabreTube successfully meets all design requirements as listed in Sections 2.2.1-2.2.3. Initially, the furnace required a 'burn-in' or conditioning period that is not well understood. After about a day of use, consistent growth results were achieved.

The users successfully grew CNTs (Figure 51), measured *in situ* CNT length (Figure 52), and monitored *in situ* temperature at the substrate (Figure 53). Dr. Hart has achieved 3 mm of growth in ten minutes, his fastest growth to date.



Figure 51: CNT growth in the SabreTube

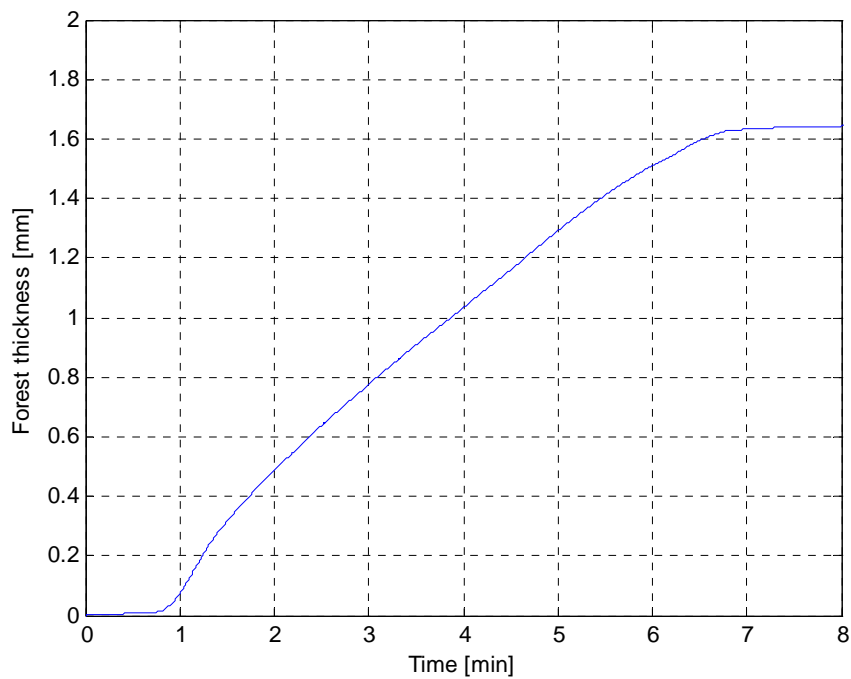


Figure 52: *In Situ* measurement of CNT length over time

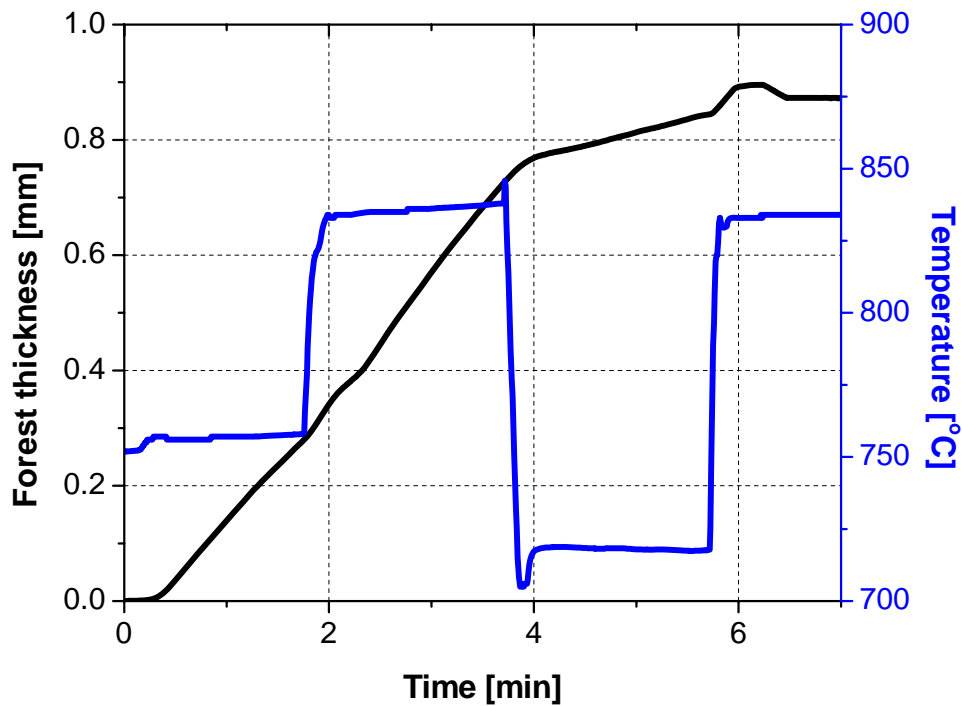


Figure 53: *In Situ* measurement of temperature and forest thickness over time

The SabreTube also enabled the first ever small angle x-ray scattering (SAXS) measurement of CNT diameter during growth. Dr. Hart measured both

length and diameter during growth using the method in [35]. The results from this study were unavailable by the time this thesis was written but will be published in the near future. Figure 8 shows the SabreTube installed in the SAXS machine.

4.1.2. Nanosled

To date, the Nanosled has not been used in any experiments. The apparatus has been tested to verify functionality but no continuous growth experiments have been conducted. These experiments should be conducted in the near future.

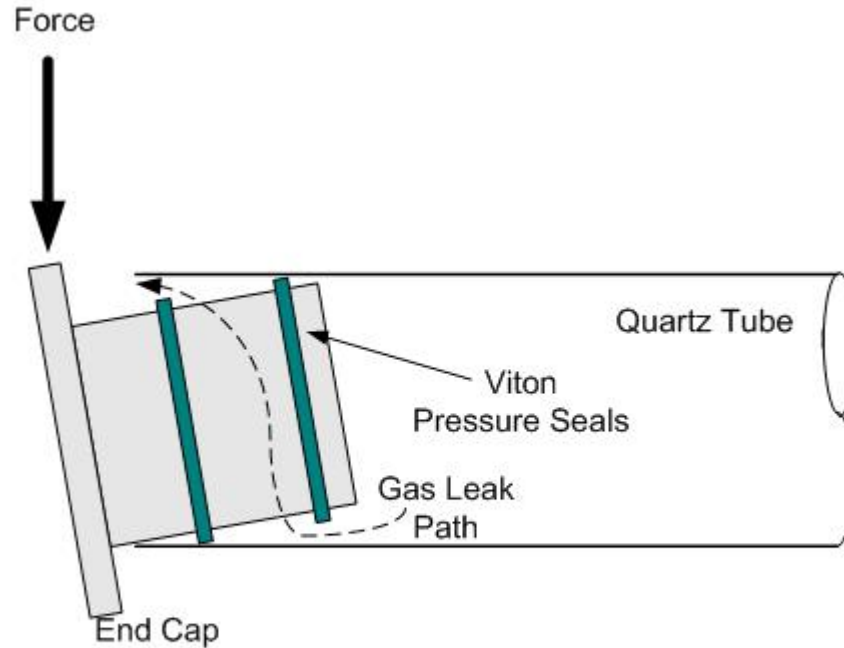
4.2. Future Work Recommendations

4.2.1. SabreTube Future Design Refinements

This section details recommended next steps in the evolution of the SabreTube design. Time did not permit the full exploration of these ideas. The electrical interlock recommended in section 4.2.1.4 is the only critical design recommendation.

4.2.1.1. Gas Sealing

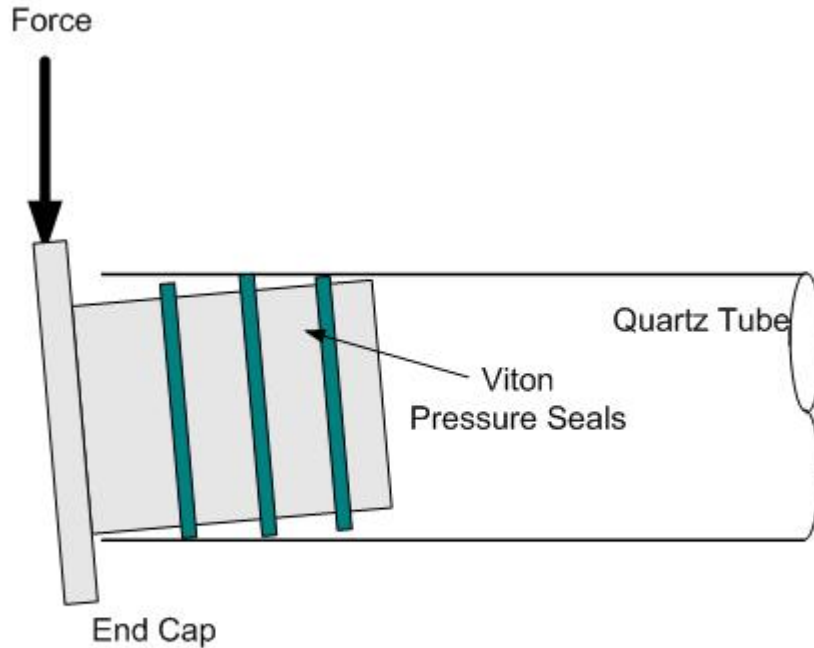
The double row Viton Lip seal has been proven through use in proximity to a hazardous gas detector to contain all gases inside the reactor tube. However, mechanical testing has shown that, if a moment is applied to the end cap, the two Viton seals can act as pivot points and a small gap can be created as shown in Figure 54.



Note: End Cap displacement is not to scale. Drawing is exaggerated for illustrative purposes.

Figure 54: Potential leak path when a moment is applied to a two seal end cap

Adding a third Viton lip Seal and/or adding spacing between the lip seals would help mitigate against the unusual case of a significant force applied at the end cap (Figure 55). Greater force would be required to create a gap at the seals and more of a labyrinthine path would be required for the gas to escape. At lower forces, two of the seals should always have contact.



Note: End Cap displacement is not to scale. Drawing is exaggerated for illustrative purposes.

Figure 55: An end cap with three Viton lip seals adds additional protection against leaks

4.2.1.2. Substrate Clip Design

The steel blocks using a screw and spring washer to provide compressive force is adequate to give good electrical contact to the silicon heater but a spring clip design could make substrate heater loading even easier for the user and might improve electrical contact. An anodized aluminum heat clip was attempted but the temperatures at the electrode caused creep and the clip lost its flexural stiffness after a few uses. Spring Steel clips also failed under the temperature conditions and a flat spring and metal clip manufacturer stated that he could not make flat spring clips able to function at 500°C.

Research is required to see if metals such as Inconel could be adapted to use as a spring clip for clamping the substrate.

4.2.1.3. Quartz Tube Retraction

Experience with the SabreTube prototype shows that the quartz tube will smoothly slide off the front end cap when a rocking twist motion is used to ease off of the Viton seals. If the user is not careful to apply a light downward force, the tube can shift upwards just a bit as it retracts and slides off the Lip seals. Experienced users will quickly become accustomed to the retraction technique but a simple refinement might remove this concern, improving the novice user experience.

Placing an arch or crossbar above the tube with a spring-loaded roller in contact with the quartz tube would provide a slight downward force and aid in keeping the tube aligned as it is retracted or shut. Some experimentation is required to see if a wheel roller, a ball transfer, or some other form factor would be best.

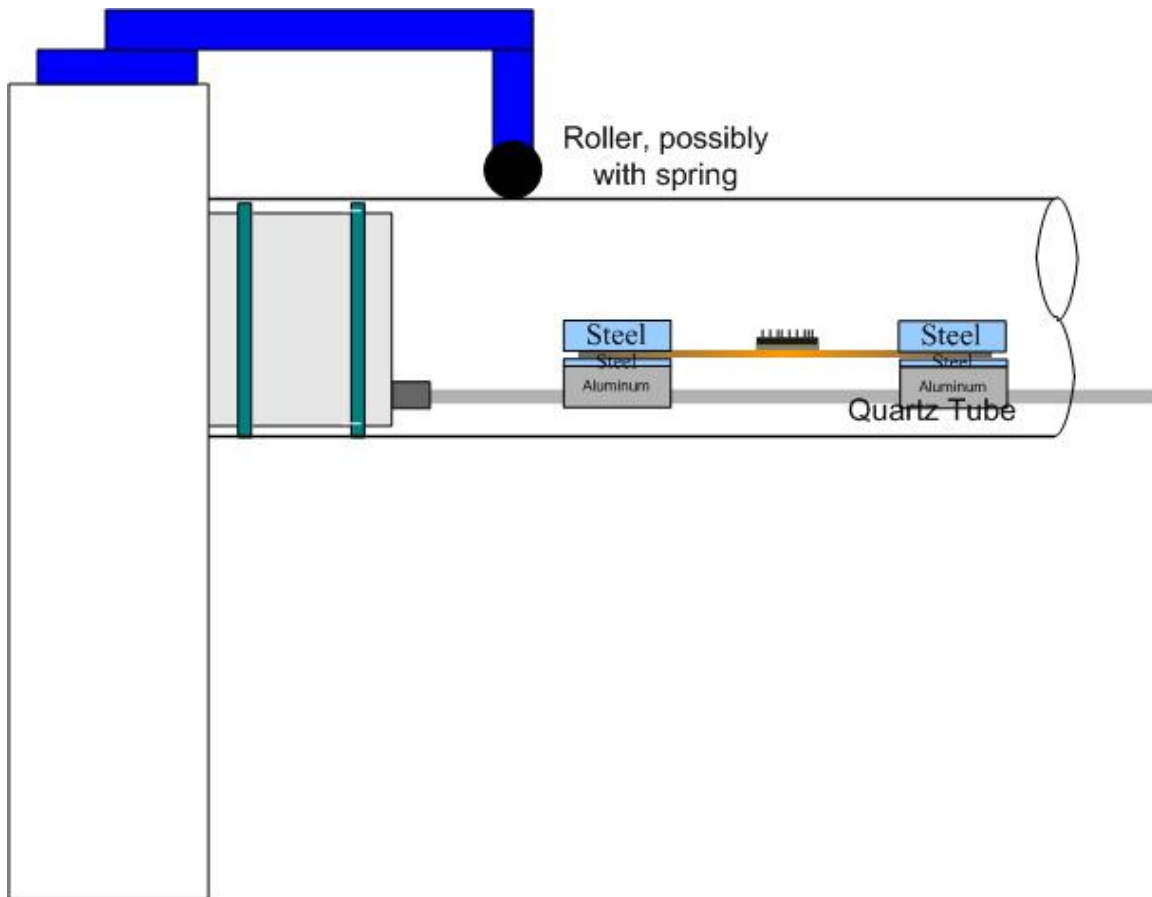


Figure 56: Possible mechanism for aiding in quartz tube alignment during retraction

4.2.1.4. Electrical Safety

As noted in Section 2.2.5.7.2, only procedural compliance guards against the user making contact with an energized substrate heater. A preferable solution would place an electrical interlock that cut off power if the quartz tube is not covering the substrate heater.

Ball transfer or snap action switches such as those shown in Figure 57 and Figure 58 could easily be fit to the front end cap. Placing one of these switches in series with the wiring for the substrate heater guarantees that the tube is covering the substrate heater.

Alternatively, the interlock could be placed on one of the aluminum support rails or above the quartz tube on the crossbar proposed in Section 4.2.1.3.



Figure 57: Ball transfer switch



Figure 58: Snap action switches

4.2.1.5. Footprint Reduction

The SabreTube already has a small footprint but there are opportunities to reduce the footprint even further. Currently, the Conax-Buffalo power sealing gland and the stainless steel pipe extend out from the pegboard. The combined stack length of the stainless steel pipe, sealing gland, front cap, reactor tube, and rear cap is determined by the length of the alumina rails and the space required to tilt the tube to lift it out of the rails and clear the rear angel bracket without striking the alumina rails or substrate heater assembly.

This distance is required because the one inch clearance slit shown in Figure 32 does not extend all the way to the top of the right angle bracket. If this slit did extend the full distance, then the retracted quartz tube could be lifted vertically from the aluminum support rails rather than tilted and carefully slid out.

The Alumina rails can also be easily shortened by simply ordering shorter rails. The reactor currently employs 8 inch long rails but the minimum distance is only governed by the maximum substrate wafer length desired. Currently, the substrate heater assembly only requires about 6 inches of length. Testing will be required to see if the temperature of the lip seals rises unacceptably for a shorter tube.

Either or both solutions together would allow the angle brackets to be positioned closer to one another. Prototyping will be required to see if all elements can be brought within the pegboard footprint. If all elements can be brought within the footprint, this would enable selling the system with an optional clear Plexiglas enclosure that could mount directly to the pegboard. This

enclosure could protect the system when not in use or may have other uses such as a secondary pressure boundary if it is ever required or desired.

4.2.1.6. Vertical Tube Holder

Presently four bolts with rubber heads provide a snug fit to the reactor tube when the tube is mounted vertically. Replacing these four bolts with a plastic conical plug with a bottom flange would provide a snug vertical mount and provide protection from a rough landing of the quartz tube against the aluminum pegboard.

4.2.1.7. Material Changes

Currently steel 'E' clips are used to route the substrate heater wires internal to the reactor. These clips probably interact with the hydrogen during the first several uses to produce methane and weaken the clip (see Section 2.1.2), introducing some error into experiments. Stainless steel or aluminum 'E' clips, if they can be found, would eliminate this concern.

4.2.1.8. Temperature Feedback Control

Though the Omega i32 temperature display / controller was installed, the control features were never used or verified as optimal for the CVD system. The substrate heater system has been found to be capable of 100°C/s temperature gradients, requiring a controller with a time constant capable of properly damping

temperature changes rather than always following the temperature change in a closed loop system.

A controller should be capable of:

- Reading a K type thermocouple analog signal from either the IR sensor or the thermocouple
- Controlling up to 10 A of DC current between 15-100 V_{DC}. (The silicon substrate heater is stable when the current is controlled vice the voltage.)
- Managing a 100°C/s temperature gradient
- Storing and managing programmed temperature profiles of up to an hour in length

4.2.1.9. Outgas Testing and Conditioning

Despite care in material selection, initial growths in the SabreTube were disappointing. Dr. Hart tried several processes known to produce good CNT growth with little success for the first few days of use. After these first few days, he observed good growth with the same processes. It is believed that both the reactor tube and the preheater tube required a 'burn-in' or conditioning period but it is not well understood. It seems that basic CVD systems like the one in Figure 4 also require a burn-in period for high-purity chemistry experiments.

Testing is required to try and understand what causes this need for conditioning and to determine whether different materials would remove this

need, whether the system will require conditioning prior to shipping, or whether a burn in procedure should be suggested in the system instruction manual.

4.2.2. Nanosled Future Work and Refinements

4.2.2.1. Increase the box CVD size

The Nanosled was constrained in size by a preexisting box furnace design. This limits the length of the crab flexures, the length of the silicon substrate sled, and time an experiment can run at a given motor rotational rate. In order to increase experimental flexibility, I recommend constructing a larger box furnace designed to accommodate continuous manufacturing experiments.

Increasing length in the axis of travel for the silicon sled allows for a longer growth zone or for a longer silicon sled travel during the course of the experiment.

Increasing the length of the box so that a wider fixture can be accommodated allows for a longer flexure arm. Stress is proportional to the inverse of length squared and is directly proportional to deflection. Therefore, a longer flexure allows a much greater deflection in case the user would like to experiment with thicker substrates.

4.2.2.2. Install Graphalloy Bushings

The Nanosled currently fastens a wire to a shaft and allows the wire to wrap around the shaft as the shaft turns. A graphalloy bearing could be installed. These bearings conduct electricity while allowing the shaft to turn. This would avoid wire wrapping.

4.2.2.3. Continuous Harvesting

If continuous growth can be achieved, then a method to continuously harvest the CNTs from the substrate will be required. If the method can also treat the substrate to allow for regeneration of the substrate to regrow CNTs then a cheaper process would result. If a circular ring instead of a linear substrate could be used then the substrate would never have to be reloaded.

This may also require a way to pass the substrate through separate atmosphere zones if the growth, harvesting, and regeneration require different chemical atmospheres.

4.3. Conclusions

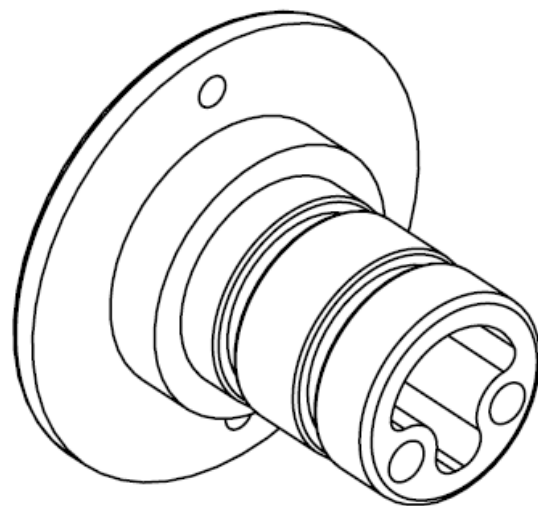
A CVD system, the SabreTube, consisting of a suspended resistively heated substrate with optical, infrared, and mechanical access was designed and built. The SabreTube has proven much easier to load and has already enabled experiments that have not been possible in the past. The SabreTube's relatively low production cost will enable many research groups to obtain this device for research.

A fixture system, the Nanosled, to enable translation of a silicon wafer through a growth zone was also designed and built. The device will enable researchers to experiment with continuous growth processes of CNTs produced via thermal CVD.

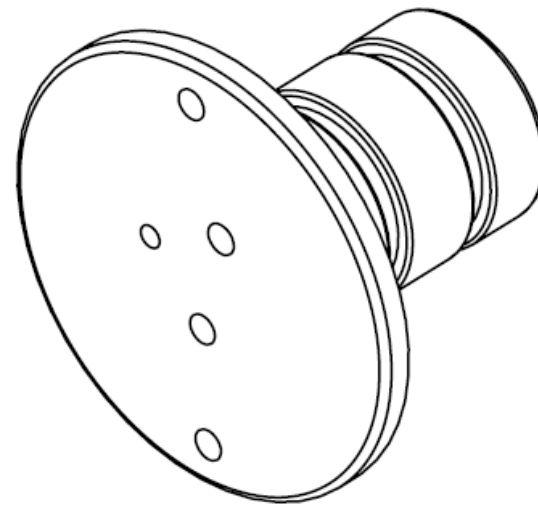
Several potential applications of CNTs would benefit the Navy. Yarn based composites seem very promising and may merit further research by the Navy. Supercapacitors are also promising and deserve research funding.

Even if these applications can be provide in the laboratory, research is required in growth and manufacturing processes to reduce the cost of CNTs. This step is critical if the Navy is to be able to afford a 313 ship force.

Appendix A: SabreTube Technical Drawings

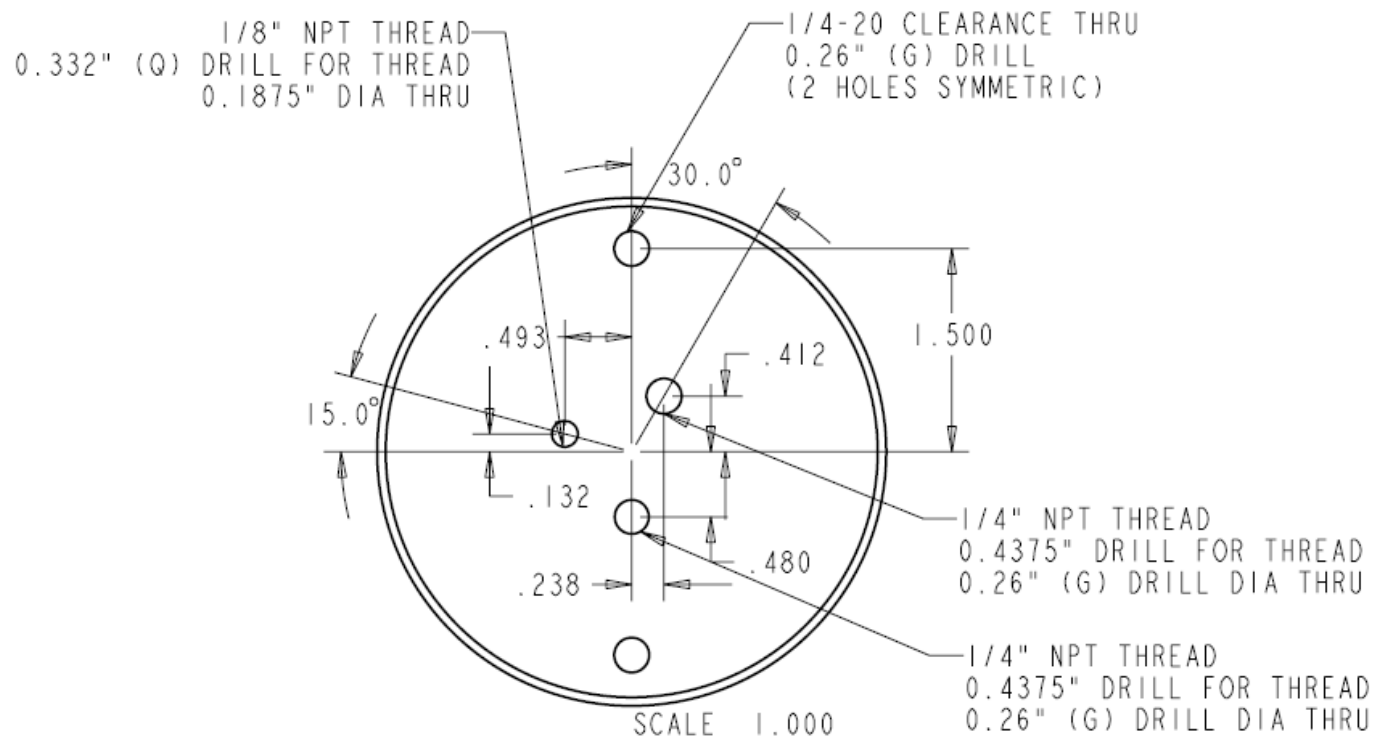


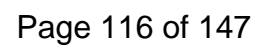
SCALE 1.000

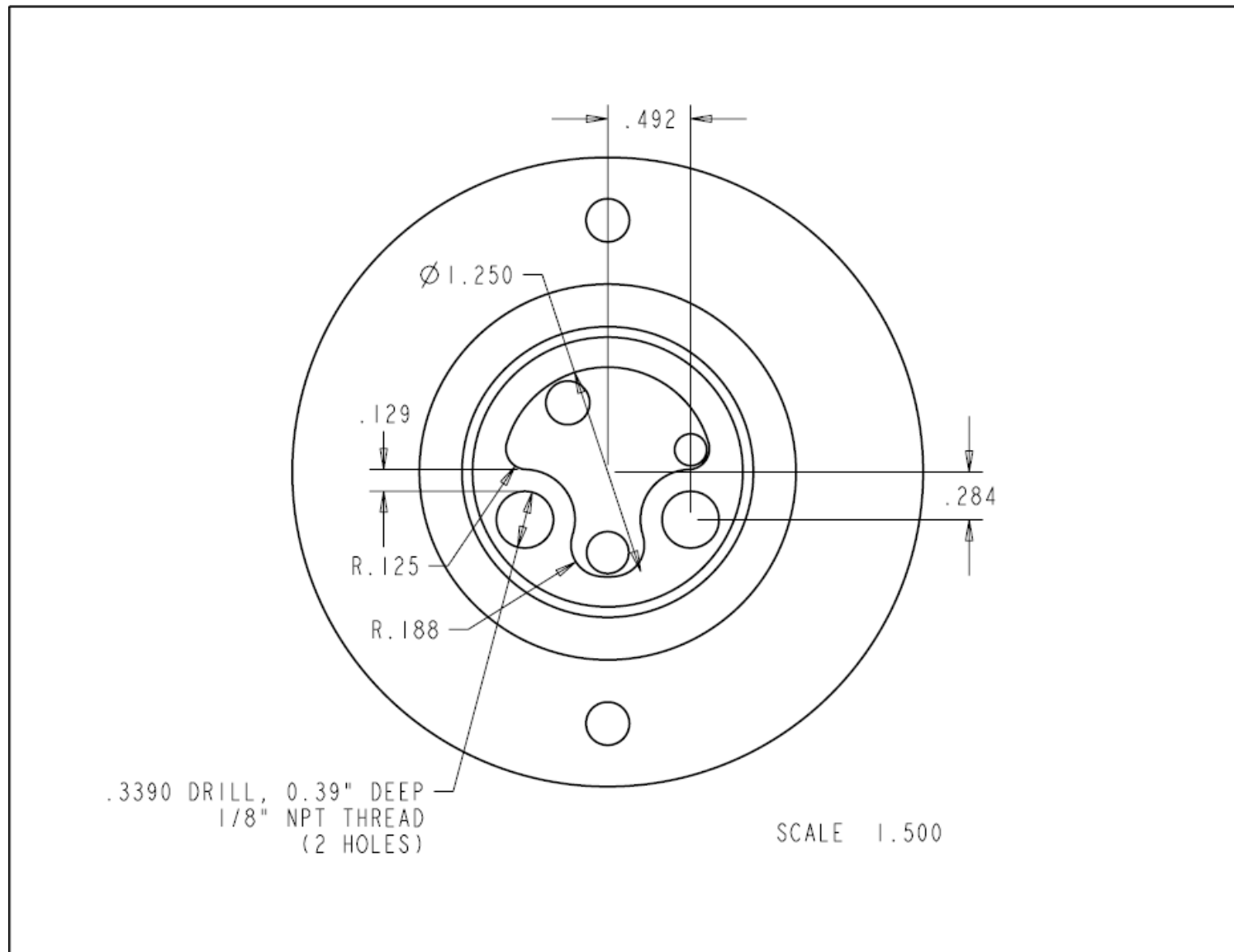


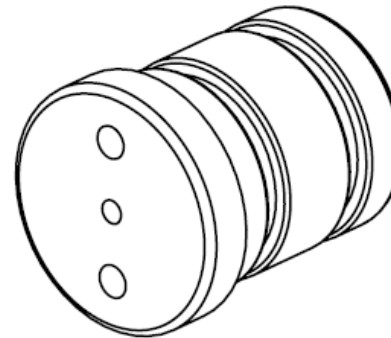
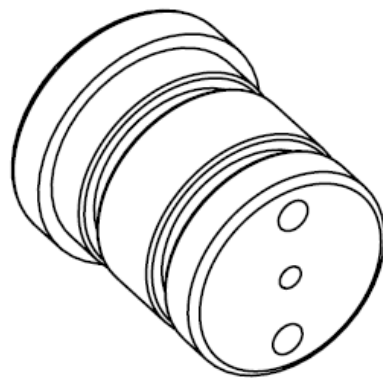
SCALE 1.000

FRONTCAP
6061 ALUMINUM
AJHART@MIT.EDU, 617.319.9617, JAN/31/07
ALL DIMENSIONS INCHES



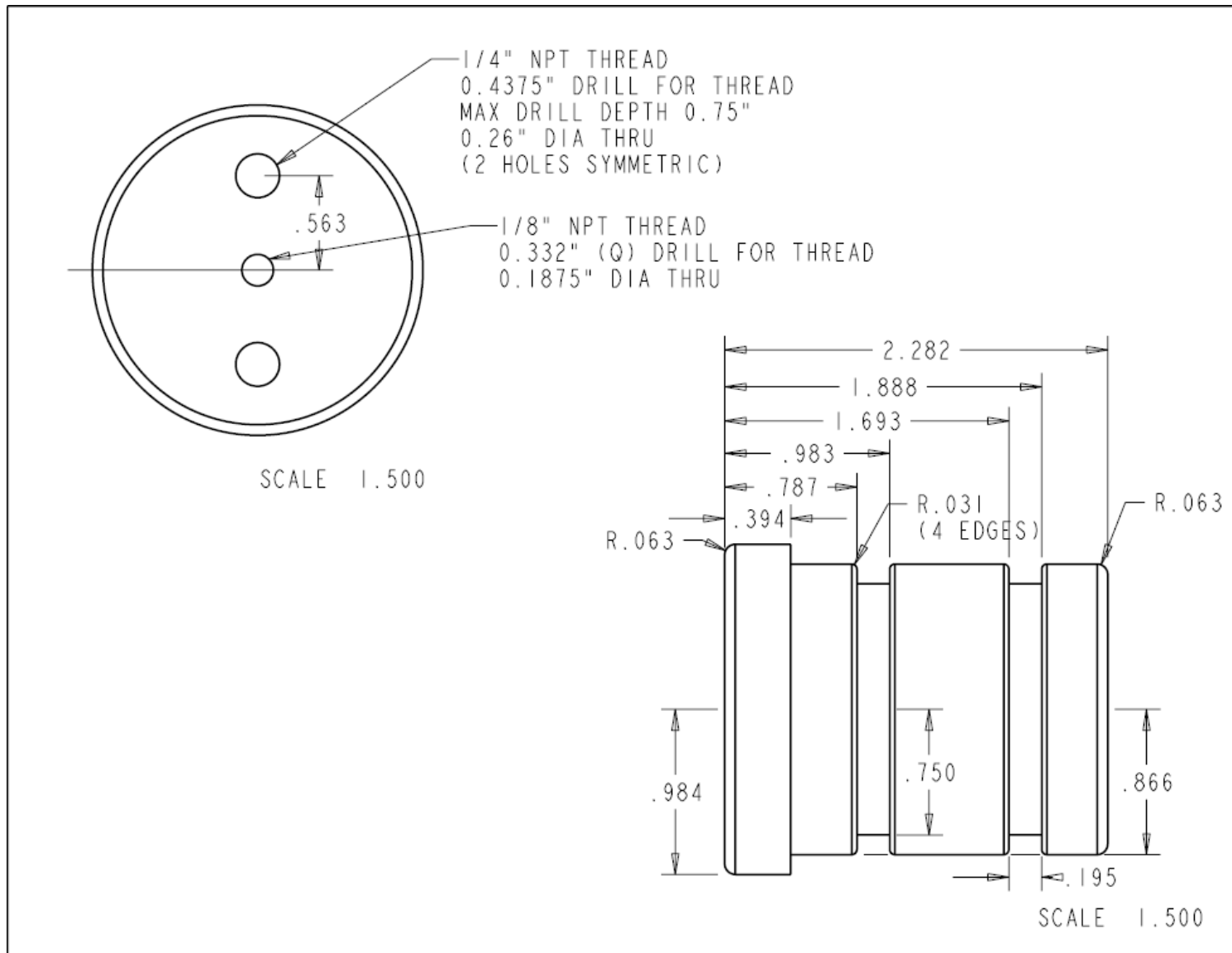


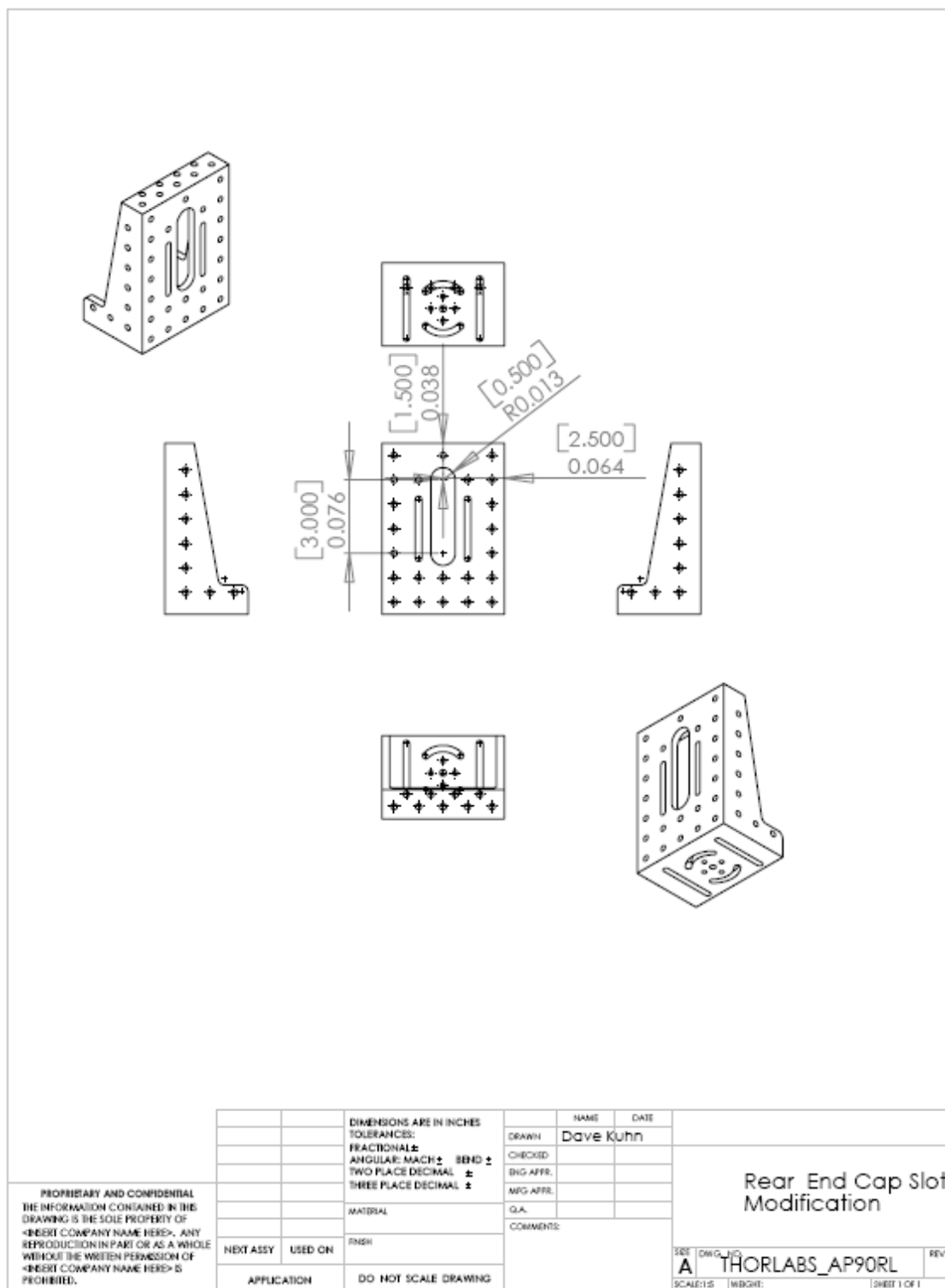


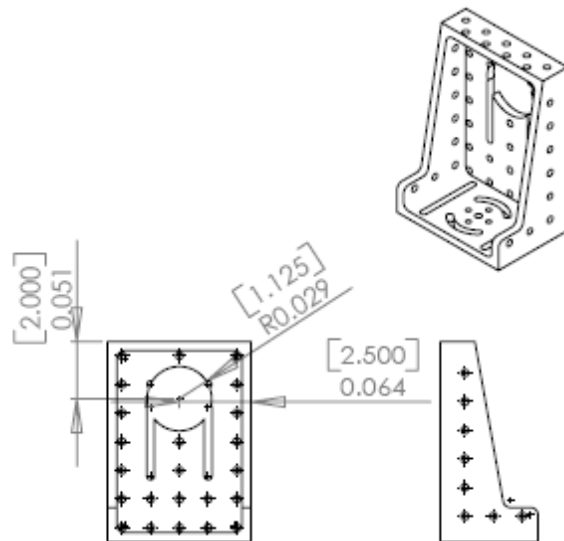


SCALE 1.000

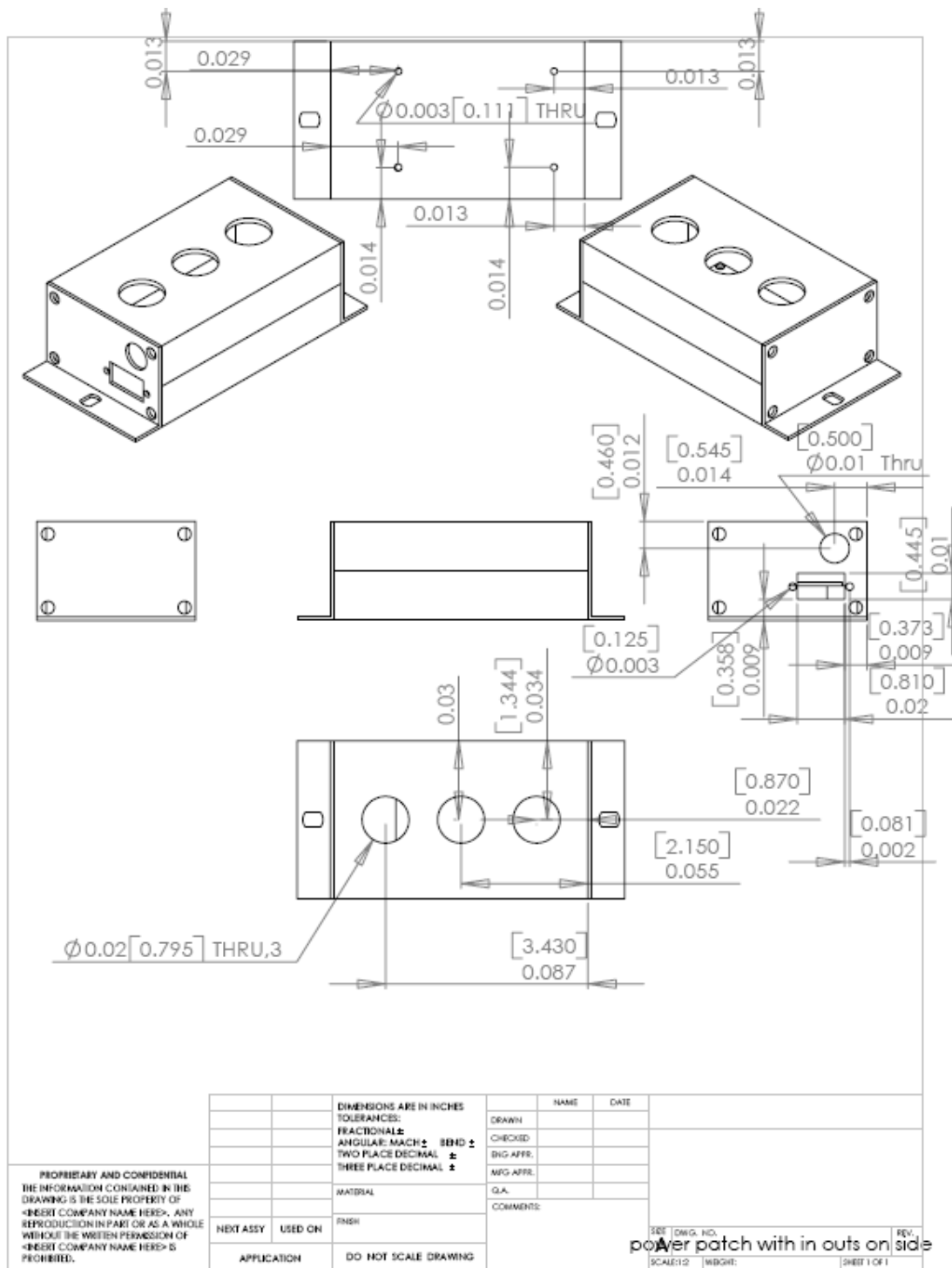
REARCAP
6061 ALUMINUM
AJHART@MIT.EDU, 617.319.9617, JAN/31/07
ALL DIMENSIONS INCHES

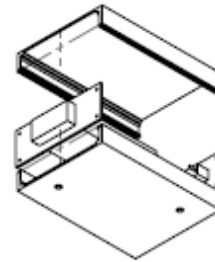
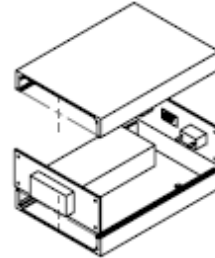
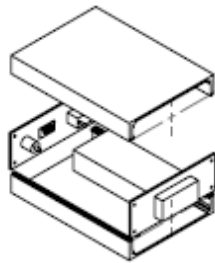






| | | | | | |
|--|---------|---|----------------------|--|--------------|
| PROPRIETARY AND CONFIDENTIAL THE INFORMATION CONTAINED IN THIS DRAWING IS THE SOLE PROPERTY OF <INSERT COMPANY NAME HERE>. ANY REPRODUCTION IN PART OR AS A WHOLE WITHOUT THE WRITTEN PERMISSION OF <INSERT COMPANY NAME HERE> IS PROHIBITED. | | DIMENSIONS ARE IN INCHES TOLERANCES: FRACTIONAL ± ANGULAR: MACH ± BEND ± TWO PLACE DECIMAL ± THREE PLACE DECIMAL ± | | NAME Dave Kuhn | DATE |
| | | MATERIAL | | CHECKED | ENG APPR. |
| | | FINISH | | MFG APPR. | Q.A. |
| | | COMMENTS: | | Right Angle Bracket Modified to Hold Front End Cap | |
| NEXT ASSY | USED ON | APPLICATION | DO NOT SCALE DRAWING | FILE: C:\DWG\JUN AUTHORLABS_AP90RL_BORE | |
| | | | | SCALE: 1:15 | SHEET 1 OF 1 |



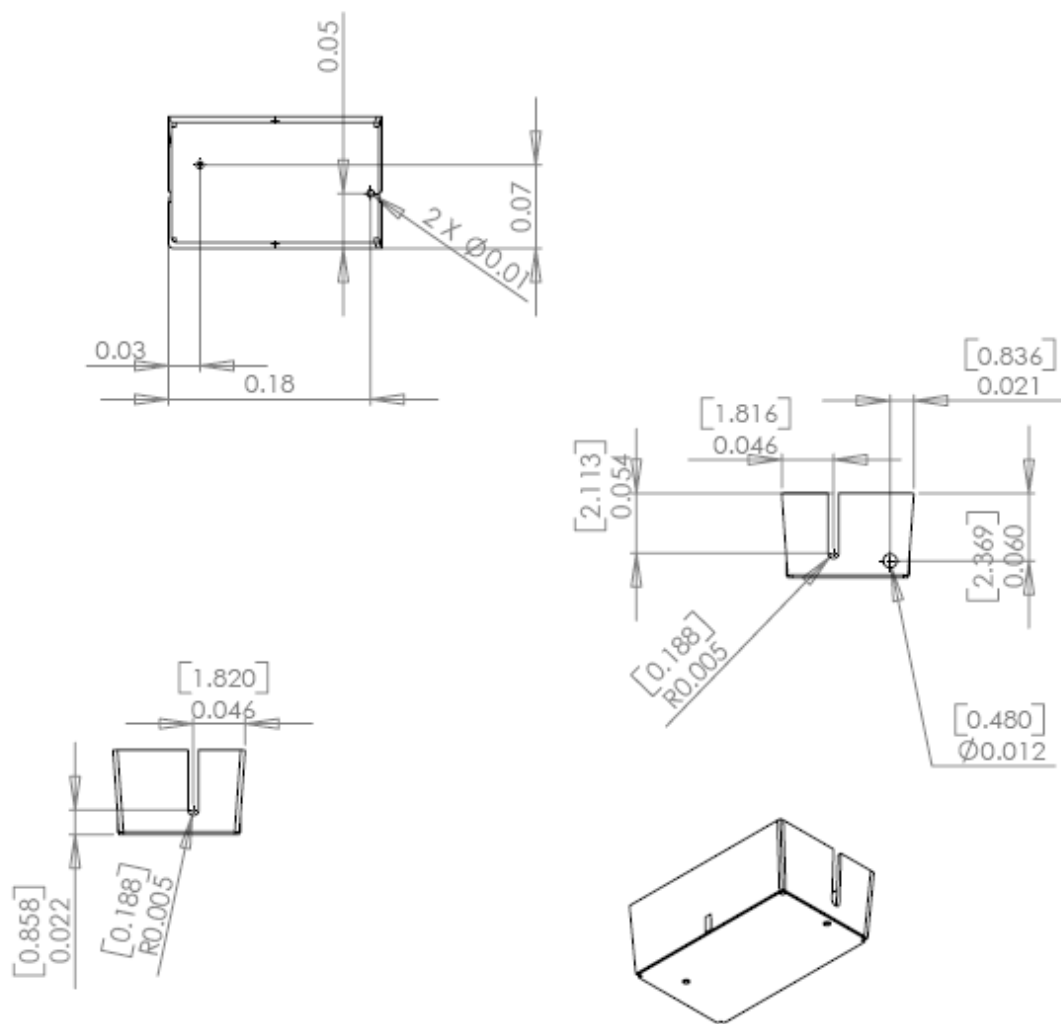


PROPRIETARY AND CONFIDENTIAL
THE INFORMATION CONTAINED IN THIS
DRAWING IS THE SOLE PROPERTY OF
<INSERT COMPANY NAME HERE>. ANY
REPRODUCTION IN PART OR AS A WHOLE
WITHOUT THE WRITTEN PERMISSION OF
<INSERT COMPANY NAME HERE> IS
PROHIBITED.

| | | | | | |
|-------------|----------------------|---|------------|---------|---|
| | | DIMENSIONS ARE IN INCHES TOLERANCES: FRACTIONAL ± ANGULAR: MACH ± BEND ± TWO PLACE DECIMAL ± THREE PLACE DECIMAL ± | NAME | DATE | Temperature Display Exploded View |
| | | | DRAWN | | |
| | | | CHECKED | | |
| | | | ENG APPR. | | |
| | | | MFG APPR. | | |
| | | MATERIAL | Q.A. | | SEE DWG. NO. temp display unit exploded view |
| | | FINISH | COMMENTS: | | |
| NEXT ASSY | USED ON | | | | |
| APPLICATION | DO NOT SCALE DRAWING | | SCALE: 1:5 | W/IGHT: | REV. SHEET 1 OF 1 |

Temperature Display
Exploded View

SEE DWG. NO. **tenAp display unit exploded view** REV.
SCALE: 1:1 WEIGHT: SHEET 1 OF 1



PROPRIETARY AND CONFIDENTIAL
THE INFORMATION CONTAINED IN THIS
DRAWING IS THE SOLE PROPERTY OF
<INSERT COMPANY NAME HERE>. ANY
REPRODUCTION IN PART OR AS A WHOLE
WITHOUT THE WRITTEN PERMISSION OF
<INSERT COMPANY NAME HERE> IS
PROHIBITED.

| | |
|--------------------------|---------|
| DIMENSIONS ARE IN INCHES | |
| TOLERANCES: | |
| FRACTIONAL | ± |
| ANGULAR | MACH ± |
| TWO PLACE DECIMAL | ± |
| THREE PLACE DECIMAL | ± |
| MATERIAL | |
| NEXT ASSY | USED ON |
| FINISH | |
| APPLICATION | |
| DO NOT SCALE DRAWING | |

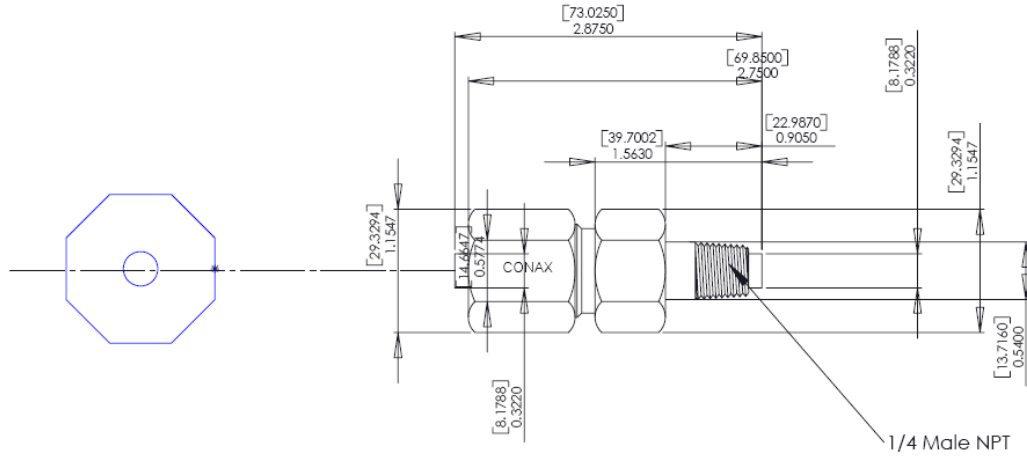
| | |
|-----------|------|
| NAME | DATE |
| DRAWN | |
| CHECKED | |
| ENG APPR. | |
| MFG APPR. | |
| Q.A. | |
| COMMENTS: | |

Enclosure Modifications
for Preheater

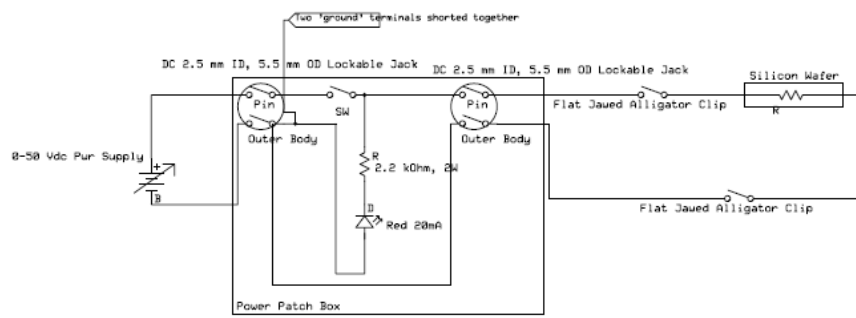
REV. 01/15/15
Preheater bottom enclosure
SCALE: 1:1 WEIGHT: SHEET 1 OF 1

Conax Buffalo Power Sealing Gland

Part # PL(PM2)-18(1K/2ALUMEL)-A4-T, 12"/12", WITHIN 1" OF THE NPT BUTT WELD 20 AWG TYPE K LEADS
AND 18 AWG ALUMEL LEADS AND REINSULATED WITH FIBERGLASS SLEEVING

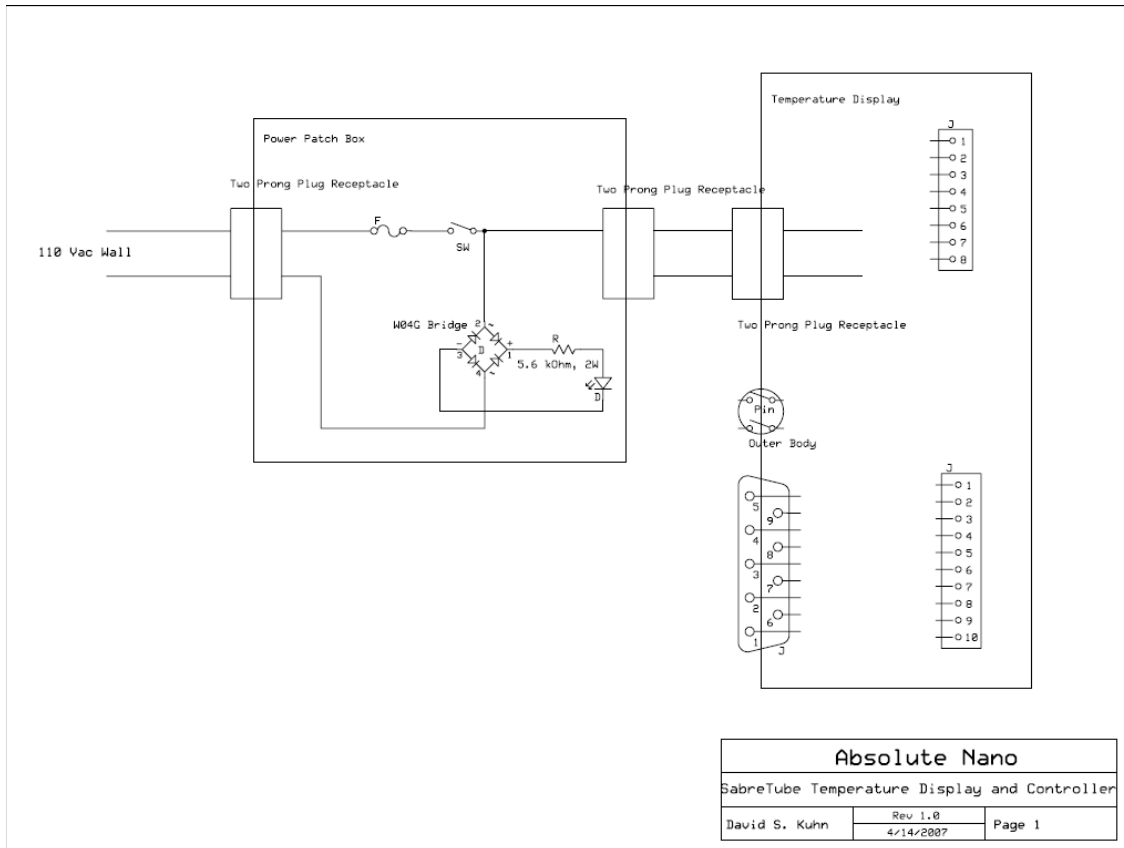


Appendix B: SabreTube Electrical Schematics

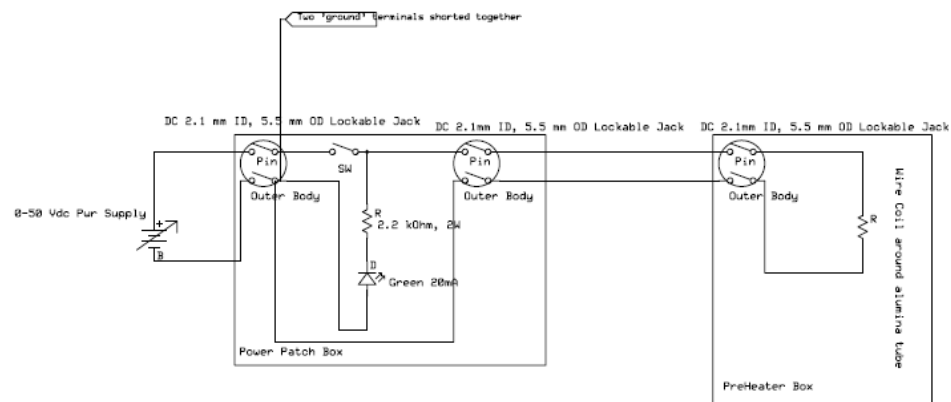


20 or 22 AWG for LED; 18 AWG for all other

| Absolute Nano | | |
|--------------------------|----------------------|--------|
| SabreTube Silicon Heater | | |
| David S. Kuhn | Rev 1.0 4/14/2007 | Page 1 |



C:\Documents and Settings\Administrator\My Documents\MIT\ NanoTube Furnace\FlowCell\circuits\SabreTube Electronic Circuits.sch - Sheet3



20 or 22 AWG for LED; 18 AWG for all other

| Absolute Nano | | |
|--------------------------|-----------|--------|
| SabreTube Gas Pre-Heater | | |
| David S. Kuhn | Rev 1.0 | Page 1 |
| | 4/14/2007 | |

Appendix C: SabreTube Parts and Cost Spreadsheet

| Item | Sub-Component ID | Supplier | ID # | Unit price | items per unit | Cost per item | # items per System | System total |
|---|------------------|------------------|--|------------|----------------|---------------|--------------------|--------------|
| #8-32 Cap Screws, nuts, and washers | Fasteners | Thorlabs | HW-KIT1 | 50.00 | 200 | \$0.25 | 12 | \$3.00 |
| 1/4"-20 Cap Screws, nuts, and washers | Fasteners | Thorlabs | HW-KIT2 | 99.00 | 200 | \$0.50 | 32 | \$15.84 |
| Optical breadboard baseplate, 12x24"x1/2", 1/4"-20 threaded | Fixture | Thorlabs | MB1224 | 297.16 | 1 | \$297.16 | 1 | \$297.16 |
| Right angle mounting bracket | Fixture | Thorlabs | AP90RL | 123.00 | 1 | \$123.00 | 2 | \$246.00 |
| Support rails (outer tusks), total length 12" | Fixture | Thorlabs | TR12 | 11.39 | 1 | \$11.39 | 2 | \$22.78 |
| Lip Seals, Type&Style BV, lip code V | Front End Cap | Chicago Rawhide | 721556 | 12.79 | 1 | \$12.79 | 2 | \$25.58 |
| Front End Cap Manufacturing | Front End Cap | custom - MIT CMS | | 541.00 | 1 | \$541.00 | 1 | \$541.00 |
| Alumina support rods (inner tusks), 0.1875" dia, 8" length | Front End Cap | Vesuvius McDanel | AXR-1292-B (+specify length) | 4.77 | 1 | \$4.77 | 2 | \$9.54 |
| SS Male BT 1/8 in NPT to 3/16 in for tusk holder | Front End Cap | Swagelok | SS-300-1-2BT | 7.30 | 1 | \$7.30 | 2 | \$14.60 |
| 3/16" Steel E Clips | Front End Cap | | | 0.25 | 1 | \$0.25 | 2 | \$0.50 |
| Front end cap stock, Al 6061, 4"dia, 6" long | Front End Cap | McMaster | 1610T43 | 57.47 | 1 | \$57.47 | 1 | \$57.47 |
| Power Sealing gland | Front End Cap | Conax-Buffalo | PL(PTM2)-18(1K/2ALUMEL)-A4-T, 12"/12", WITHIN 1" OF THE NPT BUTT WELD 20 AWG TYPE K LEADS AND 18 AWG ALUMEL LEADS AND REINSULATED WITH FIBERGLASS SLEEVING | 349.00 | 1 | \$349.00 | 1 | \$349.00 |
| 2.5 mm DC Plug (power for substrate heater) | Front End Cap | Philmore | | 2.90 | 1 | \$2.90 | 1 | \$2.90 |
| 2.1 mm DC plug (for Thermocouple) | Front End Cap | Philmore | | 2.90 | 1 | \$2.90 | 1 | \$2.90 |

| Item | Sub Component ID | Supplier | ID # | Unit price | items per unit | Cost per item | # items per System | System total |
|--|---------------------|----------|------------------|------------|----------------------|------------------|--------------------------|--------------|
| Stainless Steel Ultra-Torr Vacuum Fitting, Male Connector, 1/4 in. Ultra-Torr Fitting x 1/4 in. Male NPT bored through (Feedthrough for heated pipe) | Front End Cap | Swagelok | SS-4-UT-1-4-BT | 18.14 | 1 | \$18.14 | 1 | \$18.14 |
| 1/8" NPT SS male pipe plug when not using purge gas | Front End Cap | Swagelok | SS-2-P | 3.30 | 1 | \$3.30 | 1 | \$3.30 |
| 1/8" NPT SS male hose barb for purge gas, 1/8" ID | Front End Cap | Swagelok | SS-2-HC-1-2 | 4.70 | 1 | \$4.70 | 1 | \$4.70 |
| Heat Shrink tubing, .125" Shrink Diameter, 4' Length | Front End Cap | | | 2.90 | 4 | \$0.73 | 2 | \$1.45 |
| Alligator Clip Toothless, with Crimp Connection, 1-3/32" L, Steel, Packs of 10 | Front End Cap | McMaster | | 5.20 | 10 | \$0.52 | 2 | \$1.04 |
| Stainless Steel Hose Connector, 1/4 in. Male NPT, 1/8 in. Hose ID | Gas Routing | Swagelok | SS-2-HC-1-4 | 7.27 | 1 | \$7.27 | 1 | \$7.27 |
| Stainless Steel Ultra-Torr Vacuum Fitting, Union, 1/4 in. Tube OD | Gas Routing | Swagelok | SS-4-UT-6 | 28.39 | 1 | \$28.39 | 2 | \$56.78 |
| SS Flexible Hose Pipe with 1/4" Tubing at each end | Gas Routing | Swagelok | 321-4-X-12B2 | 73.80 | 1 | \$73.80 | 1 | \$73.80 |
| Stainless Steel Ultra-Torr Vacuum Fitting, Male Connector, 1/4 in. Ultra-Torr Fitting x 1/4 in. Male NPT bored through (Feedthrough for heated pipe) | Gas Routing | Swagelok | SS-4-UT-1-4-BT | 18.14 | 1 | \$18.14 | 1 | \$18.14 |
| IR Sensor | IR Sensing | Exergen | Irt/c.2ACF-K-LoE | 599.00 | 1 | \$599.00 | 1 | \$599.00 |
| IR Dove Tail Rail | IR Sensing | Thorlabs | RLA1200 | 66.00 | 1 | \$66.00 | 1 | \$66.00 |
| IR Rail Carrier | IR Sensing | Thorlabs | RC2 | 24.00 | 1 | \$24.00 | 1 | \$24.00 |
| 90 Degree Angle Plate | IR Sensing | Thorlabs | MSAP90 | 39.00 | 1 | \$39.00 | 1 | \$39.00 |
| Vee Mount | IR Sensing | Thorlabs | VC3 | 41.50 | 1 | \$41.50 | 1 | \$41.50 |
| 2.1 mm DC plug | IR Sensing | Philmore | | 1.90 | 1 | \$1.90 | 1 | \$1.90 |

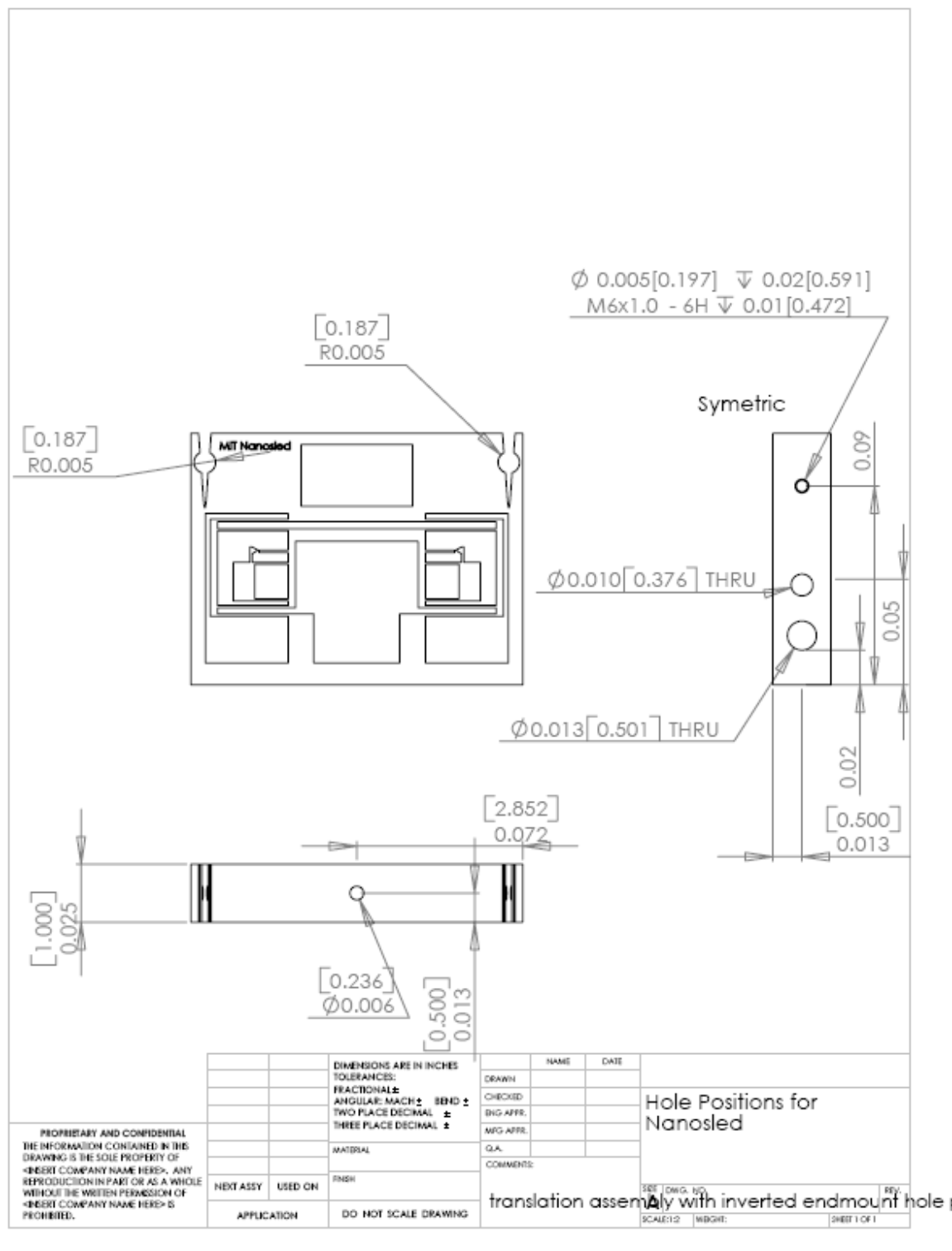
| Item | Sub Component ID | Supplier | ID # | Unit price | Items per unit | Cost per item | # items per System | System total |
|--|--------------------|----------------|-------------|------------|----------------|---------------|--------------------|--------------|
| Heat Shrink tubing, .125" Shrink Diameter, 4' Length | IR Sensing | | | 2.90 | 4 | \$0.73 | 2 | \$1.45 |
| Keyence Laser Displacement Sensor | Laser Displacement | Keyence | LK-G150 152 | 8000.00 | 1 | \$8,000.00 | 1 | \$8,000.00 |
| Horizontally Adjustable Mounting Base | Laser Displacement | Thorlabs | BA2T1 | 19.00 | 1 | \$19.00 | 1 | \$19.00 |
| 90 Deg Counter Bored Construction Post | Laser Displacement | Thorlabs | TR3C | 14.00 | 1 | \$14.00 | 2 | \$28.00 |
| Post .499" dia x 8" 32 stud 1/4-20 tapped hole | Laser Displacement | Thorlabs | TR8 | 8.55 | 1 | \$8.55 | 1 | \$8.55 |
| Post .499" dia x 4" 32 stud 1/4-20 tapped hole | Laser Displacement | Thorlabs | TR4 | 6.18 | 1 | \$6.18 | 2 | \$12.36 |
| Post Holder with Spring-Loaded Thumbscrew L-2inch | Laser Displacement | Thorlabs | PH2-ST | 8.10 | 1 | \$8.10 | 1 | \$8.10 |
| Power Patch Enclosure | Power Patch | LMB Heeger Inc | EAF100BLANO | 16.40 | 1 | \$16.40 | 1 | \$16.40 |
| SPST LED Switch | Power Patch | | | 3.90 | 1 | \$3.90 | 3 | \$11.70 |
| 2.1 mm DC Coax Jack | Power Patch | | | 1.49 | 1 | \$1.49 | 2 | \$2.98 |
| 2.5 mm DC Plug (power for substrate heater) | Power Patch | Philmore | | 2.90 | 1 | \$2.90 | 1 | \$2.90 |
| Two Prong AC Plug | Power Patch | | | 3.59 | 1 | \$3.59 | 2 | \$7.18 |
| 20 mm fuse holder | Power Patch | | | 1.49 | 1 | \$1.49 | 1 | \$1.49 |
| Circuit Board | Power Patch | | | 3.00 | 1 | \$3.00 | 1 | \$3.00 |
| Silicon Bridge Rectifier, 120 Vac to 120 Vdc | Power Patch | | | | 1 | \$0.00 | 1 | \$0.00 |
| Resistor 2.2kOhm, 2 Watt | Power Patch | | | | 2 | \$0.00 | 2 | \$0.00 |
| Resistor 5.6kOhm, 2 Watt | Power Patch | | | | 2 | \$0.00 | 1 | \$0.00 |
| 20 mm, 100 mA fuse | Power Patch | | | 3.00 | 4 | \$0.75 | 1 | \$0.75 |
| Insulating Circuit Board Mounts | Power Patch | Radio Shack | | | 4 | \$0.00 | 4 | \$0.00 |
| 18 AWG Power Wire | Power Patch | | | 6.99 | 540 | \$0.01 | 24 | \$0.31 |
| PreHeater Enclosure | PreHeater | Hammond | 1590E | 24.60 | 1 | \$24.60 | 1 | \$24.60 |
| Fire Brick | PreHeater | McMaster | 9355K1 | 9.82 | 1 | \$9.82 | 1 | \$9.82 |

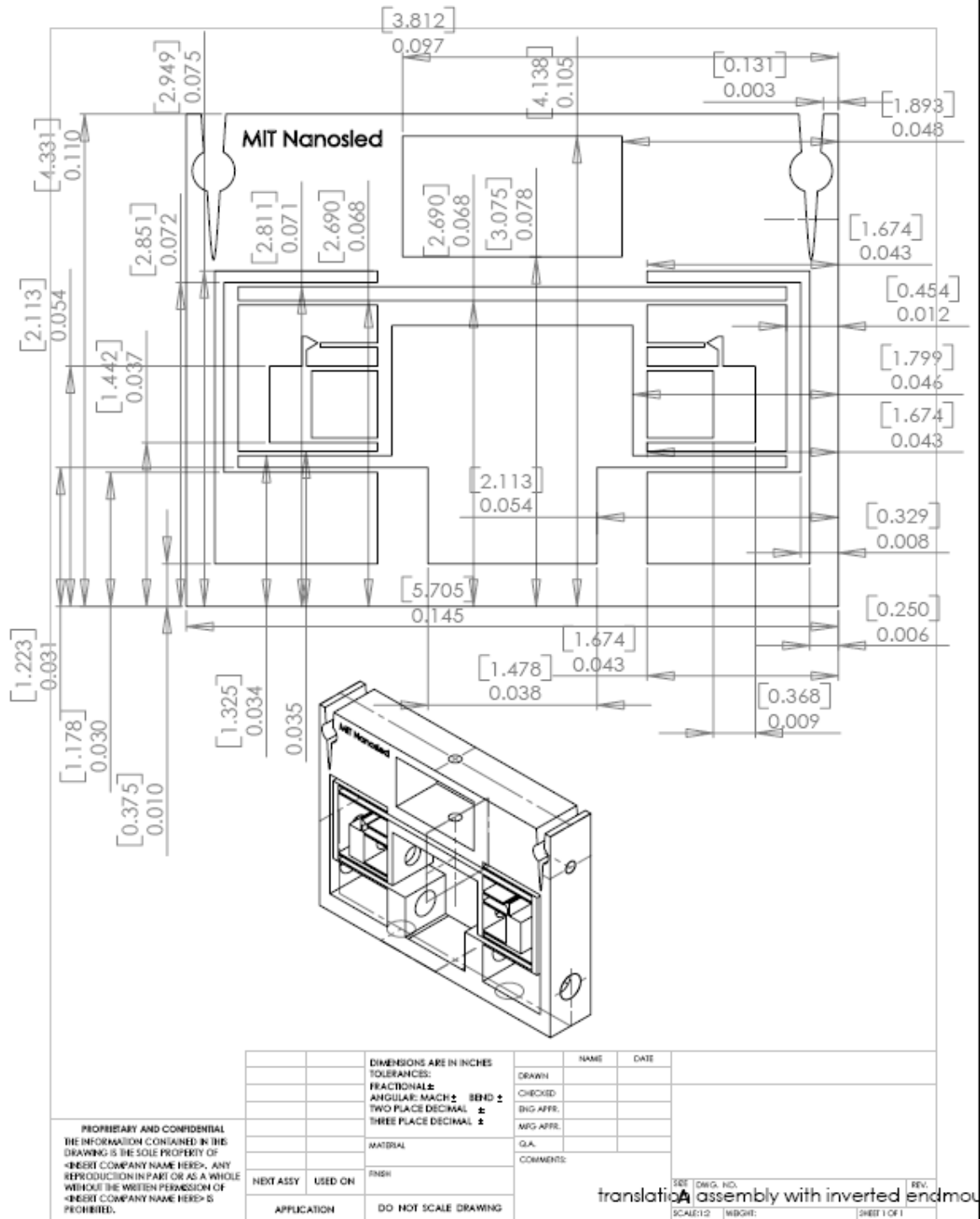
| Item | Sub Component ID | Supplier | ID # | Unit price | items per unit | Cost per item | # items per System | System total |
|--|---------------------------|--------------------|-------------|------------|----------------|---------------|--------------------|--------------|
| 99.8% Alumina Four Bore Tube, 1/4" Diameter, 6 in length | PreHeater | McDaniel | AXF-1165 | 4.98 | 1 | \$4.98 | 1 | \$4.98 |
| 1/4" Diameter Quartz Tube, 6 in length | PreHeater | Finkenbeiner Glass | | | 1 | \$0.00 | 1 | \$0.00 |
| 2.1 mm DC Coax Jack | PreHeater | | | 1.49 | 1 | \$1.49 | 1 | \$1.49 |
| 18 AWG Single Strand Wiring | PreHeater | | | 6.99 | 540 | \$0.01 | 12 | \$0.16 |
| 30 AWG Alumel Heater Wire | PreHeater | Omega | NI80-010 | 10.00 | 15 | \$0.67 | 0.4 | \$0.27 |
| Insulation | PreHeater | McMaster | | | 1 | \$0.00 | | \$0.00 |
| Nextel Ceramic Wiring Insulation, 3/16 ID | PreHeater | Omega | XC-316 | 3.25 | 1 | \$3.25 | 2 | \$6.50 |
| Two Screw Uninsulated Terminal Block | PreHeater | | | | 1 | \$0.00 | 2 | \$0.00 |
| Power supply | Pwr | | | | 1 | \$0.00 | 2 | \$0.00 |
| 18 AWG Dual Strand Insulated Wire | Pwr Patch to PreHeater | | | 1.90 | 1 | \$1.90 | 1 | \$1.90 |
| 2.1 mm DC plug | Pwr Patch to PreHeater | Philmore | | 2.90 | 1 | \$2.90 | 2 | \$5.80 |
| 18 AWG Power Cord | Pwr Patch to Temp Display | | | 1.90 | 1 | \$1.90 | 1 | \$1.90 |
| Two Prong AC Plug | Pwr Patch to Temp Display | | | 2.29 | 1 | \$2.29 | 2 | \$4.58 |
| Quartz tube: 52mmx48mmx12" (ODxDxlength), fire polished ends, round bottom | Reactor | Finkenbeiner Glass | | 50.00 | 1 | \$50.00 | 1 | \$50.00 |
| Lip Seals, Type&Style BV, lip code V | Rear End Cap | Chicago Rawhide | 721556 | 12.79 | 1 | \$12.79 | 2 | \$25.58 |
| 1/8" NPT SS male pipe plug when not using purge gas | Rear End Cap | Swagelok | SS-2-P | 3.30 | 1 | \$3.30 | 1 | \$3.30 |
| 1/8" NPT SS male hose barb for purge gas, 1/8" ID | Rear End Cap | Swagelok | SS-2-HC-1-2 | 4.70 | 1 | \$4.70 | 1 | \$4.70 |
| Rear End Cap Manufacturing | Rear End Cap | custom - MIT CMS | | 329.00 | 1 | \$329.00 | 1 | \$329.00 |
| Rear end cap Stock, Al 6061, 2.125" dia, 12" long | Rear End Cap | McMaster | 8974K731 | 23.77 | 1 | \$23.77 | 1 | \$23.77 |
| Stainless Steel Hose Connector, 1/4 in. Male NPT, 1/8 in. Hose ID | Rear End Cap | Swagelok | SS-2-HC-7-4 | 7.27 | 1 | \$7.27 | 1 | \$7.27 |

| Item | Sub Component ID | Supplier | ID # | Unit price | items per unit | Cost per item | # items per System | System total |
|---|------------------|------------------|-------------|------------|----------------|---------------|--------------------|--------------|
| 1/8" NPT SS Female Check Valve, Viton Seat. .3psi cracking pressure | Rear End Cap | Swagelok | SS-4CP2-1/3 | 23.80 | 1 | \$23.80 | 1 | \$23.80 |
| 1/4" NPT SS male pipe plug for rear end plate | Rear End Cap | Swagelok | SS-4-P | 4.00 | 1 | \$4.00 | 1 | \$4.00 |
| Stainless Steel Hose Connector, 1/4 in. Male NPT, 1/8 in. Hose ID | Rear End Cap | Swagelok | SS-2-HC-1-4 | 7.27 | 1 | \$7.27 | 1 | \$7.27 |
| Stainless Steel Belleville Disc Spring .156" ID, .312" OD, .011" Thick, Packs of 12 | Substrate Heater | McMaster | | 5.12 | 12 | \$0.43 | 2 | \$0.85 |
| Heat sink contact blocks; post-milling with 0.25" end mill Alloy 3003 | Substrate Heater | Aavid Thermalloy | 63620 | 27.50 | 50 | \$0.55 | 2 | \$1.10 |
| Aluminum Tube 1/4" OD, .222" ID, 12" Length, Packs of 10 | Substrate Heater | McMaster | 7237K18 | 10.88 | 60 | \$0.18 | 4 | \$0.73 |
| .125" SS 304 bar | Substrate Heater | McMaster | | 12.52 | 76 | \$0.16 | 2 | \$0.33 |
| 304 Stainless Steel Sheet W/#8 Mirror Finish 0.030" Thick, 12" X 12" | Substrate Heater | McMaster | | 18.36 | 144 | \$0.13 | 2 | \$0.26 |
| Silicon substrate, 6" wafer, 0.3 mm thickness, DSP, p++-doped | Substrate Heater | Silicon Quest | | | 1 | \$0.00 | | \$0.00 |
| Temperature Display aluminum enclosure | Temp Display | LMB Heeger Inc | EAS300BLANO | 19.03 | 1 | \$19.03 | 1 | \$19.03 |
| 2.1 mm DC Coax Jack | Temp Display | | | 1.49 | 1 | \$1.49 | 1 | \$1.49 |
| DB9 Female Jack | Temp Display | | | 0.99 | 1 | \$0.99 | 1 | \$0.99 |
| Two Prong AC Jack | Temp Display | | | 0.99 | 1 | \$0.99 | 1 | \$0.99 |
| 18 AWG Power Wire | Temp Display | | | 1.90 | 1 | \$1.90 | 1 | \$1.90 |
| Omega i32 Temperature Display and Controller | Temp Display | Omega | DPI32-C24 | 210.00 | 1 | \$210.00 | 1 | \$210.00 |

| <u>Item</u> | <u>Sub Component ID</u> | <u>Supplier</u> | <u>ID #</u> | <u>Unit price</u> | <u>items per unit</u> | <u>Cost per item</u> | <u># items per System</u> | <u>System total</u> |
|-----------------------------|-----------------------------|-----------------|-------------|-------------------|-------------------------------|--------------------------|-----------------------------------|---------------------|
| Type K Thermocouple Wire | Temp Display | | | | 1 | \$0.00 | 6 | \$0.00 |
| 1/4-20 2" Hex Cap Screw | Vertical Tube Holder | | | 1.20 | 1 | \$1.20 | 4 | \$4.80 |
| 3/8" Rubber Tip | Vertical Tube Holder | | | 1.29 | 4 | \$0.32 | 4 | \$1.29 |

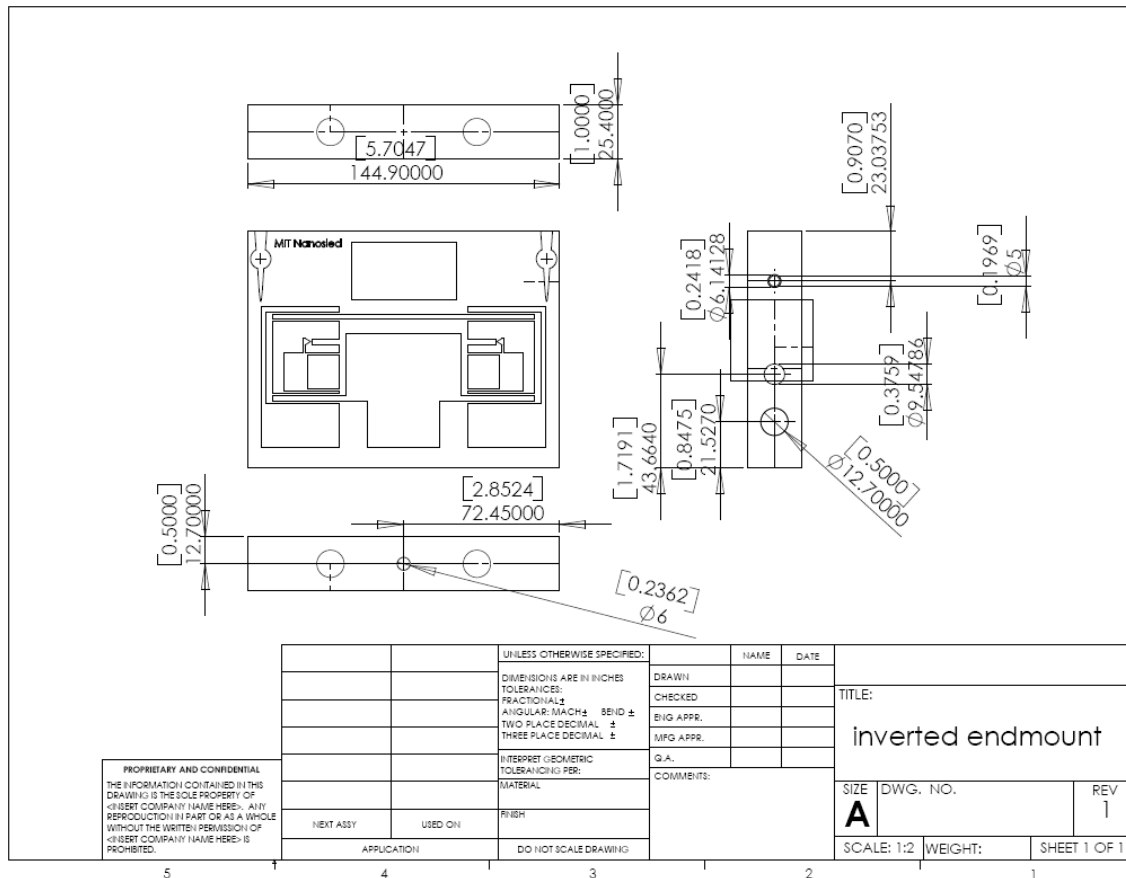
Appendix D: Nanosled Technical Drawings





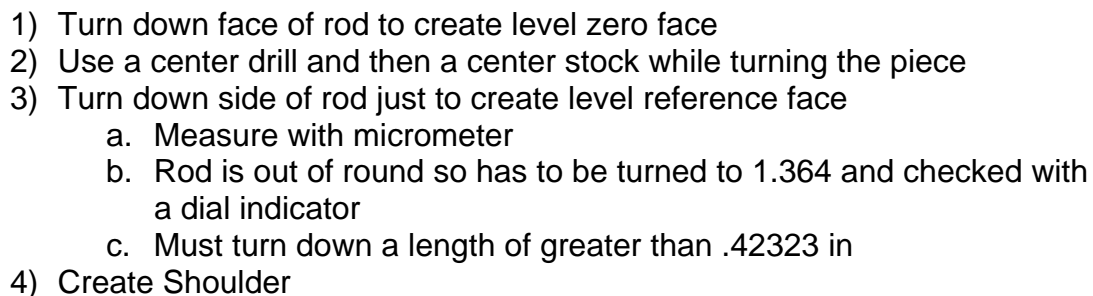
Appendix E: Nanosled Manufacturing

End Fixture Manufacturing



- 1) Face and cut rectangle
 - a. 5.7047 in long by 4.3307 in high by 1in thick (thickness is non-critical)
- 2) Drill Bottom Shaft Hole
 - a. Drill or Mill a 31/64 in hole
 - b. Hole center located
 - i. .8475 in from bottom
 - ii. .5 in from front edge (centerline of thickness)
- 3) Drill Top Shaft Hole
 - a. Drill or Mill a 23/64 hole
 - b. Hole center located
 - i. 1.7191 in from bottom
 - ii. Centerline of thickness
- 4) Drill Clamp Screw Hole
 - a. Drill or Mill a M6 hole
 - i. Use a #9 drill into .75in
 - ii. Use a M6 tap
 - b. For first end fixture, use ¼" screw

- ## Shoulder Bushing Manufacturing



- a. Shoulder Depth is .0076 in (diameter)
 - b. Shoulder ends at .30612 in from the end face
 - c. Used 800 rpm, feed of .002 and .025 removal at a time on CNC lathe. Use a smaller radius tip tool.
- 5) Create Deep Shoulder
 - a. Shoulder diameter is .3750 in
 - b. Shoulder finishes at .19685 in from the end
- 6) Drill or Mill Through Hole
 - a. Shaft diameter is measured at .186 in
 - b. Machine Hole of 11/64 in
 - i. Recommend drilling longer hole than required in order to allow chips from reaming to have a relief point in front as well as up the reamer flutes
 - c. Ream hole to 3/16 in
 - i. Don't ream later because this will produce a bur on the side
- 7) File any burred edges off of piece while in the lathe
- 8) Cut off machined piece from rod
- 9) Turn machined piece 180 degrees and use lathe to remove excess material on other side and produce flat face
 - a. Used 750 rpm and no more than .001 in removed at a time worked well. Used collet chuck.
 - b. File off any burred edges while in the lathe
- 10) Tap Set screw hole
 - a. Use a 39 drill in the milling machine to drill the hole
 - b. File any burs
 - c. Tap hole
 - i. Put center in the milling machine and use the descending arm to hold the tap vertical

Appendix F: Department of Defense Technology Readiness Levels

[39]

| TRL | Definition | Description | Supporting Information |
|-----|---|---|---|
| 1 | Basic principles observed and reported. | Lowest level of technology readiness. Scientific research begins to be translated into applied research and development (R&D). Examples might include paper studies of a technology's basic properties. | Published research that identifies the principles that underlie this technology. References to who, where, when. |
| 2 | Technology concept and/or application formulated. | Invention begins. Once basic principles are observed, practical applications can be invented. Applications are speculative, and there may be no proof or detailed analysis to support the assumptions. Examples are limited to analytic studies. | Publications or other references that outline the application being considered and that provide analysis to support the concept. |
| 3 | Analytical and experimental critical function and/or characteristic proof of concept. | Active R&D is initiated. This includes analytical studies and laboratory studies to physically validate the analytical predictions of separate elements of the technology. Examples include components that are not yet integrated or representative. | Results of laboratory tests performed to measure parameters of interest and comparison to analytical predictions for critical subsystems. References to who, where, and when these tests and comparisons were performed. |
| 4 | Component and/or bread-board validation in a laboratory environment. | Basic technological components are integrated to establish that they will work together. This is relatively "low fidelity" compared with the eventual system. Examples include integration of "ad hoc" hardware in the laboratory. | System concepts that have been considered and results from testing laboratory-scale breadboard(s). References to who did this work and when. Provide an estimate of how breadboard hardware and test results differ from the expected system goals. |
| 5 | Component and/or breadboard validation in a relevant environment. | Fidelity of breadboard technology increases significantly. The basic technological components are integrated with reasonably realistic supporting elements so they can be tested in a simulated environment. Examples include "high-fidelity" laboratory integration of components. | Results from testing a laboratory breadboard system are integrated with other supporting elements in a simulated operational environment. How does the "relevant environment" differ from the expected operational environment? How do the test results compare with expectations? What problems, if any, were encountered? Was the breadboard system refined to more nearly match the expected system goals? |

| TRL | Definition | Description | Supporting Information |
|-----|---|---|--|
| 6 | System/subsystem model or prototype demonstration in arelevant environment. | Representative model or proto-type system, which is well be-yond that of TRL 5, is tested in a relevant environment. Repre-sents a major step up in a tech-nology's demonstrated readiness. Examples include testing a prototype in a high-fidelity laboratory environment or in a simulated operational environment. | Results from laboratory testing of a prototype system that is near the desired configuration in terms of performance, weight, and volume. How did the test environment differ from the operational environment? Who performed the tests? How did the test compare with expectations? What problems, if any, were encountered? What are/were the plans, options, or actions to resolve problems before moving to thenext level? |
| 7 | System prototype demon-stration in an operationalenvironment. | Prototype near or at planned operational system. Represents a major step up from TRL 6 by requiring demonstration of an actual system prototype in an operational environment (e.g., in an aircraft, in a vehicle, or in space). Examples include testing the prototype in a testbed aircraft. | Results from testing a proto-type system in an operational environment. Who performed the tests? How did the test compare with expectations? What problems, if any, were encountered? What are/were the plans, options, or actions to resolve problems beforemoving to the next level? |
| 8 | Actual system completed and qualified through test and demonstration. | Technology has been proven to work in its final form and under expected conditions. In almost all cases, this TRL represents the end of true system develop-ment. Examples include devel-opmental test and evaluation of the system in its intended wea-pon system to determine if itmeets design specifications. | Results of testing the system in its final configuration under the expected range of environ-mental conditions in which it will be expected to operate. Assessment of whether it will meet its operational require-ments. What problems, if any, were encountered? What are/ were the plans, options, or actions to resolve problemsbefore finalizing the design? |
| 9 | Actual system proven through successful missionoperations. | Actual application of the tech-nology in its final form and under mission conditions, such as those encountered in opera-tional test and evaluation (OT&E). Examples include using the system under operationalmission conditions. | OT&E reports. |

References

- [1] Hart AJ. Discussion on state of the art in growing CNT forests by CVD. In: Kuhn DS, ed. *Conversation*. Cambridge 2007.
- [2] Hart AJ. *Chemical, Mechanical, and Thermal Control of Substrate-Bound Carbon Nanotube Growth*. Cambridge: Massachusetts Institute of Technology; 2006.
- [3] Baughman RH, Zakhidov AA, de Heer WA. Carbon Nanotubes—the Route Toward Applications. *Science*. 2002 2002/08/02;297:787-92.
- [4] Endo M, Hayashi T, Kim YA, Terrones M, Dresselhaus MS. Applications of carbon nanotubes in the twenty-first century. *The Royal Society*. 2004 2004/08/13:2223-38.
- [5] Coleman JN, Khan U, Blau WJ, Gun'ko YK. Small but strong: A review of the mechanical properties of carbon nanotube–polymer composites. *Carbon*. 2006 2006/02/23.
- [6] Hart AJ. *Carbon Nanotube Fundamentals Short Course*. ISNM; 2006; Cambridge, MA; 2006.
- [7] Huang H, Liu C, Wu Y, Fan S. Aligned Carbon Nanotube Composite Films for Thermal Management. *Advanced Materials*. 2005;17:1652-6.
- [8] Tománek D, Enbody RJ. *Science and Application of Nanotubes*. New York: KLUWER ACADEMIC PUBLISHERS 2002.
- [9] Zhang M, Atkinson KR, Baughman RH. Multifunctional Carbon Nanotube Yarns by Downsizing an Ancient Technology. *Science*. 2004 2004/11/19;306:1358-61.
- [10] LennTech. Properties of 304 Stainless Steel. [cited; Available from: <http://www.lenntech.com/Stainless-steel-304.htm>]
- [11] Gale WF, Totemeier TC, eds. *Smithells Metals Reference Book*. 8th ed. Burlington, MA: Elsevier Butterworth-Heinemann 2004.
- [12] 5456 H112 Series Aluminum. [cited; Available from: <http://www.matweb.com/search/SpecificMaterial.asp?bassnum=MA5456H112>]
- [13] University CfNEaIS. Electrical Conductivity of Aluminum and It's Alloys. [cited; Available from: http://www.ndt-ed.org/GeneralResources/MaterialProperties/ET/Conductivity_Al.pdf]
- [14] Matweb. 6000 Series Aluminum. [cited; Available from: <http://www.matweb.com/search/SpecificMaterial.asp?bassnum=MA6016>]
- [15] Zhang M, Fang S, Zakhidov AA, Lee SB, Aliev AE, Williams CD, et al. Strong, Transparent, Multifunctional, Carbon Nanotube Sheets. *Science*. 2005 2005/08/19;309:1215-9.
- [16] Dalton AB, Collins S, Muñoz E, Razal JM, Ebron VH, Ferraris JP, et al. Super-tough carbon-nanotube fibres. *Nature*. 2003 2003/06/12;423:703.
- [17] (ABS) ABoS. High Speed Naval Craft Rules, Part 2, Materials and Welding, 2007. In: (ABS) ABS, ed. 2006.
- [18] HY80 Properties. [cited; Available from: <http://www.matweb.com/search/SpecificMaterial.asp?bassnum=MSHY80>]

- [19] Committee on High-Performance Structural Fibers for Advanced Polymer Matrix CNMAB, Division on Engineering and Physical Sciences. High-Performance Structural Fibers for Advanced Polymer Matrix Composites. Washington D.C.: The National Academies Press 2005.
- [20] (ABS) ABoS. High Speed Naval Craft Rules, Part 2, Rules for Materials and Welding - Aluminum and Fiber Reinforced Plastics (FRP). In: (ABS) ABS, ed. 2005.
- [21] DuPont. Kevlar Technical Guide; 2007.
- [22] Endo M, Kim YJ, chino t, shinya o, matsuzawa y, suezaki h, et al. High-performance electric double-layer capacitors using mass-produced multi-walled carbon nanotubes. *Applied Physics A: Material Science & Processing*. 2006 2004/10/07;82:559-65.
- [23] Hayashi T, Kim YA, Matoba T, Esaka M, Nishimura K, Tsukada T, et al. Smallest freestanding single-walled carbon nanotube. *Nano Letters*. 2003;3(7):887-9.
- [24] Atomate. Atomate Company Website. [cited; Available from: www.atomate.com]
- [25] firstnano. Company Website. [cited; Available from: www.firstnano.com]
- [26] Lucas van Laake AJH, and Alexander H. Slocum. A Suspended Heated Silicon Platform for Rapid Thermal Control of Surface Reactions with Application to Carbon Nanotube Synthesis. Cambridge: Massachusetts Institute of Technology 2006:29.
- [27] Scientific G. GFI Scientific. [cited; Available from: <http://www.finkenbeiner.com/QTZPROP.htm>]
- [28] Vesuvius-McDanel. Technical Specifications for 99.8% Alumina. 2007 [cited; Available from: <http://www.techceramics.com/pdf/99.8Alumina.pdf>]
- [29] International SQ. Properties of N-type silicon wafer. [cited; Available from: <http://www.siliconquest.com/eng/products/substrates.htm>]
- [30] Mech T. Product Marketing Engineer, Conax-Buffalo. Email ed 2007.
- [31] Perry RHG, D.W. . Perry's Chemical Engineers' Handbook. 7th ed: McGraw-Hill 1997.
- [32] Purdue University DoPF. Material Safety Data Sheet for Ethylene. [cited; Available from: <http://www2.itap.purdue.edu/MSDS/detail.cfm?MSDSID=5448>]
- [33] van Laake L, Hart AJ, Slocum AH. A Suspended Heated Silicon Platform for Rapid Thermal Control of Surface Reactions with Application to Carbon Nanotube Synthesis. Cambridge: Massachusetts Institute of Technology 2006:29.
- [34] Hart AJ, Laake Lv, Slocum AH. Desktop Growth of Carbon-Nanotube Monoliths with In Situ Optical Imaging. *Small*. 2007;3(5):772-7.
- [35] Wang BN, Bennett RD, Verploegen E, Hart AJ, Cohen RE. Quantitative Characterization of the Morphology of Multiwall Carbon Nanotube Films by Small-Angle X-ray Scattering. *Journal of Physical Chemistry C Nanomaterials and interfaces*. 2007;111(16):5859-65.
- [36] Thermalloy A. Specifications for the 63620 Extruded Heat Sink. [cited; Available from: <http://www.aavidthermalloy.com/cgi->]

[bin/exdisp.pl?Pnum=63620&therm=2.73592322527705&therm=&airflow=57.2&AirUnits=LFM&CType=Natural&ExLength=1&LengthUnits=in](#)

[37] Site GSW. [cited; Available from:

<http://www.finkenbeiner.com/QTZPROP.htm>

[38] Omega. Nickel/Chromium 80/20 Resistive Heating Wire Data. 2007

[cited; Available from: www.omega.com

[39] Technology DUoDfSa. Technology Readiness Assessment (TRA)

Deskbook. In: Defense Do, ed. 2005.

[40] Force USNRACNPoRtaEN. Roadmap to an Electric Naval Force. In: Navy U, ed. 2002:90.

[41] Hackenberger W, Technologies T. Very High Energy Density Capacitors for Miniaturized, Modular Power Electronics. State College, PA: ONR.

[42] Atkinson K, Hawkins S, Huynh C, Skourtis C, Wassenberg J, Jane Dai MZ, et al. Multifunctional Carbon Nanotube Yarns and Transparent Sheets: Fabrication, Properties, and Applications. NanoTechnology 2006 (NT'06); 2006; Nagano, Japan; 2006.